

Surface-Crosslinked Gelatin Nanoparticles As New Tool for the Delivery of Hydrophilic Macromolecular Drugs

Dissertation
zur Erlangung des Grades
des Doktors der Naturwissenschaften
der Naturwissenschaftlich-Technischen Fakultät
der Universität des Saarlandes

Von
Abdul Baseer

Saarbrücken

2019

Tag des Kolloquiums:	12.02.2020
Dekan:	Prof. Dr. Guido Kickelbick
Berichterstatter:	Prof. Dr. Marc Schneider
Berichterstatter	Prof. Dr. Gerhard Wenz
Vorsitz:	Prof. Dr. Claus-Michael Lehr
Akad. Mitarbeiter:	Dr. Josef Zapp

Dedicated to

my Family

Table of Contents

Table of Contents	I
List of Figures	VI
List of Tables	XIII
Abstract	XVI
1 Background and Literature Survey	1
1.1. Introduction.....	2
1.2. Delivery challenges of macromolecules.....	2
1.3. Nanoparticle-based delivery of hydrophilic macromolecules.....	3
1.4. Proteins as a construction material for nanoparticles.....	4
1.5. Gelatin as a construction material for delivery systems.....	5
1.5.1. Gelatin nanoparticles as a carrier for hydrophilic macromolecules.....	6
1.5.1.1. Formulation methods of GNPs.....	8
1.5.2. Crosslinking of gelatin nanoparticles.....	11
1.5.2.1. Aldehydes.....	11
1.5.2.2. Genipin.....	12
1.5.2.3. Carbodiimide/ <i>N</i> -hydroxysuccinimide (CDI/NHS).....	13
1.5.2.4. Microbial transglutaminase (MTG).....	14
1.5.3. Purification methods of nanoparticles.....	15
1.5.3.1. Centrifugation based purification.....	16
1.5.3.2. Tangential flow filtration.....	16
2 Aim and Scope of the Thesis	19
2.1. Formulation optimization for the design of surface-crosslinked gelatin nanoparticles (scGNPs).....	20
2.2. Optimization of purification procedures for the surface-crosslinked GNPs.....	22

2.3. Characterization and loading of surface-crosslinked GNPs with hydrophilic macromolecules.....	23
3 Formulation Optimization for the Design of Surface-Crosslinked Gelatin Nanoparticles (scGNPs)	24
3.1. Abstract	25
3.2. Introduction.....	26
3.2.1. Challenges of GNPs crosslinking.....	27
3.3. Experimental	29
3.3.1. Materials.....	29
3.3.2. Nanoparticles by nanoprecipitation.....	29
3.3.3. Optimization of crosslinking.....	30
3.3.3.1. Type B GNPs.....	30
3.3.3.2. Type A GNPs	31
3.3.4. Nanoparticle characterization.....	32
3.3.4.1. Determination of size and zeta potential.....	32
3.3.4.2. Morphology of nanoparticles by scanning electron microscopy (SEM).....	32
3.3.5. Determination of crosslinking extent	33
3.3.6. Measurement of un-reacted DIC	34
3.3.7. Measurement of diisopropylurea.....	34
3.3.8. Cytotoxicity evaluation	35
3.4. Results and Discussion.....	36
3.4.1. Optimization of crosslinking conditions	39
3.4.1.1. Type B GNPs.....	39
3.4.1.2. Type A GNPs	46
3.4.2. Investigation of crosslinking	54
3.4.2.1. Determination of crosslinking degree – TNBS Assay.....	54
3.4.2.2. Monitoring of crosslinking.....	58
3.4.3. Zeta potential of DIC-crosslinked GNPs	63

3.4.4.	Morphology of nanoparticles – Scanning Electron Microscopy.....	65
3.4.5.	Cytotoxicity Evaluation.....	67
3.5.	Conclusions.....	69
4	Optimization of Purification Procedures for Surface-Crosslinked Gelatin Nanoparticles	70
4.1.	Abstract.....	71
4.2.	Introduction.....	72
4.3.	Experimental.....	74
4.3.1.	Materials.....	74
4.3.2.	Preparation of DIC-crosslinked gelatin nanoparticles.....	74
4.3.3.	Purification of DIC-crosslinked GNPs.....	74
4.3.3.1.	Centrifugation.....	75
4.3.3.2.	Dialysis.....	75
4.3.3.3.	Tangential flow filtration (TFF).....	75
4.3.4.	Evaluation of purification performance.....	77
4.3.4.1.	Quantification of poloxamer.....	77
4.3.4.2.	Quantification of un-reacted crosslinker (DIC).....	79
4.3.4.3.	Quantification of crosslinking by product (DIU).....	79
4.3.4.4.	Fourier Transform-Infrared (FT-IR) analysis of crosslinked GNPs.....	80
4.3.5.	Measurement of particle size.....	80
4.3.6.	Morphological Characterization.....	81
4.3.6.1.	Scanning Electron Microscopy (SEM).....	81
4.4.	Results and Discussion.....	81
4.4.1.	Nanoparticles preparation.....	82
4.4.2.	Optimization of purification.....	82
4.4.2.1.	Centrifugation.....	82
4.4.2.2.	Dialysis and cross-flow filtration.....	83
4.4.3.	Evaluation of purification performance.....	84

4.4.3.1.	Removal of Poloxamer-188	84
4.4.3.2.	Removal of un-reacted crosslinker (DIC).....	86
4.4.3.3.	Removal of crosslinking by product (DIU)	86
4.4.3.4.	Fourier Transform-Infrared (FT-IR) analysis of crosslinked GNPs	87
4.4.4.	Measurement of particle size and size distribution	89
4.4.4.1.	Effect of membrane type and pore size	89
4.4.4.2.	Effect of amount of water in re-circulation.....	91
4.4.5.	Morphological Characterization.....	91
4.4.5.1.	Scanning Electron Microscopy (SEM)	91
4.5.	Conclusions	93
5	Characterization and loading of Surface -Crosslinked Gelatin Nanoparticles with Hydrophilic Macromolecules	94
5.1.	Abstract	95
5.2.	Introduction	96
5.3.	Experimental	98
5.3.1.	Materials.....	98
5.3.2.	Preparation of loaded gelatin nanoparticles	98
5.3.2.1.	Loading with FITC-dextran.....	98
5.3.2.2.	Loading with lysozyme	99
5.3.3.	Physicochemical Characterization	102
5.3.3.1.	Determination of size and size distribution	102
5.3.3.2.	Determination of zeta potential.....	102
5.3.4.	Entrapment and loading efficiency.....	102
5.3.4.1.	FITC-dextran	102
5.3.4.2.	Lysozyme	103
5.3.5.	Investigation of <i>in vitro</i> release	105
5.3.5.1.	FITC-dextran	105
5.3.5.2.	Lysozyme	106
5.3.6.	Determination of the biological activity.....	107
5.4.	Results and Discussion.....	108

5.4.1.	Effect of loading on mean size and size distribution.....	109
5.4.1.1.	FITC-dextran loaded GNPs.....	109
5.4.1.2.	Lysozyme loaded GNPs.....	111
5.4.2.	Optimization of crosslinking time for lysozyme loading.....	113
5.4.3.	Determination of zeta potential	117
5.4.4.	Entrapment and loading efficiency.....	118
5.4.4.1.	FITC-dextran	118
5.4.4.2.	Lysozyme	120
5.4.5.	Summary of the physicochemical properties of lysozyme-loaded GNPs	124
5.4.6.	Investigation of <i>in vitro</i> release	125
5.4.6.1.	FITC-dextran	125
5.4.6.2.	Lysozyme	127
5.4.7.	Determination of biological activity.....	129
5.5.	Conclusions.....	134
	Summary and Outlook.....	135
	Bibliography	139
	Scientific Output.....	149
	Curriculum Vitae.....	150
	Acknowledgment	151

List of Figures

Figure 1-1. Challenges of macromolecular drug delivery (adapted from Agrahari V <i>et al.</i> (2016) [2]).	3
Figure 1-2. Mechanism of glutaraldehyde-based crosslinking of gelatin forming Schiff's bases within gelatin peptidal chains.	12
Figure 1-3. Mechanism of genipin induced crosslinking of gelatin. A. Fast nucleophilic attack of gelatin's L-lysine amino groups on the ring structure of genipin to form a stable transition intermediate product; and B. slower reaction with nucleophilic substitution of free lysine amino molecules of a second gelatin chain (Adapted from James B Rose <i>et al.</i> 2014 [109]).	13
Figure 1-4. Mechanism of crosslinking caused by CDI/NHS crosslinkers (adapted from Qazvini <i>et al.</i> , 2011 [110]).	14
Figure 1-5. Microbial transglutaminase catalysed crosslinking reaction in gelatin nanoparticles. This involves the conjugation of primary amino groups of glutamine and lysine. During this crosslinking, one mole of ammonium is produced (adapted from S. Fuchs <i>et al.</i> , (2010) [112]).	15
Figure 1-6. Comparison between (a) dead-end or normal flow filtration and (b) tangential flow filtration.	17
Figure 1-7. TFF-based ultra-filtration in (a) concentration mode and (b) diafiltration mode.	18
Figure 2-1. Summary of the work packages addressed in the present thesis.	20
Figure 3-1. (a) Schematic illustration of glutaraldehyde-crosslinked GNPs loaded with a protein-based drug. (b) A closer look of Schiff's base crosslink between gelatin and protein-based drug substance.	28
Figure 3-2. Reaction of the tetrazolium salt MTT to formazan during the cell viability test.	35
Figure 3-3. (a) Schematic representation of the procedure to form GNPs via nanoprecipitation and crosslinking the particles by DIC. (b) Schematic representation of DIC-mediated	

crosslinking mechanism. Step 1: Formation of diisopropylcarbodiimide-mediated activation of (-COOH) to form an unstable intermediate O-Acylisourea. Step 2: Secondary reaction with nucleophilic substitution of free primary amino groups presented by lysine into the formerly formed DIC activated ester leading to formation amide crosslink at GNPs interface [131-137].	38
Figure 3-4. Effect of crosslinker concentration (DIC) on particle size and size distribution. The nanoparticles were measured in water after 10 times dilution before purification with three independent experiments (n = 3).	41
Figure 3-5. Mean size and size distribution analysis at different incubation times at room temperature (concentration of DIC in nanosuspension. (a) 5 mg/mL (b) 15 mg/mL).	43
Figure 3-6. Mean size and size distribution analysis at different crosslinking reaction times at room temperature, 30°C and 50°C for DIC concentration of 15 mg/mL.....	45
Figure 3-7. Effect of gelatin concentration on mean size and polydispersity index of GNPs. The samples were measured in triplicates for three independent experiments. Acetone was used as dispersion medium and samples were diluted 10 times with acetone before DLS measurements. <i>Statistics</i> (N.S: statistically non-significant on the basis of $p > 0.05$ as per one-way ANOVA). * statistically significant $p < 0.05$ as per one-way ANOVA.....	51
Figure 3-8. Comparison between mean sizes of DIC-crosslinked gelatin A NPs measured in acetone and water as dispersion media. * $p < 0.05$: statistically significant according to paired two-tailed t -test.....	54
Figure 3-9. Relationship between % crosslinking extent and concentrations of crosslinker (DIC) for 18 h crosslinking reaction time. The volumes were kept constant during the preparations. Values determined from TNBS assay by using the absorption maximum of $\lambda_{\text{max}} = 349$ nm, n = 3. <i>Statistics</i> (N.S: Non-significant statistically on the basis of $p > 0.05$ as per one-way ANOVA). * Statistically significant $p < 0.05$ as per one-way ANOVA.....	55

Figure 3-10. Relationship between % crosslinking degree and concentration of crosslinker for 48 h crosslinking reaction time. Values determined by TNBS assay using an absorption maximum of $\lambda_{\max} = 349$ nm, $n = 3$. <i>Statistics</i> (NS: Non-significant on the basis of $p > 0.05$ as per one-way ANOVA).....	57
Figure 3-11. Proposed hypothetical model of DIC-crosslinked GNP based on TNBS assay. $V_{(\text{sphere})}$: Total volume of GNP sphere. $V_{(\text{internal sphere})}$: Volume of non-crosslinked sphere, $V_{(\text{crosslinked})}$: Volume of crosslinked part of GNP, $R_{(\text{un-crosslinked sphere})}$: Radius of uncross linked part of GNP which is the interior of GNP. $R_{(\text{sphere})}$: Total radius of GNP. $D_{(\text{crosslinked})}$: Thickness of the crosslinked edge (nm).	58
Figure 3-12. Quantification of the reaction by-product (DIU). (A) ^1H -NMR-spectrum of the supernatant of the crosslinked GNPs. The close-up in green shows the spectrum of the supernatant between 1.00 and 1.06 ppm; in red the signal of DIU methyl protons and in blue the high field satellite peak of DIC. (B) Shows the integration of the DIU methyl resonances and of the DIC methyl carbon-13 satellites.....	61
Figure 3-13. Quantification of the reaction by-product DIU. The diagram shows the results of the DIU quantification, calculated by the integral of the corresponding peaks for different amounts of crosslinker. Negative control: sample without gelatin. <i>Statistics</i> (* $p < 0.05$ as per one-way ANOVA, N.S: Non-significant statistically).....	62
Figure 3-14. Theoretical scheme of pH dependent surface charge of type A and Type B GNPs.	64
Figure 3-15. Zeta potential of type A and type B GNPs crosslinked with DIC [15 mg/mL] measured at different pH values.....	65
Figure 3-16. SEM images of DIC-crosslinked type B GNPs washed via tangential flow filtration (TFF) set-up containing modified regenerated cellulose membrane (Hydrosart) of 100 kDa pore size. (a) concentrated sample. (b) Diluted sample.....	66

Figure 3-17. Cell viability analysis of DIC-crosslinked GNPs by MTT assay after 4 h incubation on A549 cells. The % viability for all concentrations of GNPs is above 80 %. MTT assay was performed in triplicates and data is average of three independent experiments.....	68
Figure 4-1. Schematic representation of TFF assembly used for the purification of sc-GNPs. (a). External overview of TFF assembly. (adapted from product operational manual provided by Sartorius) (b). Scheme of the working principal of TFF assembly.	77
Figure 4-2. Purification efficiency of TFF and dialysis-based purification in terms of % clearance of poloxamer and effect of critical parameters. (a) Effect of membrane pore size, and (b) effect of water amounts used in re-circulation using 100 kDa membrane using TFF based purification.	85
Figure 4-3. GC chromatograms. (a). DIC-crosslinked GNPs washed with dialysis. (b) Reference compound of DIC. (c). DIC-crosslinked GNPs washed with TFF filtration.	86
Figure 4-4. Proton NMR (¹ H-NMR) spectra of supernatant of washed nanoparticles taken in deuterated acetone. (a) ¹ H-NMR spectrum of standard compound of DIU. (b) ¹ H-NMR spectrum of TFF purified scGNPs samples. (c) ¹ H-NMR spectrum of dialysis washed scGNPs sample.....	87
Figure 4-5. FT-IR spectra of GNPs crosslinked with different amounts of crosslinker (DIC) purified with tangential flow filtration.	89
Figure 4-6. Mean size and size distribution of DIC-crosslinked GNPs purified with dialysis and TFF-based purification, using membranes of different pore sizes and type (RC: regenerated cellulose; PES: polyethersulfone). <i>Statistics</i> : N.S: statistically non-significant on the basis of $p > 0.05$ as per one-way ANOVA.....	90
Figure 4-7. Particle size & size distribution versus volume of water used for TFF washing. <i>Statistics</i> : N.S: statistically non-significant on the basis of $p > 0.05$ using one-way ANOVA.	91
Figure 4-8. SEM micrographs of GNPs suspension purified with different techniques (a) DIC-crosslinked GNPs purified with centrifugation ($3000 \times g$; $t = 10$ min), (b) DIC-crosslinked	

GNPs purified with dialysis (regenerated cellulose membrane of 50 kDa), (c) DIC-crosslinked GNP purified with tangential flow filtration (membrane 100 kDa pore size, concentrated sample), (d) same formulation with diluted sample.	92
Figure 5-1. Chemical structure of lysozyme. (a) Primary structure. (b) Secondary structure. (Reprinted from Phillips <i>et al.</i> (1966) [177].	99
Figure 5-2. Schematic representation of the procedure lysozyme and FITC-dextran loaded GNP via nanoprecipitation and crosslinking the particles by DIC.	101
Figure 5-3. Effect of FITC-dextran (1mg) loading of different molecular weights on mean size and size distribution of produced gelatin nanoparticles. The FITC-dextran to gelatin mass ratio was 1:20. <i>Statistics:</i> (N.S: Not significant statistically as per one-way ANOVA ($p > 0.05$)	110
Figure 5-4. Mean size and size distribution analysis of DIC-crosslinked GNP loaded with different drug to polymer mass ratio at room temperature for DIC concentration of 15 mg/mL. The samples were measured in acetone as a dispersant and were diluted 10 times with acetone before DLS measurements. <i>Statistics</i> (N.S.: statistically non-significant on the basis of $p > 0.05$ as per one-way ANOVA). (*) $p < 0.05$: Statistically significant as per one-way ANOVA.	112
Figure 5-5. Mean size and size distribution analysis of lysozyme-loaded GNP loaded with different amounts of lysozymes at different incubation times at room temperature (concentration of DIC was 15 mg/mL). Samples were measured in water as a dispersant for DLS measurements and each sample was diluted 10 times in water before measurements. .	114
Figure 5-6. Mean size and size distribution analysis of DIC-crosslinked GNP loaded with different lysozyme amounts. The DIC concentration used was 15 mg/mL. The samples were measured both in acetone and water as dispersion media and were diluted 10 times before DLS measurements. Each sample was measured in triplicates with three independent	

experiments. <i>Statistics</i> : (*) $p < 0.05$: Statistically significant according to paired two-tail t -test.	115
Figure 5-7. Zeta potential of DIC-crosslinked GNPs loaded with different amounts of lysozyme measured at pH 6. <i>Statistics</i> (N.S: non-significant statistically ($p > 0.05$), (*) $p < 0.05$: Statistically significant as per one-way ANOVA.	118
Figure 5-8. Comparison of entrapment efficiency between GTA-crosslinked and DIC-crosslinked GNPs and effect of molecular weight of FITC-dextran on entrapment potential of both types of GNP systems. <i>Statistics</i> (n.s.: statistically non-significant on the basis of $p > 0.05$ using t -test. (*) Statistically significant $p < 0.05$	120
Figure 5-9. Mean sizes of free lysozyme having concentration of 2 mg/mL in water dispersed in acetone. The mean sizes are in the micro-range.....	122
Figure 5-10. Microfiltration of free lysozyme dispersed in acetone and lysozyme-loaded GNPs. (a). Entrapment efficiency of lysozyme-loaded un-crosslinked GNPs with and without microfiltration of nanosuspension using PTFE syringe filters (0.45 μm pore size). (b) % lysozyme retained on membrane surface after microfiltration of free lysozyme dispersion in acetone using μm 0.45 PTFE filter. <i>Statistics</i> (N.S: statistically non-significant on the basis of $p > 0.05$ using t -test.....	123
Figure 5-11. (a) Entrapment efficiency of DIC-crosslinked GNPs loaded with different amounts of lysozyme (% EE was calculated for lysozyme-loaded GNPs without microfiltration. (b) Loading efficiency of GNPs loaded with different amounts of lysozyme. Loaded GNPs without microfiltration were analysed. <i>Statistics</i> (N.S.: statistically non-significant on the basis of $p > 0.01$ as per one-way ANOVA and t -test; (*) $p < 0.05$).....	124
Figure 5-12. <i>In vitro</i> release profile of DIC-crosslinked gelatin nanoparticles loaded with FITC-dextran of different molecular weight in phosphate buffer saline (PBS) pH 7.4 as release medium at 37 °C.....	127

Figure 5-13. <i>In vitro</i> release profile of DIC-crosslinked and glutaraldehyde crosslinked GNPs loaded with different amounts of lysozyme in phosphate buffer saline (PBS) pH 7.4 as a release medium at 37°C. <i>Statistics</i> (N.S.: statistically non-significant on the basis of $p > 0.05$ as per one-way ANOVA).....	128
Figure 5-14.(a): Relationship between enzyme concentration ($\mu\text{g/mL}$) and corresponding enzymatic activity ($\Delta A/\text{min}$). (b): Calibration curve of lysozyme based on turbidimetric assay (Linearity between enzyme concentration and corresponding enzymatic activity in the concentration range of 5-80 $\mu\text{g/mL}$)	130
Figure 5-15. Standard kinetic curves using turbidimetric assay. The enzymatic activity is high initially which slowly declines with the passage of time. The calibration curve was constructed after 1 st minute.	131
Figure 5-16. Calibration curve of lysozyme based on RP-HPLC	132

List of Tables

Table 1-1. Compiled research investigations for numerous active loaded protein nanoparticles	5
Table 3-1. Summary of the GC chromatographic conditions.....	34
Table 3-2. Relationship between attenuator index and transmission value [141]	40
Table 3-3. Mean size and size distribution of DIC-crosslinked GNPs crosslinked at different concentrations of crosslinker (DIC) at room temperature. (Crosslinking time: 24 - 48 h).....	41
Table 3-4. Relationship between mean particle size, size distribution and attenuator index of ZetaSizer at two concentrations of DIC. The attenuator index range (6-9) is an indicator of enough concentration of stable crosslinked GNPs due to sufficient crosslinking.	43
Table 3-5. Relationship between particle size and attenuator index of DLS machine for DIC concentration of 15 mg/mL at different crosslinking times at room temperature, 30°C and 50°C. The attenuator index range (6-9) is an indicator of enough concentration of stably crosslinked GNPs in aqueous medium due to sufficient crosslinking.	45
Table 3-6. Summary of the optimum crosslinking times of DIC-crosslinked GNPs at different crosslinker concentration and temperatures.	46
Table 3-7. Relationship between bloom number and molecular mass [139].	48
Table 3-8. Relationship between mean particle size/size distribution of DIC-crosslinked type A GNPs of different blooms and attenuator index. The crosslinker concentration was 15 mg/mL at room temperature. The attenuator indices (6-9) is an indicator enough nanoparticles concentration of stable crosslinked GNPs in aqueous media due to sufficient crosslinking. ..	50
Table 3-9. Effect of gelatin type, bloom number and concentration on particle size and size distribution. All samples were measured in acetone as dispersion medium before particles purification and diluted 10 times with acetone before DLS analysis.....	52

Table 3-10. Effect of gelatin type, bloom number and concentration on mean particle size and size distribution. All samples were measured in water as dispersion medium before particles purification and diluted 10 times with water before DLS measurements.	53
Table 3-11. Relationship between crosslinker amounts (mg) used initially for crosslinking and amounts of DIC consumed in crosslinking of GNPs	59
Table 3-12. Size characterization of DIC crosslinked Type-B GNPs purified <i>via</i> tangential flow filtration (TFF)	66
Table 4-1. Effect of centrifugation speed and time on mean size and size distribution. (*) Particles were centrifuged once.....	83
Table 4-2. Impurities of DIC crosslinked GNPs	84
Table 4-3. IR absorptions bands of gelatin and corresponding vibrational frequencies and functional groups.....	88
Table 4-4. Comparison of TFF and dialysis in terms of removal of poloxamer 188, DIC and DIU from crude nanosuspension of DIC-crosslinked GNPs.....	89
Table 4-5. Size characterization of DIC-crosslinked GNPs purified via different purification techniques.....	92
Table 5-1. Mean sizes and size distribution of FITC-dextran loaded GNPs crosslinked with DIC used in a concentration of 15 mg/mL in nanosuspension.....	110
Table 5-2. Effect of lysozyme loading on mean size, size distribution and optimum crosslinking time (h) of DIC-crosslinked GNPs loaded with different amounts of lysozyme. The DIC concentration used for the crosslinking was 15 mg/mL.....	114
Table 5-3. Zeta potential profile of Lysozyme-loaded GNPs crosslinked with DIC at pH 6.	118
Table 5-4. Comparison of entrapment efficiencies of lysozyme-loaded GNPs with and without microfiltration using PTFE syringe filters (0.45 μ m pore size).	123
Table 5-5. Summary of the physicochemical properties of lysozyme-loaded GNPs crosslinked with diisopropylcarbodiimide (DIC concentration used for crosslinking: 15 mg/mL).....	125

Table 5-6. Comparison between lysozyme amounts analysed via bioassay and HPLC assay
..... 132

Abstract

For the delivery of hydrophilic macromolecules, a novel flexible, hydrophilic delivery system based on gelatin nanoparticles is developed. Stabilization of gelatin in water is addressed using an apolar zero length crosslinker, *i.e.*, diisopropylcarbodiimide (DIC). Crosslinking of GNPs with polar crosslinkers has certain limitations not only crosslinking gelatin nanoparticles but also the loaded proteins, which interfere not only in the release of cargo but also their biological activity. Therefore, we introduced a novel crosslinking approach termed as interfacial crosslinking with the application of DIC which specifically crosslink the colloidal interface and not diffusing into the interior of nanoparticle. In this context, critical process parameters involved in the crosslinking process have been investigated in order to obtain optimum preparation conditions.

The main challenge while formulating these surface crosslinked gelatin nanoparticles (scGNPs) was purification. The centrifugation results in the formation of non-redispersible pellet. Therefore, we optimized tangential flow filtration as a promising alternative purification tool.

For the final proof of our hypothesis that the hydrophobic crosslinker crosslink only the colloidal interface of GNPs without crosslinking the loaded protein, the surface crosslinked GNPs were loaded with a model hydrophilic protein, *i.e.*, lysozyme. This proved scGNPs as a flexible delivery system for protein-based drugs.

Zusammenfassung

Gelatine-Nanopartikel haben sich als eines der geeignetsten Wirkstoffträgersysteme für hydrophile Makromoleküle erwiesen, insbesondere für Therapeutika auf Proteinbasis. Während der Formulierung ist die Vernetzung von Gelatine-Nanopartikeln (GNPs) ein unvermeidlicher Stabilisierungsschritt, der mit unerwünschten Konsequenzen einhergeht, die die GNPs zu einem weniger flexiblen Trägersystem für proteinbasierte Moleküle machen. Wasserlösliche Quervernetzer verknüpfen nicht nur die Gelatine, sondern auch die enthaltenen Biologicals. Dies beeinflusst nicht nur ihre Freisetzung *in vivo*, sondern führt auch zum Verlust der biologischen Aktivität. Im Rahmen dieser Arbeit wurde ein Ansatz zur Vermeidung dieser unspezifischen Reaktion untersucht. Es wurde eine alternative Stabilisierungsstrategie eingeführt: die Grenzflächenvernetzung unter Verwendung des apolaren Quervernetzers Diisopropylcarbodiimid (DIC). Ziel war es, GNPs zu entwickeln, die nur an ihrer Oberfläche vernetzt sind. In diesem Zusammenhang wurden verschiedene am Vernetzungsprozess beteiligte Prozessparameter untersucht, um optimale Herstellungs- und Reaktionsbedingungen zu finden.

Eine Hauptherausforderung bestand in der Aufreinigung der stabilisierten Partikel. Zentrifugation resultierte in einem nicht aufschüttelbaren Pellet weswegen die Tangentialflussfiltration (TFF) etabliert werden konnte.

Das System konnte erfolgreich mit dem hydrophilen Modellprotein Lysozym beladen werden ohne die Aktivität zu kompromittieren.

1 Background and Literature Survey

1.1. Introduction

The field of molecular biotechnology with the help of latest technologies, such as, combinatorial chemistry and high-throughput screening, has produced a significant number of active pharmaceutical compounds (APIs). Majority of these APIs are hydrophilic macromolecules which are regarded as novel therapeutic compounds being used for the treatment of numerous major pathologies, such as cancer and cardiovascular disease. These macromolecular therapeutic compounds include recombinant proteins, antisense oligonucleotides, genes and small interfering RNAs [1]. Amongst these novel therapeutic compounds, protein-based active pharmaceutical ingredients are being predominantly utilized in clinics [2]. These hydrophilic proteinaceous compounds offer many advantages as compared to small molecules which include high potency, low unspecific binding, minimum toxicity and low probability of drug–drug interaction [3]. Their significance is, however, hampered by lack of effective, safe and specific delivery.

1.2. Delivery challenges of macromolecules

The delivery of these macromolecules to the desired site of action is affected by certain obstacles which, consequently, lead to a low biological half-life at the desired site of action. These obstacles decrease the therapeutic potential and clinical applications of these potent therapeutic compounds. Some of the major obstacles associated to delivery of these compounds are structure instability, short *in vivo* half-life due to extensive first-pass metabolism as well as the phagocytic metabolism and low permeability across biological membranes [3-5]. Some of the important challenges associated with delivery of macromolecular drugs have been elaborated in Figure 1-1. Therefore, in order to achieve the highest therapeutic efficacy of macromolecules, appropriate and effective delivery systems are needed.

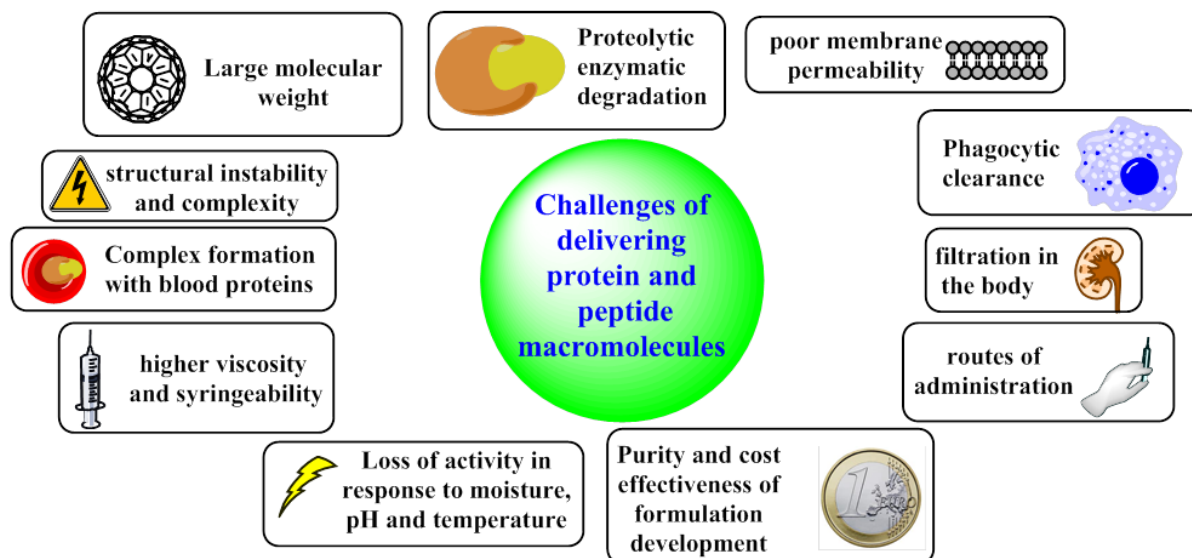


Figure 1-1. Challenges of macromolecular drug delivery (adapted from Agrahari V *et al.* (2016) [2]).

1.3. Nanoparticle-based delivery of hydrophilic macromolecules

For the effective treatment of human illnesses, the delivery of therapeutic proteins specifically to the diseased sites is a rate limiting factor [2]. The conventional administration of these compounds require comparatively high dose due to non-specific bio-distribution and fast metabolism of free drugs before reaching to their targeted sites. To overcome these challenges, nanoparticulate delivery systems have been demonstrated as a promising alternative for the delivery of macromolecules, peptides and nucleic acid-based molecules [6, 7]. The nano-size dimension of these particle systems enhance the intracellular uptake as compared to larger carriers [8, 9]. Besides, these nanoparticulate formulations offer advantages over conventional drug delivery systems. These include higher bioavailability at the target site due to enhanced solubility of low solubility drugs [10-14], reducing the side effects of chemotherapeutic drugs due to a localization at the site of action by the enhanced permeability and retention (EPR) effect [15] and controlling the release of drug and enhancement of permeation of drugs across the cell membrane [16]. However, these

nanomaterials are mostly composed of hydrophobic polymers, which possess some demerits. They may cause unfolding and hence inactivation of protein-based hydrophilic macromolecules [17-19]. Furthermore, they also have low encapsulation potential for the hydrophilic protein based drugs [20, 21]. Due to this fact, water soluble polymers of natural origin have always been under investigations as a delivery vehicle for these sensitive macromolecular drugs [22, 23]. Different types of biopolymeric materials including polysaccharides (*e.g.*, chitosan, dextran), and proteins (*e.g.*, albumins, gelatin, gliadin, zein, soy protein, etc.) have been investigated as a constitutive materials of these nanoparticles. The selection criteria of appropriate nanoparticle materials depends on several factors including (a) the desired size of nanoparticles (b) the physicochemical properties of drug, *e.g.*, aqueous solubility and stability (c) desired drug release profile (d) surface charge (e) immunogenicity and toxicity of the final product and (f) biodegradability and biocompatibility of the fabricated nanomaterials [24]. In recent years, the protein-based biopolymeric nanoparticles have offered numerous advantages due to some desirable attributes such as low toxicity and biodegradability [25]. They have been exploited both for pharmaceutical as well as nutraceutical delivery [26].

1.4. Proteins as a construction material for nanoparticles

Protein-based nanomaterials possess excellent biocompatibility and biodegradability [27]. Nanoparticles formulated from proteins are biodegradable, metabolizable, and provide excellent opportunities for surface modification by attaching different targeting ligands [28]. They can be prepared from both water soluble proteins (*e.g.*, bovine and human serum albumin) and water insoluble protein (*e.g.*, gliadin, zein) [29, 30].

Albumins and gelatins were the first naturally occurring proteins from which protein nanoparticles were fabricated [31-33]. The albumin- and gelatin-derived colloidal systems are promising due to biodegradability, low immunogenicity [34] and non-toxicity. They show

high stability in biological environment [35]. Various nanoparticle formulations prepared from proteins have been displayed in Table 1-1.

Table 1-1. Compiled research investigations for numerous active loaded protein nanoparticles

Proteins	Source	Delivery system	Reference
Albumin	bovine serum human serum	nanospheres and nanocapsules	[36-39]
Gelatin	Animal bones and skin	microspheres and nanoparticles.	[25]
Gliadin and Legumin	Gliadin: wheat gluten Legumin: pea seeds	oral and topical drug systems. Used in the mucoadhesive formulations	[29, 40]
Elastin	Connective tissue	Nanoparticles	[41]
Zein	Maiz (corn)	Nanoparticles formed from zein proteins to encapsulate bioactive compound (<i>e.g.</i> , coumarin, 5-fluorouracil).	[30, 42, 43]
B-lactoglobulin & Casein	Milk		[44]
Soy Proteins	Soybeans		[45, 46]

1.5. Gelatin as a construction material for delivery systems

Gelatin is a hydrophilic bio-macromolecular polymer which is obtained from collagens of mammals, *e.g.* bovine and porcine sources. Besides, gelatin from fish and marine sources has also been used [47-49]. It is isolated after denaturation of collagen using partial acidic or alkaline hydrolysis. It has widespread applications in pharmaceuticals, cosmetics and food industry with high level of safety. Due to its biodegradability and biocompatibility, it is generally regarded as safe (GRAS) material by the United States Food and Drug Administration (FDA) [50-52]. It possesses a highly heterogeneous molecular weight distribution consisting of mixture of water-soluble protein fragments of different molecular masses. There are two types of gelatin, *i.e.*, type A and type B. Type A gelatin is manufactured from porcine skins after its acidic treatment. This acidic treatment does not cleave the amide bonds of asparagine and glutamine residues of the collagen. This leads to a higher isoelectric

point (IEP), *i.e.*, 7-9 [53]. On the other hand, gelatin B is obtained from bovine hides and skin with alkaline treatment. This alkaline treatment cleaves the amide bonds of asparagine and glutamine to aspartate and glutamate, respectively. The production of higher amounts of acidic amino acids leads to a greater proportion of carboxylic groups which make type B gelatin as negatively charged protein at neutral pH. Consequently, this leads to lowering of IEP (*i.e.*, 4.5–6.0) [54]. In the field of drug delivery, gelatin has been exploited as a fabrication material for different delivery systems [55] which include hydrogels [56], films [57], microcapsules [58] and nanoparticles [59, 60].

1.5.1. Gelatin nanoparticles as a carrier for hydrophilic macromolecules

Gelatin nanoparticles (GNPs) have been repeatedly reported in the literature as carrier system for a wide range of therapeutic compounds. These include peptide-, non-peptide- and gene-based therapeutic compounds. Some of the non-peptide-based compounds include paclitaxel [61], pilocarpine [62], amphotericin B [63], FITC-dextran [64], methotrexate [65], cytarabine [66], hydrocortisone [62], doxorubicin [67-69], didanosine [70], sulphamethaxazole [71], cyclosporine [72], rosiglitazone [73] and cycloheximide [74].

GNPs have been exploited as an excellent delivery platform for a variety of protein- and peptide-based drugs. Some researchers have reported bovine serum albumin as a model proteinaceous cargo for GNPs without causing any physicochemical instability to protein primary structure [75]. In another attempt, a composite delivery system composed of BSA-loaded GNPs which were subsequently microencapsulated in poly (lactic-co-glycolic acid) microspheres. This composite architecture was found promising in terms of maintaining a sustained release pattern and the ability to prevent the denaturation of protein [76]. In another study, FITC-BSA was encapsulated in recombinant human gelatin (rHG) nanoparticles which showed safety, sustained release and lower degree of initial burst release [77]. Some other examples of proteins encapsulation in GNPs are angiogenic basic fibroblast growth factor

(bFGF) [77], insulin [78], alkaline phosphatase (ALP) [79], tissue-type plasminogen activator (t-PA) [80, 81] and bone morphogenetic protein-2 (BMP-2). All these formulations utilizing GNPs as a carrier system for different proteins retained the *in vitro* biological activity of the encapsulated protein-based drugs.

The GNPs have also been proven as a promising carrier system in immunotherapy. It has been reported that GNPs are effectively and significantly up-taken by murine bone marrow dendritic cells (DCs) and therefore, they are intended for targeting antigens to dendritic cells, hence acting as an immunoadjuvant [26]. Following the subcutaneous administration of tetanus toxoid (TT)-encapsulated GNPs in BALB/c mice, the systemic immune response was effectively stimulated. This was confirmed by a comparable amount of IgG production in the mice blood circulation. In contrast to conventional alum-TT vaccine, the cytokine response expressed in terms of IL-2 and IFN γ level was significantly higher [82]. After uptake by antigen presenting cells (APC), these TT vaccine-loaded GNPs are digested by enzymes present in the lysosomal compartment (*e.g.*, collagenase) thus releasing the tetanus toxoid payload intracellularly. Another advantage is that GNPs can be loaded with a large amount of antigens, therefore, leading to an antigen specific immunological response.

The first gelatin nanoparticulate-based formulation was carried out by C. Oppenheim *et al.*, employing coacervation-phase separation using sodium sulphate as a coacervating agent [33]. It was observed that the gelatin nanodispersion system obtained with simple coacervation possess broader size distribution and colloidal instability. Since then, various formulation approaches have been adopted depending upon the intended application in order to get physicochemically stable colloidal gelatin particles. The drug substances can be loaded to these nanocarriers either prior to nanoparticle formation via incorporation to gelatin aqueous solution or by post-nanoparticle formation via electrostatic adsorption. The former method has been found to be more effective in terms of encapsulation efficiency. Since, gelatin nanoparticles have multiple functional groups due to its proteinaceous nature which provides

excellent opportunities for modification, *e.g.*, attachment of targeting-ligands and crosslinkers [83-85]. There are numerous formulation methods which have been reported so far for the preparation of gelatin nanoparticles. Some of the commonly used methods are elaborated as following.

1.5.1.1. Formulation methods of GNPs

Coacervation-phase separation

In coacervation-phase separation, nanoparticles are formed as a result of liquid-liquid phase separation from a homogeneous solution of charged macromolecules. In fact, two distinguishable phases are formed. The polymer rich, dense phase (coacervate phase), tends to sediment at the bottom and a relatively transparent layer in the supernatant layer [86]. The phase separation is initiated following the addition of salt, *e.g.*, sodium sulphate to aqueous gelatin solution containing surfactant, *e.g.*, tween 20 followed by addition of isopropanol to dissolve the precipitate by sodium sulphate. Subsequently, the sub-microparticles are crosslinked by the addition of glutaraldehyde. This leads to formation of gelatin particles in the size range of 600 to 1000 nm [86].

Emulsification-solvent evaporation

In this approach, an aqueous phase containing gelatin and drug is emulsified with organic or oil phase, *e.g.*, polymethylmethacrylate [65, 66] or paraffin oil [87] forming an water-in-oil emulsion system (w/o) accompanied by vigorous shaking. Afterwards, the emulsion system consisting of gelatin nano-droplets as a dispersed phase is crosslinked after addition of glutaraldehyde [65] or genipin [87]. Finally, the dispersion medium (organic phase) is evaporated leaving behind GNPs (100 to 400 nm) [65].

Reverse Phase Preparation Technique

Reverse phase involves the formation of gelatin nanoparticles after encapsulation of gelatin aqueous solution inside the core of reverse micellar droplets made by surfactant bis (2-ethylhexyl sulphosuccinate) in n-hexane [88]. Subsequently, the entrapped gelatin aqueous solution is crosslinked with a crosslinker. With this method, gelatin nanoparticles in the range of 40 nm can be formulated [88].

Inverse Mini-emulsion Technique

Inverse mini-emulsions approach is characterized by the formation of gelatin nanoparticles employing two inverse mini-emulsion systems, *i.e.*, mini-emulsion A and mini-emulsion B. Emulsion A consists of gelatin droplets in *p*-Xylene stabilized by tween 80 as an emulsifier. Emulsion B is obtained after emulsification of the aqueous phase of crosslinker agents, *e.g.*, glutaraldehyde or carbodiimide/*N*-hydroxysuccinimide (CDI/NHS) in *p*-xylene as dispersion medium. Both types of crude emulsions are sonicated to get a homogeneous dispersion system. Subsequently, both crude emulsions are mixed together in an ice bath with continuous sonication. This leads to fusion of the droplets thus forming crosslinked gelatin nanoparticles. The working principal of the inverse mini-emulsion is fusion and fission which is responsible for the formation of nanoparticles [89-91]. With this technique, GNPs in the size range of 150-200 nm can be produced with a relatively broad size distribution [91].

Desolvation Technique

In the desolvation technique, the gelatin solution is dehydrated following the addition of a dehydrating agent, *e.g.*, alcohol or acetone to an aqueous gelatin solution. Desolvation involves transition from stretched conformation to coil conformation. Afterwards, crosslinkers are added to gelatin nanoparticles for stabilization [92, 93]. The main disadvantage of this technique is that it leads to formation of large particles with in-homogeneous size distribution

due to heterogeneity in molecular weight of gelatin. In order to solve this problem, two-step desolvation was introduced by Coester *et al.*, [26]. With two step-desolvation, smaller nanoparticles with a narrower distribution are obtained. In two step desolvation, the high molecular weight gelatin fragments are extracted in the first desolvation step from low molecular weight gelatin. Then, the high molecular weight gelatin is re-dissolved and desolvated again. With two-step desolvation, GNPs with a size of 100-300 nm are obtained [94, 95].

Nanoprecipitation Technique

The nanoprecipitation technique is also known as solvent displacement technique. It involves two miscible solvents; the solvent phase in which the polymer is soluble and the non-solvent phase in which the polymer is not soluble containing poloxamer as a stabilizer. While producing gelatin nanoparticles via nanoprecipitation, gelatin is dissolved in water and is then slowly added to an organic solvent, *e.g.*, methanol, ethanol, acetone or acetonitrile which act as non-solvent containing poloxamer as a stabilizer. Due to instantaneous diffusion of the solvent phase into the non-solvent phase, interfacial turbulences are created which forms nanodroplets at the interface. Finally, the gelatin polymer precipitates within these droplets which ultimately lead to formation of nanoparticles. Subsequently, glutaraldehyde is added to crosslink the nanoparticles [96, 97]. Nanoprecipitation has many advantages. It is a rapid, straightforward and easy to perform technique. It enables the production of nanoparticles in the size range of 250-350 nm with narrow unimodal distribution [98]. Nanoprecipitation does not involve shear forces, sonication or very high temperatures, which could inactivate the API and it does not involve the formation of oily–aqueous interfaces also known to impair protein drug functionality [99]. These interfaces are known to interfere with the three dimensional (3-D) structure and function of encapsulated proteins ultimately leading to loss of intended activity [99-101].

It is evident that the physicochemical stabilization via chemical crosslinking is common to all the above mentioned production methods. It is because the un-crosslinked GNPs are readily dissolved on contact with hydrophilic environment.

1.5.2. Crosslinking of gelatin nanoparticles

Due to hydrophilicity, gelatin-based delivery systems dissolve in aqueous environment and thus cannot maintain its structural integrity without crosslinking. Therefore, crosslinking of gelatin nanoparticles is indispensable in order to get mechanical stability in aqueous environment, shape and enhanced *in vivo* circulation time [50, 93]. The un-crosslinked GNPs have been found to be unstable and consequently, they tend to dissolve in the aqueous media with the passage of time [102]. Different methods to crosslink GNPs have been reported and are described in the following.

1.5.2.1. Aldehydes

The literature survey shows that glyoxal-induced crosslinked GNPs exhibits an instantaneous mass aggregation which results in precipitation of nanoparticles [103]. Therefore, in order to avoid these instabilities, researchers have demonstrated glutaraldehyde as an alternative effective crosslinker for stabilization of GNPs [64, 67]. The GNPs crosslinked with glutaraldehyde show stability for more than 10 months at 2–8 °C. Glutaraldehyde is a homo-bifunctional crosslinker forming poly- or bi-functional crosslinks into the protein network by bonding free amino groups of lysine or hydroxylysine amino acids, known as Schiff's base [67, 104] (see Figure 1-2). As glutaraldehyde becomes a part of the crosslink, therefore, a very low amount remained unreacted, hence the residual crosslinker is removed following particle purification. In order to avoid the expected toxicity associated with glutaraldehyde, another aldehyde, D, L-glyceraldehyde is regarded as a non-toxic crosslinking agent. The D-enantiomer is normally metabolized in the body through glycolytic pathway following

phosphorylation by triokinase producing D-glyceraldehyde-3-phosphate. The metabolite, D-glyceraldehyde-3-phosphate, is an important intermediate of the glycolytic pathway. In the near past, the DL-glyceraldehyde induced crosslinked gelatin was recognized as a new material for pharmaceutical purposes [105]. In this connection, insulin-loaded GNPs crosslinked with DL-glyceraldehyde were synthesized being intended for pulmonary administration. After subcutaneous as well as intra-tracheal administration of nanoparticles into rats, no toxicity was observed [78]. Nevertheless, some level of toxicity has been reported in oral toxicology studies as well as skin dermatitis when used in skin applications. Therefore, it has always been a demand to use non-toxic crosslinking agents for stabilization of GNPs [106].

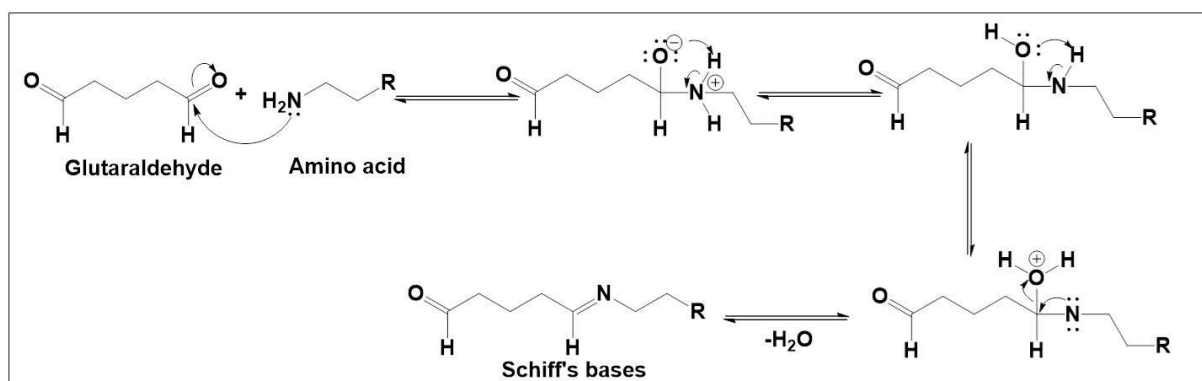


Figure 1-2. Mechanism of glutaraldehyde-based crosslinking of gelatin forming Schiff's bases within gelatin peptidal chains.

1.5.2.2. Genipin

In order to avoid the toxicities arising from glutaraldehyde, it has always been a topic to search for less toxic crosslinkers. One such example is genipin which is a natural crosslinker obtained from gardenia fruit. Genipin has been demonstrated to be 10,000 times less toxic than glutaraldehyde [107]. The crosslinking time with genipin is longer and the crosslinking involves the bond formation between two free amino groups of lysine residue on the protein molecule with one molecule of genipin [108]. One such example is the genipin-crosslinked rHG nanoparticles which showed an effective internalization into the cells without any

significant cytotoxicity [77]. The crosslinking reaction mechanism of genipin within the gelatin fragments can be schematically represented in Figure 1-3.

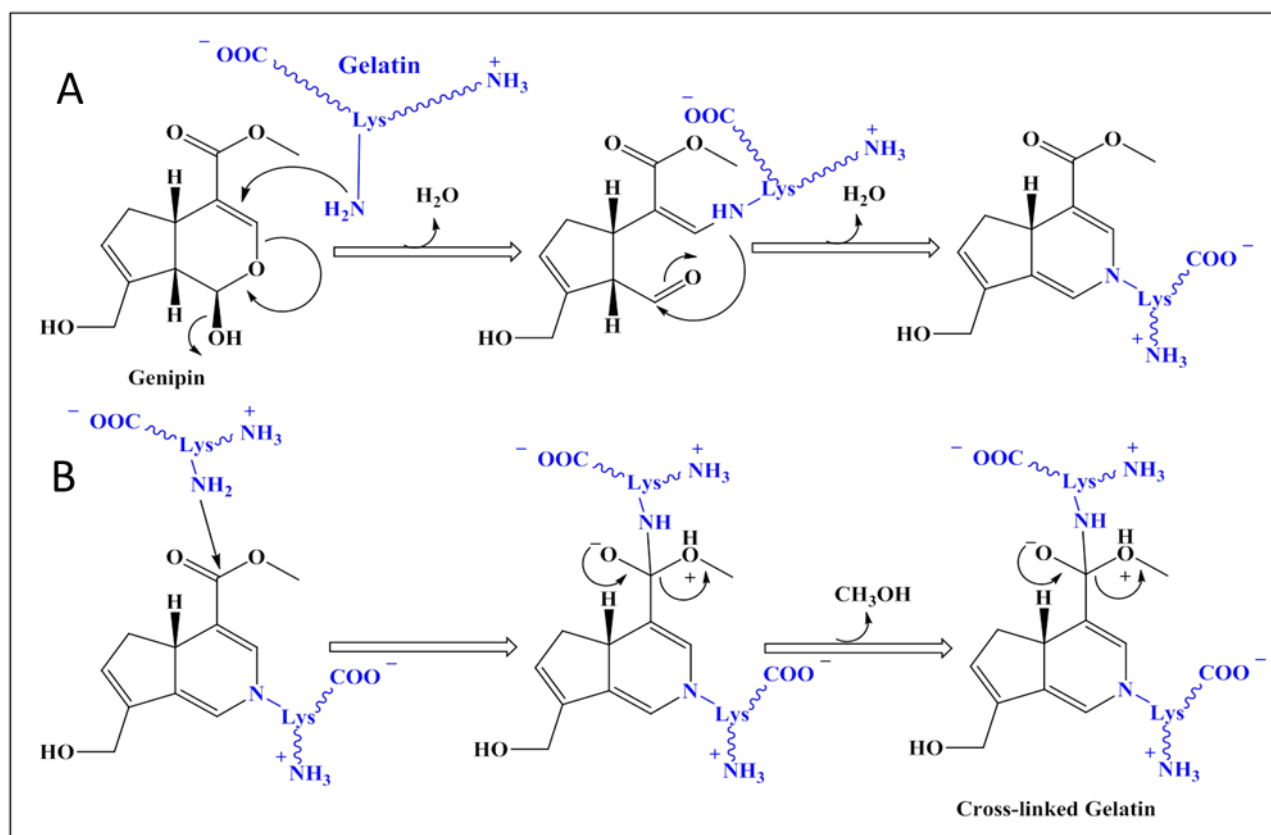


Figure 1-3. Mechanism of genipin induced crosslinking of gelatin. A. Fast nucleophilic attack of gelatin's L-lysine amino groups on the ring structure of genipin to form a stable transition intermediate product; and B. slower reaction with nucleophilic substitution of free lysine amino molecules of a second gelatin chain (Adapted from James B Rose *et al.* 2014 [109]).

1.5.2.3. Carbodiimide/*N*-hydroxysuccinimide (CDI/NHS)

A mixture of two water soluble carbodiimide, carbonyldiimidazole (CDI) and *N*-hydroxysuccinimide (NHS) was employed as crosslinking mixture for the stabilization of GNPs [110]. The crosslinking mechanism of this crosslinking mixture has been illustrated in Figure 1-4. As a result, nanoparticles with relatively smaller sizes and narrower size distribution with smoother morphology are obtained as compared to GNPs crosslinked with glutaraldehyde. In this research, paracetamol was used as a model drug. The drug entrapment as well as loading efficiencies were higher in the CDI/NHS crosslinked nanoparticles. The release kinetics profile was comparable to that of glutaraldehyde (GTA)-crosslinked

nanoparticles. Other physicochemical differences between glutaraldehyde-crosslinked GNPs and CDI/NHS are due to different chemistry of crosslink formation induced by the two crosslinkers [110].

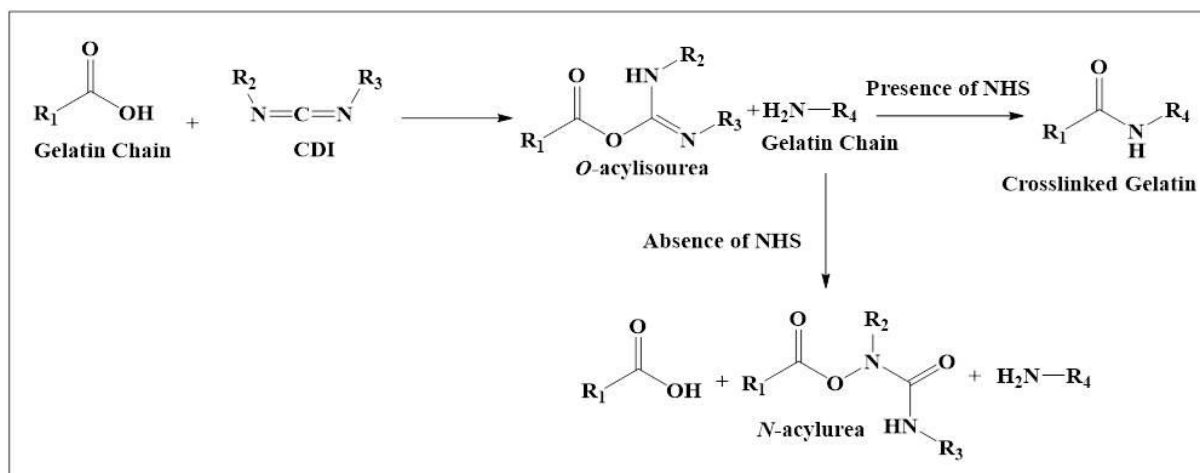


Figure 1-4. Mechanism of crosslinking caused by CDI/NHS crosslinkers (adapted from Qazvini *et al.*, 2011 [110]).

1.5.2.4. Microbial transglutaminase (MTG)

The enzyme-based crosslinking is a promising strategy owing to high specificity of the enzyme catalysis. This catalysis is controlled to a certain extent by changing pH and temperature [111]. The crosslinking of GNPs with recombinant microbial transglutaminase (MTG) was investigated by Fuchs *et al.*, [112]. The GNPs were formulated by a two-step desolvation technique using acetone as a desolvating agent followed by crosslinking with microbial transglutaminase. The MTG favours the formation of intra- and intermolecular isopeptide bonds within the protein networks by connecting the ϵ -amino groups of lysine with the amide group of glutamine. This enzyme-catalysed crosslinking reaction is accompanied by the elimination of ammonium ion (NH_4^+) as a by-product (see Figure 1-5). The optimum temperature for the MTG-catalysed crosslinking reactions was observed to be at 25 °C at a neutral pH using an ion-free solvent. With this approach, GNPs with a mean size below 250 nm and narrow size distribution were produced successfully [112].

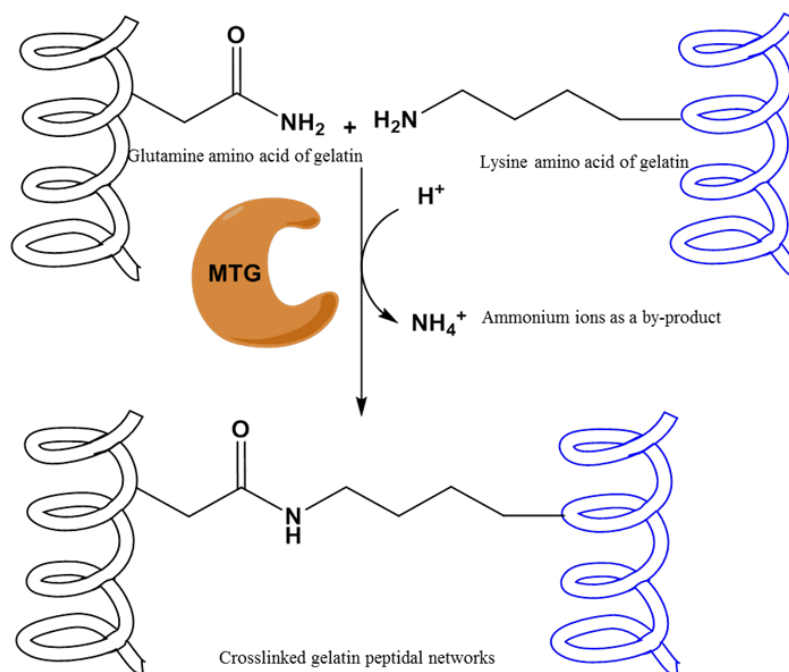


Figure 1-5. Microbial transglutaminase catalysed crosslinking reaction in gelatin nanoparticles. This involves the conjugation of primary amino groups of glutamine and lysine. During this crosslinking, one mole of ammonium is produced (adapted from S. Fuchs *et al.*, (2010) [112]).

1.5.3. Purification methods of nanoparticles

After preparation of nanoparticles, purification is a necessary step to remove the toxic unwanted substances present in the crude nano-dispersion systems. These include chemical initiators, crosslinkers, excessive amounts of stabilizers and un-encapsulated APIs. Purified nanoparticles also minimize the variability in biological applications. The characteristic features of an effective and efficient purification procedure is that it should remove satisfactorily all the above mentioned impurities from the nanoparticles suspensions without influencing the physicochemical properties of nanoparticles such as size, shape and surface charge.

Some of the reported purification methods are: size exclusion chromatography [113], size selective precipitation [114], magnetic field flow fractionation filtration [115], cross-flow filtration [116], electrophoresis [117], density gradient centrifugation [118] and centrifugation

[119]. Gel filtration chromatography, ultra-filtration and centrifugation are most commonly reported purification methods for polymeric nanoparticles. The main disadvantage of these methods is the problem of scale up of these methods. On the other hand, ultra-filtration-based purification can be automated and hence cost effective for industrial purposes.

1.5.3.1. Centrifugation based purification

Large amounts of impurities can be removed from the nanodispersion system using centrifugation followed by re-dispersion in water. This is a straightforward method, but sometimes it leads to formation of non-dispersible aggregates of nanoparticles. Another disadvantage is the low yield of nanoparticles due to loss of finer nanoparticles in the supernatant [120]. Therefore, centrifugation is applicable to purification of nanoparticles on laboratory scale, but is not applicable to for industry applications [120].

1.5.3.2. Tangential flow filtration

Tangential flow filtration (TFF) also known as crossflow filtration, has been frequently reported for the purification of proteins [121]. Since the size dimensions of nanoparticles are almost in the same range as proteins, therefore TFF-based ultrafiltration can also be employed effectively for the purification of nanoparticles [116, 120]. The difference between normal or dead-end) flow filtration and tangential flow filtration is the direction of the flow (see Figure 1-6). By pumping the feed tangentially along the membrane, the pressure which is built up due to particles on the membrane that can pose a problem in normal flow filtration, is minimized. Particles that are too large to pass the membrane are swept along, instead of accumulating at the membrane surface.

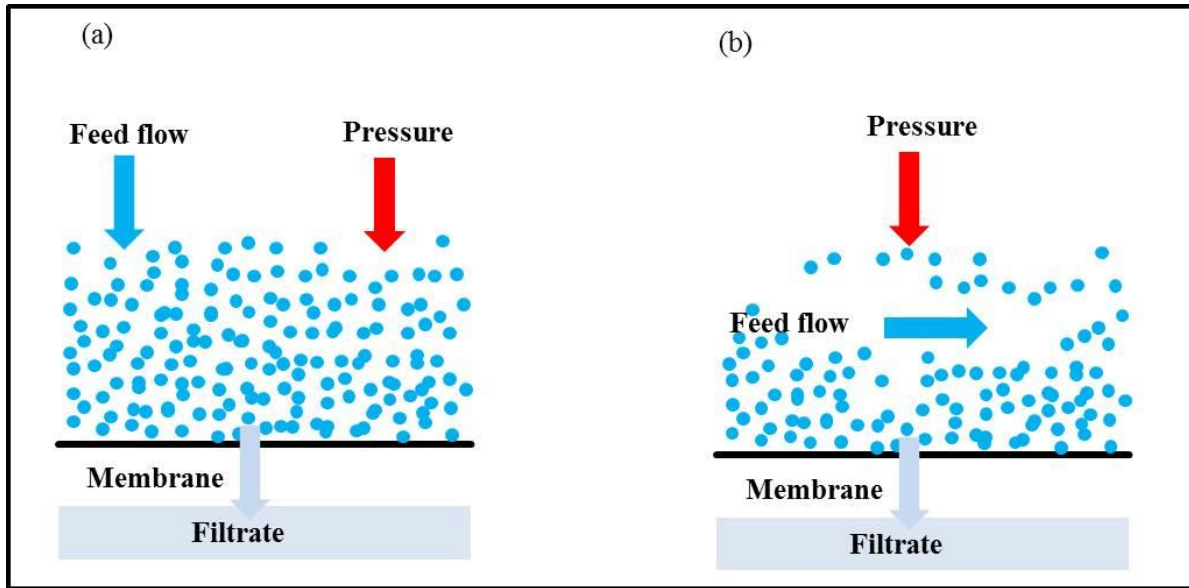


Figure 1-6. Comparison between (a) dead-end or normal flow filtration and (b) tangential flow filtration.

During cross-flow filtration, the starting particles suspensions known as feed will be divided into two solutions, the retentate and the filtrate. The retentate (also known as concentrate) is composed of particles which are too large to pass through the membrane and therefore are retained. In normal flow filtration, the retentate consists only of large particles, but because of the tangential flow, some solute and small molecules will be pushed past the membrane, and make the retentate a concentrated one. The retentate can be either collected in a separate vessel, or returned to the feed vessel. The solutions passing through the membrane is called as filtrate or permeate, as the membrane is permeable for it (see Figure 1-7). Tangential flow filtration can be performed in either concentration or diafiltration mode (Figure 1-7). In concentration mode, the feed volume is reduced by filtration, and thereby the particle concentration increased. On the other hand, during diafiltration, the suspension volume is kept constant by adding new buffer as filtrate is removed. By doing so, buffer exchange is possible. As the buffer is exchanged, all undesired species that were dissolved in it, will be removed. This is why filtration is a potentially good method for purification of nanoparticles. In this

thesis, the tangential flow filtration has been optimized for the purification of crosslinked gelatin nanoparticles.

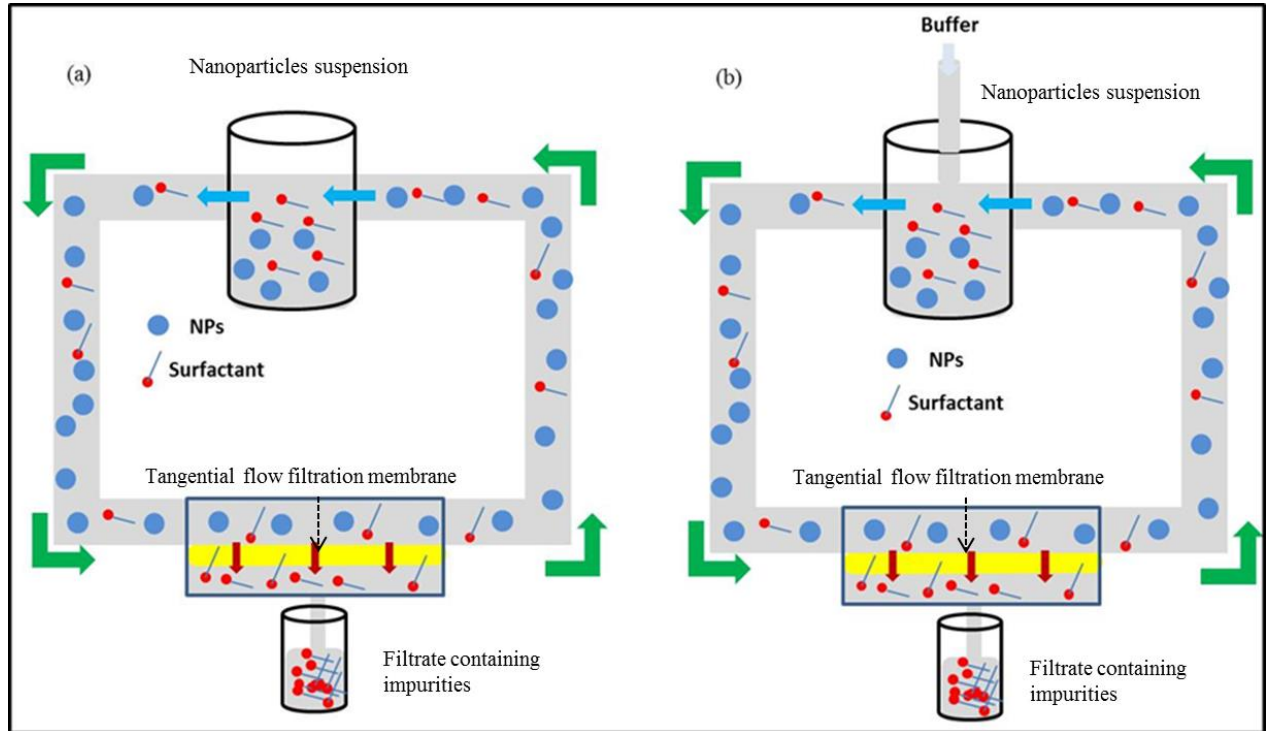


Figure 1-7. TFF-based ultra-filtration in (a) concentration mode and (b) diafiltration mode.

2 Aim and Scope of the Thesis

The aim of this thesis can be divided in three work packages. In the following diagram, these work packages are briefly summarized.

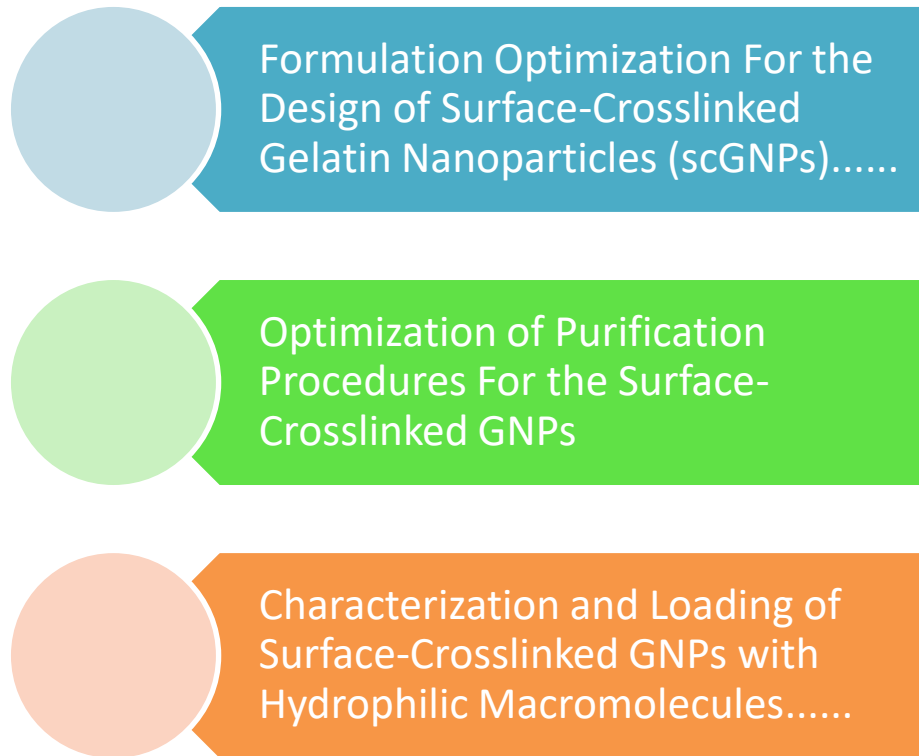


Figure 2-1. Summary of the work packages addressed in the present thesis.

2.1. Formulation optimization for the design of surface-crosslinked gelatin nanoparticles (scGNPs)

Majority of the hydrophilic macromolecules are proteins in nature, therefore, the nanoparticulate-based formulation should guarantee the maximum physicochemical stability as well as biological activity of the encapsulated macromolecular compound. In most of preparation techniques for gelatin nanoparticles reported so far, the stabilization with hydrophilic crosslinker is common. These hydrophilic crosslinkers, *e.g.*, glutaraldehyde, glyoxal, genipin, enzymatic crosslinking, *etc.*, are mostly used to gain mechanical stability in aqueous environment. The demerit of hydrophilic crosslinkers is that due to their non-specific

crosslinking of the gelatin networks with the loaded cargo, they cause interference in the release of loaded hydrophilic drug from the gelatin matrix [122]. Therefore, the core objective was to physicochemically stabilize the gelatin nanoparticles, using zero-length hydrophobic crosslinker, diisopropylcarbodiimide (DIC). The idea is to avoid diffusion of crosslinker into the hydrophilic interior of nanoparticles. This will provide an opportunity to encapsulate protein-based drugs. In this context, the formation of gelatin nanoparticles using both gelatin A and B was carried out using nanoprecipitation technique followed by crosslinking with a hydrophobic zero-length crosslinker to obtain surface crosslinked gelatin nanoparticles that are stable in aqueous environment. The hypothesis of the surface crosslinking caused by zero length hydrophobic crosslinker, *i.e.*, diisopropylcarbodiimide was investigated in terms of both direct measurements as well as indirect measurements. The direct measurements are concerned about the evaluation of crosslinking degree of crosslinked GNPs using TNBS assay to quantify the un-crosslinked primary amino groups in gelatin matrix after crosslinking GNPs with diisopropylcarbodiimide. On the other hand, the indirect measurements involve the determination of residual amounts of the crosslinker (DIC) remained unreacted in the crosslinking of GNPs and the amounts of crosslinking by-product of this crosslinker, *i.e.*, diisopropylurea formed in the mixture after completion of crosslinking reaction. For these investigations, validated methods of gas chromatography and proton NMR spectroscopy were employed.

To get a stable formulation, some critical parameters were investigated such as optimum crosslinker concentration, optimum crosslinking time and crosslinking reaction temperature with regard to the effect on particle size, size distribution and zeta potential of gelatin nanoparticles.

2.2. Optimization of purification procedures for the surface-crosslinked GNPs

After establishing a validated formulation composed of DIC-surface crosslinked GNPs following the standard formulation optimized in work package 1, the next step was the purification of these novel gelatin-based nanocarriers systems from hazardous impurities, *e.g.*, unreacted crosslinker, *i.e.*, diisopropylcarbodiimide, its by product known as diisopropyl urea (DIU) and the stabilizer (Poloxamer 188). Centrifugation is the most frequently used purification tool for nanoparticles. However, in some situations, centrifugation results in the formation of a hard pellet which cannot be easily re-dispersed in water. This phenomenon is mostly observed when the organic solvents (*e.g.*, acetone, alcohol) are the dispersion phases of polymeric nanoparticles. In our scenario, the DIC-crosslinked GNPs are also non-dispersible in water following centrifugation because of dispersion medium which is predominantly acetone.

Therefore, in order to avoid the formation of non-dispersible pellet and to avoid particle loss as well, we evaluated and optimized the performance of tangential flow filtration (TFF) for the purification of DIC surface-crosslinked gelatin nanoparticles and compared the results with dialysis and centrifugation. During the optimization of TFF-based purification, the influence of different process parameters, *e.g.*, membrane type, pore size and amount of recirculating water on physicochemical properties of DIC-crosslinked GNPs was evaluated. Besides, the effectiveness of TFF-based purification in terms of removal of aforementioned hazardous impurities from the DIC-crosslinked GNPs suspensions was also focussed in this chapter.

2.3. Characterization and loading of surface-crosslinked GNPs with hydrophilic macromolecules

This work package is mainly focused on the provision of more experimental evidences in order to prove the working hypothesis of surface-crosslinking. This would be possible in terms of loading these surface crosslinked gelatin nanocarriers with a model hydrophilic therapeutic protein-based payload. For this purpose, lysozyme was selected as model protein in the present study. The main aim of this investigation was the evaluation of crosslinkability of loaded protein-based cargo (*i.e.*, lysozyme) with the nanoparticulate matrix composed of gelatin. The hypothesis was characterized in terms of recovery of encapsulated lysozyme after performing *in vitro* release experiment and also monitoring the biological activity of loaded lysozyme. For comparison, the glutaraldehyde crosslinked GNPs loaded with similar amount of lysozyme were also evaluated for *in vitro* release extent and biological activity of the released lysozyme. So, in both types of crosslinked GNPs, *i.e.*, glutaraldehyde and DIC-crosslinked GNPs, the biological activity of loaded lysozyme was evaluated after releasing the lysozyme in phosphate buffer saline (PBS) to make sure whether the polypeptide after undergoing a few formulation steps, *i.e.*, co-precipitation with gelatin, nanoencapsulation in GNPs and crosslinking with DIC and glutaraldehyde, retains its intended biological activity or not. Besides, a non-peptide based hydrophilic macromolecular cargo, *i.e.*, FITC dextran was also loaded into these DIC-surface crosslinked GNPs to investigate the *in vitro* release kinetics pattern of non-peptidal hydrophilic macromolecular drugs from these novel types of surface-crosslinked GNPs and subsequently comparing with glutaraldehyde-crosslinked GNPs.

3 Formulation Optimization for the Design of Surface-Crosslinked Gelatin Nanoparticles (scGNPs)

Parts of this chapter have been published in:

Abdul Baseer, Aljoscha Koenneke, Joseph Zapp, Saeed A. Khan, Marc Schneider, Design and Characterization of Surface Crosslinked Gelatin Nanoparticles for the Delivery of Hydrophilic Macromolecular Drugs. *Macromolecular Chemistry and Physics*. 2019. **220**(18): p. 1900260.

3.1. Abstract

This chapter is focused on the formulation development of surface-crosslinked gelatin nanoparticles thus providing a flexible hydrophilic nano-delivery platform for both peptide- and non-peptide-based hydrophilic macromolecular drugs. The physicochemical stabilization of gelatin nanoparticles is achieved while employing the zero-length hydrophobic crosslinker, diisopropylcarbodiimide. The basic idea is that the hydrophobic crosslinker cannot diffuse into the interior of the nanoparticle due to its apolar nature rather than it would establish the crosslinks on the surface of nanoparticles after conjugating primary amino groups of lysine and hydroxy-lysine with the carboxylic acid groups of aspartate and glutamate residues of the gelatin matrix. So far, we have developed a new methodology for the physicochemical stabilization of gelatin nanoparticles through a selective and diffusion limited crosslinking process using diisopropylcarbodiimide as a crosslinker. The formation of GNPs was carried out following the standard protocols of nanoprecipitation. Subsequently, the crosslinker diisopropylcarbodiimide was added to the nanosuspension followed by overnight (20-24 h) mixing to favour crosslink formation in gelatin nanoparticles. The crosslinking process was optimized both for type A and type B gelatin with different bloom numbers and concentrations and its possible impact on the physicochemical properties of gelatin nanoparticles. The gelatin nanoparticles fabricated from type B gelatin possess mean sizes of 200 - 300 nm and a narrow size distribution ($PDI < 0.2$). On the other hand, type A gelatin leads to formation of surface-crosslinked nanoparticles which possess mean sizes of 200 – 500 nm ($PDI < 0.2$) depending upon the bloom number and the concentration of gelatin used. To assure the biocompatibility, cytotoxicity against A549 cells was conducted which indicated no significant toxicity up to 1 mg/mL.

3.2. Introduction

Until now, different formulation approaches have been adopted for the design of gelatin nanoparticles. These methods have been discussed in chapter 1 in section 1.5.1.1. Since, gelatin is a hydrophilic biopolymer; therefore, on contact with aqueous environment, these gelatin nanoparticulates cannot maintain their mechanical and structural integrity. Consequently, they swell up and rapidly dissolve in the aqueous medium. Therefore, crosslinking is the necessary step for the physicochemical and mechanical stabilization of these GNPs in hydrophilic environments. For this purpose, different hydrophilic crosslinkers have been used which have already been discussed in detail in chapter 1 section 1.5.2.

The demerit of these hydrophilic crosslinkers is that due to their non-specific crosslinking of the gelatin networks with the loaded cargo, they may cause interference in the release of loaded hydrophilic macromolecular drugs from the gelatin matrix. Besides, the activity of encapsulated protein-based drug molecule is also affected after crosslinking. Therefore, a novel strategy for the stabilization of gelatin nanoparticles is needed.

Keeping under consideration this non-specific crosslinking caused by these hydrophilic crosslinkers, we intended to crosslink gelatin nanoparticles on the colloidal interface of GNPs using hydrophobic zero-length crosslinkers in order to avoid the diffusion of crosslinker inside the nanoparticles' matrix. To the best of our knowledge, the stabilization of GNPs with the application of hydrophobic zero-length crosslinkers is not reported so far. The aim of this study was to design nano-sized hydrophilic gel (gelatin)-based particles (GNPs) using the previously established standard protocols of nanoprecipitation [123]. Following the nanoprecipitation, the gelatin nanoparticles were crosslinked with hydrophobic crosslinker to overcome the main drawback for flexible protein delivery. For this selective interfacial crosslinking of GNPs, we employed diisopropylcarbodiimide (DIC) which is a zero-length

hydrophobic crosslinker. The basic idea is that the crosslinker (DIC) due to its hydrophobicity may not diffuse into the core of nanoparticle rather than it would cause its crosslinking action on the colloidal interface following the conjugation of primary amino groups with the carboxylic functional groups which are present on the colloidal interface of un-crosslinked GNPs. This conjugation leads to formation of amide-bonds between the polypeptide chains of gelatin on the surface of GNPs. These crosslinks provide stability to the GNPs in hydrophilic environment and at the same time avoid crosslinking of the proteinaceous payload in the carrier.

Furthermore, the formulation was optimized with respect to different process parameters, *e.g.*, crosslinker concentration, crosslinking time and crosslinking reaction temperature with regard to the effect on particle size, size distribution and zeta potential. The nano-formulation of surface-crosslinked GNPs was optimized both for type A and type B GNPs. As type B gelatin acts as anionic biopolymer at pH 7 while type A as a cationic biopolymer, which offer good opportunity to load both positively and negatively charged hydrophilic macromolecules.

3.2.1. Challenges of GNPs crosslinking

Since gelatin's peptidal chains are interconnected through covalent bonds after treatment with chemical crosslinkers as discussed in section 1.5.2, the crosslinked gelatin nanoparticles maintain their structural integrity in the aqueous media [124]. The main disadvantage of these hydrophilic crosslinkers is their non-specific crosslinking behaviour. Due to the polar nature, the crosslinkers diffuse into the core of the nanoparticles after crossing the colloidal interface. This results also in crosslinking of the loaded macromolecules if the respective chemical functional groups are present (NH_2). These newly established crosslinks are either intra-molecular (protein cargo-protein cargo crosslinks) or inter-molecular (protein cargo-gelatin molecule crosslinks) [125], see Figure 3-1 for non-specific crosslinking. Consequently, this

non-specific crosslinking lead to a potential interference in the release of loaded hydrophilic macromolecular drugs from the gelatin matrix [67] as well as to diminished biological activity of the encapsulated bioactive compound. Therefore, it is judicious that this non-specific crosslinking impedes the effective loading and hence the utilization of gelatin nanoparticles as a delivery tool for hydrophilic macromolecular APIs [126].

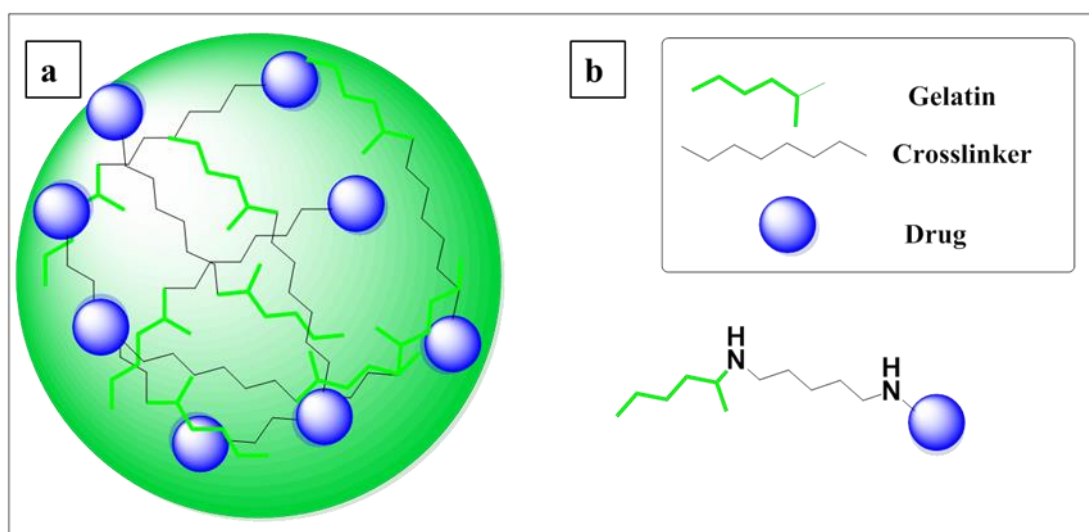


Figure 3-1. (a) Schematic illustration of glutaraldehyde-crosslinked GNPs loaded with a protein-based drug. (b) A closer look of Schiff's base crosslink between gelatin and protein-based drug substance.

In order to avoid this non-specific crosslinking dynamics due to the application of hydrophilic crosslinkers, it is demanded to use hydrophobic crosslinkers which should specifically and selectively crosslink the colloidal interface of GNPs only without diffusion into the core of GNPs.

In this research work, I will introduce a novel stabilization mechanism, termed as surface crosslinking of GNPs by using a zero-length hydrophobic crosslinker; DIC. This thesis is aimed to prove the hypothesis that the hydrophobic crosslinker (DIC) would localize its crosslinking action on the colloidal interface of GNPs rather than diffusing into the interior of the nanoparticle (NP) due to its hydrophobic nature. These surface-crosslinked GNPs will

provide a flexible delivery system for protein-based therapeutic compounds as the load will be affected only to a minor extent.

3.3. Experimental

3.3.1. Materials

Gelatin type B Bloom 75 from bovine skin, gelatin type A from porcine skin with three blooms (90-100, 175 and 300), Poloxamer 188 and diisopropylcarbodiimide (reagent grade) were purchased from Sigma-Aldrich (Steinheim, Germany). Acetone was obtained from Fischer Chemicals Ltd., (Loughborough, U.K). Milli-Q water with a resistivity of 18.2 M Ω .cm was used throughout the experiments. Tangential flow filtration (TFF) cassettes fitted with modified regenerated cellulose material (hydrosart) with molecular weight cut-off (MWCO) of 100 kDa was purchased from Sartorius Stedim Biotech Ltd. (Goettingen, Germany). The validated procedure of TFF-based purification will be discussed in detail in the next chapter 4.

3.3.2. Nanoparticles by nanoprecipitation

Gelatin nanoparticles were formulated using the pre-established formulation recipe based on nanoprecipitation technique [123]. Briefly, the solvent phase was obtained after dissolving 20 mg of gelatin in 1 mL of Milli-Q water at 50 °C. Subsequently, the solvent phase was added dropwise to the anti-solvent phase consisting of acetone containing poloxamer 188 (3 % w/v) as a stabilizer. Afterwards, the GNPs were crosslinked with different amounts of diisopropylcarbodiimide solution in acetone from its stock solution (69.16 % [w/v] for varying crosslinking time intervals. As a last step, the crude nanosuspension was washed employing tangential flow filtration (TFF) to remove impurities. The validated procedure of TFF-based purification will be discussed in detail in the next chapter 4. For the measurements

of the zeta potential, the TFF-based purified particles were used while for optimization of crosslinking conditions; GNPs without purification were analysed for DLS measurements.

3.3.3. Optimization of crosslinking

3.3.3.1. Type B GNPs

Chemical crosslinking is a necessary step for the physicochemical stabilization of gelatin nanoparticles in aqueous environment. Hence, gelatin nanoparticles using gelatin B (bloom 75) were crosslinked with varying concentrations of crosslinker (*i.e.*, diisopropylcarbodiimide) for varying crosslinking time intervals in order to get stable nanoparticles. In this context, different parameters, *e.g.*, concentration of crosslinker, crosslinking time and temperature of crosslinking reaction were investigated for their influence on particle size, size distribution and zeta potential.

Varying crosslinker concentration

The crosslinker, *i.e.*, diisopropylcarbodiimide with different concentration range (0.99 mg/mL - 15 mg/mL) was added to the uncrosslinked suspension of GNPs to evaluate its impact on mean size and size distribution. The concentration of gelatin in the aqueous phase was 20 mg/mL, the volumetric ratio of water to acetone was 1:15, and the stabilizer, *i.e.*, poloxamer 188, was 3 % (w/v) [123].

Varying crosslinking time

To investigate the minimum crosslinking reaction time, the GNPs dispersion system was subjected to react with the crosslinker at fixed for different crosslinking time intervals (0.5 h to 48 h). Other parameters, *e.g.*, gelatin concentration in the aqueous phase (water) and poloxamer concentration in the organic phase (acetone) was kept constant, *i.e.*, 20 mg/mL and

the 3 % (w/v), respectively. The crosslinking time was investigated for DIC concentration of 5 mg/mL and 15 mg/mL.

Varying Temperature

In addition to the optimization experiments regarding the concentration and crosslinking time of the crosslinker, the crosslinking of GNPs suspension was conducted at different temperatures, *i.e.*, room temperature, 30°C and 50°C. The effect of temperature on the physicochemical stabilization of crosslinked GNPs was investigated employing DLS measurements of the crosslinked GNPs at different time points at given temperatures.

3.3.3.2. Type A GNPs

Varying crosslinking time

The gelatin concentration in the solvent phase was 20 mg/mL, the solvent/non-solvent ratio was 1:15, and the stabilizer concentration was 3 % (w/v). Gelatin nanoparticles of type A with three blooms, *i.e.*, bloom 90-100, bloom 175 and bloom 30 were prepared following the standard protocols of nanoprecipitation [123]. Subsequently, the nanosuspension was crosslinked with 0.347 mL taken from stock solution of DIC in acetone having concentration of 69.16 % [w/v]. The concentration of crosslinker in the nanosuspension was 15 mg/mL which was previously optimized for type B gelatin nanoparticles at room temperature. The gelatin A nanosuspension was allowed to react with the crosslinker in above amount for various crosslinking time with intermittent DLS measurements until a stable colloidal system is formed with lowest size distribution (PDI < 0.2) while measuring in water as a dispersion medium. Hence, the crosslinking time at which the PDI was less than 0.2 with an attenuator value between 6-9 was regarded as optimum crosslinking time.

Varying gelatin concentration

Different concentrations of gelatin A of each bloom, *i.e.*, 10, 20, 30 and 40 mg/mL in the solvent phase were used for particles preparation. The objective was to investigate the impact of gelatin concentration in the solvent phase on mean size and size distribution of DIC-crosslinked GNPs.

3.3.4. Nanoparticle characterization

3.3.4.1. Determination of size and zeta potential

The mean particle size and size distribution of DIC-crosslinked gelatin nanoparticles was measured after varying crosslinking times before purification. The mean size (Z-average mean) and surface charge (zeta potential) were evaluated by dynamic light scattering (DLS) and laser Doppler anemometry, respectively using Zetasizer nano-ZS (Malvern instruments, Ltd., Worcestershire, UK). The samples were diluted 10 times with Milli-Q water before DLS measurements. Each sample was measured in triplicate for each formulation.

3.3.4.2. Morphology of nanoparticles by scanning electron microscopy (SEM)

Regarding the sample preparation for SEM visualization, these protocols were followed: a silicon wafer was placed on the top of a metal hub using carbon adhesive tape. Afterwards, a drop of TFF-washed nanosuspension was deposited onto the silicon wafer. Subsequently, samples were subjected to overnight drying for the evaporation of dispersion medium, *i.e.*, water, under ambient conditions. Then, using a current of 20 mA, the samples were sputtered for 50 s with a gold layer of ~15 nm using sputter coater (Q150R ES, Quorum Technologies Ltd, East Grinstead, UK). Finally, SEM images were obtained using SEM (EVO HD15, Carl Zeiss Microscopy, GmbH, Jena, Germany) with an acceleration voltage of 5 kV.

3.3.5. Determination of crosslinking extent

For the determination of % crosslinking extent of DIC-crosslinked gelatin nanoparticles, an already established quantification method known as trinitro-benzene sulfonic (TNBS) assay was employed [127]. This assay is a spectrophotometry-based determination of primary un-crosslinked amino groups attached to epsilon (ϵ) carbon atom of lysine amino acid residues of proteins. Briefly, the gelatin nanoparticles suspension (DIC-crosslinked and un-crosslinked) was firstly lyophilized. Next to lyophilisation, 10 mg gelatin nanoparticles from crosslinked and un-crosslinked were separately dispersed in 1 mL of sodium bicarbonate solution (4%) and 1 mL of TNBS solution (0.5% w/v). The mixture was then heated at 40°C for 4 h. Afterwards, 3 mL of HCl (6 N) was added to it followed by autoclaving at 120°C using 1.03-1.17 bar for 1h. The hydrolysed mass was diluted to 10 mL with Milli-Q water. Subsequently, ethyl acetate (5 mL) was added to this aqueous hydrolysate to remove the un-reacted TNBS. Afterwards, 5 mL aliquot of the aqueous phase was diluted to 25 mL with Milli-Q water and the absorbance was checked at $\lambda_{\text{max}} = 349$ nm using a UV-Vis spectrophotometer (Perkin-Elmer Lambda35, Rodgau, Germany) against a blank.

The blanks were prepared following the same procedure without the addition of gelatin. The number of primary amino groups was utilized as measure for crosslinking extent using the following equation (1).

$$\frac{\text{Moles of } \epsilon\text{-primary amino groups}}{\text{gelatin (g)}} = \frac{2(\text{absorbance})(0.02\text{L})}{1.46 \times \frac{10^4 \text{ L}}{\text{mole} \times \text{cm}} \times b \times x} \dots\dots\dots(1)$$

Where 1.46×10^4 L/mol.cm is the molar absorptivity of TNB-lys, b is the path length in cm, and x is the sample weight in grams.

3.3.6. Measurement of un-reacted DIC

A validated method of gas chromatography (Table 3-1) was employed for the quantification of un-reacted diisopropylcarbodiimide present in the GNPs suspension. For this purpose, gas chromatograph (GC) (Shimadzu GC-2010, Japan) connected with a flame ionization detector (FID) (Shimadzu GC-2010, Japan) was employed. The details of the validated GC method are given in Table 3-1.

Table 3-1. Summary of the GC chromatographic conditions

Chromatographic parameter	Details
GC column	Supreme-5 MS
Length of column	25 m
Packing material	5 % Phenylpolysilphenylsiloxane
Flow rate	1.24 mL/min
Injection mode	Split, split ratio of 1:10
Carriers gas	Nitrogen/Air
Oven temperature program	40°C for 5 minutes, rising temperature at 10°C/min followed by holding at 220°C for 5 minutes
Detector	Flame ionization detector (FID)

The sample for GC analysis was prepared following these protocols. Briefly, the supernatant was isolated after centrifugation of DIC-crosslinked GNPs (24,000 g for 20 minutes). Afterwards, the supernatant was isolated and analyzed for the quantification of un-reacted DIC present in the GNPs dispersion using the aforementioned validated procedure of gas chromatography (Table 3-1).

3.3.7. Measurement of diisopropylurea

During crosslinking of GNPs with diisopropylcarbodiimide, diisopropylcarbodiimide is believed to be converted to its by-product, diisopropyl urea (DIU). Therefore, for the analysis of diisopropyl urea, proton NMR spectroscopy was exploited. For this purpose, ¹H NMR spectra were recorded at 298 K in acetone-d₆ with a Bruker Avance 500 spectrometer (Bruker, BioSpin GmbH, Rheinstetten, Germany) equipped with a 5 mm BBO probe. The chemical

shifts were represented in parts per million (ppm) relative to the acetone peak at δ H 2.05. The 1 H NMR spectra were taken with a sufficient number of scans, typically NS=128, to give an acceptable S/N, because the peaks of interest, the DIU methyl protons, were in the same range as those achieved for the carbon-13 satellites of the DIC methyl groups.

3.3.8. Cytotoxicity evaluation

The *in-vitro* cytotoxicity potential of DIC-crosslinked GNPs was evaluated using the 3-(4, 5-dimethylthiazol-2-yl)-2, 5-diphenyl tetrazolium bromide (MTT) assay. MTT assay is the colorimetry-based determination of metabolically active cells after incubation of DIC-crosslinked GNPs formulations with different particle concentrations for a proper incubation time (4 hours). The dye compound, MTT undergoes reduction by mitochondrial succinate dehydrogenase produced by viable cells converting to dark purple coloured formazan product. Subsequently, the product formazan is solubilized with DMSO and measured spectrophotometrically at a wavelength of 550 nm [128]. The reaction is illustrated in (Figure 3-2).

In the MTT assay adenocarcinoma human alveolar basal epithelium cells A549 were used. The cells were cultured in RPMI-1640 with 2 mM glutamine and 10 % FCS in sterile 96-well plates until a cell density of approximately 1×10^4 cells per well.

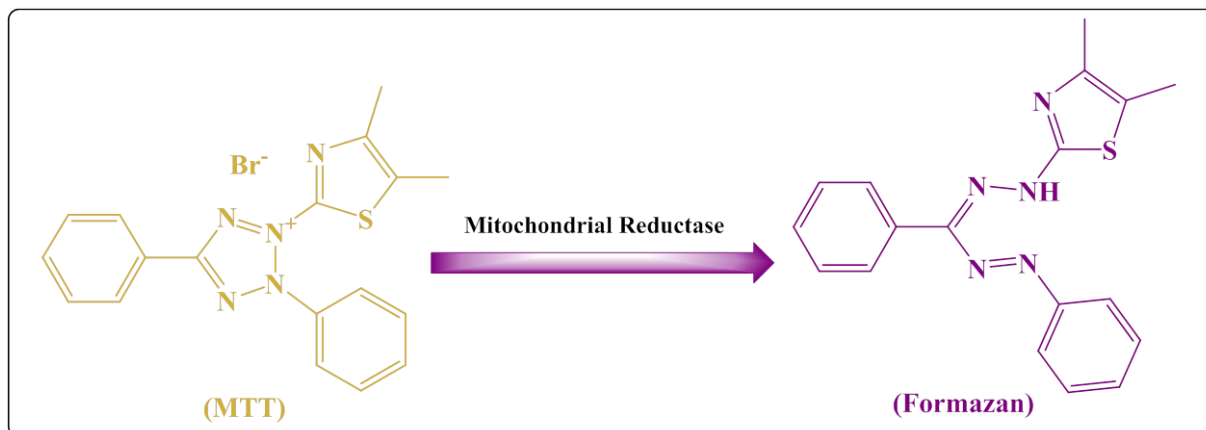


Figure 3-2. Reaction of the tetrazolium salt MTT to formazan during the cell viability test

Cells were washed two times with HBSS buffer and incubated with 200 μ L of a known concentration of DIC-crosslinked GNPs for 4 h in incubator at 37 $^{\circ}$ C with careful shaking. For the comparative evaluation, positive and a negative control were also included in the experiment. For a positive control the cells were treated with 2 % Triton X-100 which causes cell lysis due to the surface activity. For negative control, HBSS was used, to keep the cells in non-harmful conditions, so no cell death occurs during the incubation time (4 h). After incubating for 4 h, cells were washed again with 200 μ L HBSS buffer followed by the addition of 200 μ L of 10 % MTT reagent. The cells were then incubated for further 4 h at 37 $^{\circ}$ C with careful shaking. After 4 h, they were again washed with HBSS buffer followed by the addition of 100 μ L DMSO in each well to dissolve the product formazan. After the incubation time allowing for uptake of the tetrazolium salt and reduction to formazan the supernatant was removed. The formed formazan gives a deep purple colour which was measured at 550 nm with an Infinite[®]M200 plate reader (Tecan group Ltd., Männedorf, Switzerland). The percentage viability for DIC-crosslinked GNPs suspension with different nanoparticles concentrations was determined from positive and negative controls using the following equation (2).

$$\text{Cell Viability [\%]} = \frac{\text{Absorption of sample} - \text{Absorption of positive control}}{\text{Absorption of negative control} - \text{Absorption of positive control}} \times 100 \dots \dots \dots (2)$$

3.4. Results and Discussion

The current research work is focussed on introducing a novel strategy for the physicochemical and mechanical stabilization of gelatin nanoparticles, with the application of a zero-length apolar crosslinker, *i.e.*, diisopropylcarbodiimide (DIC). According to our hypothesis, the apolar crosslinker due to its low polarity is believed to be confined in the organic phase, *i.e.*, acetone (non-solvent phase for gelatin), hence might not diffuse into the hydrophilic core of GNPs. Therefore, only the amino and carboxylic functional groups on the colloidal interface

will get conjugated thus making an amide bond on the surface of nanoparticles. Gelatin nanoparticles were formulated according to the already established protocols of nanoprecipitation [123]. Briefly, the aqueous phase containing gelatin was added slowly in dropwise manner to the organic phase, *i.e.*, acetone containing 3 % [w/v] poloxamer 188 as stabilizer) [129, 130]. Due to diffusion of solvent phase into non-solvent phase, a strong interfacial turbulence is produced which leads to precipitation of gelatin at the interface in the form of gelatin nanoparticles. After particles formation via nanoprecipitation, the apolar crosslinker, *i.e.*, diisopropylcarbodiimide was added slowly in a dropwise manner to the GNPs suspension followed by stirring for varying time intervals to allow the formation of crosslinks in gelatin nanoparticles. The preparation methodology and proposed crosslinking mechanism is schematically shown in Figure 3-3.

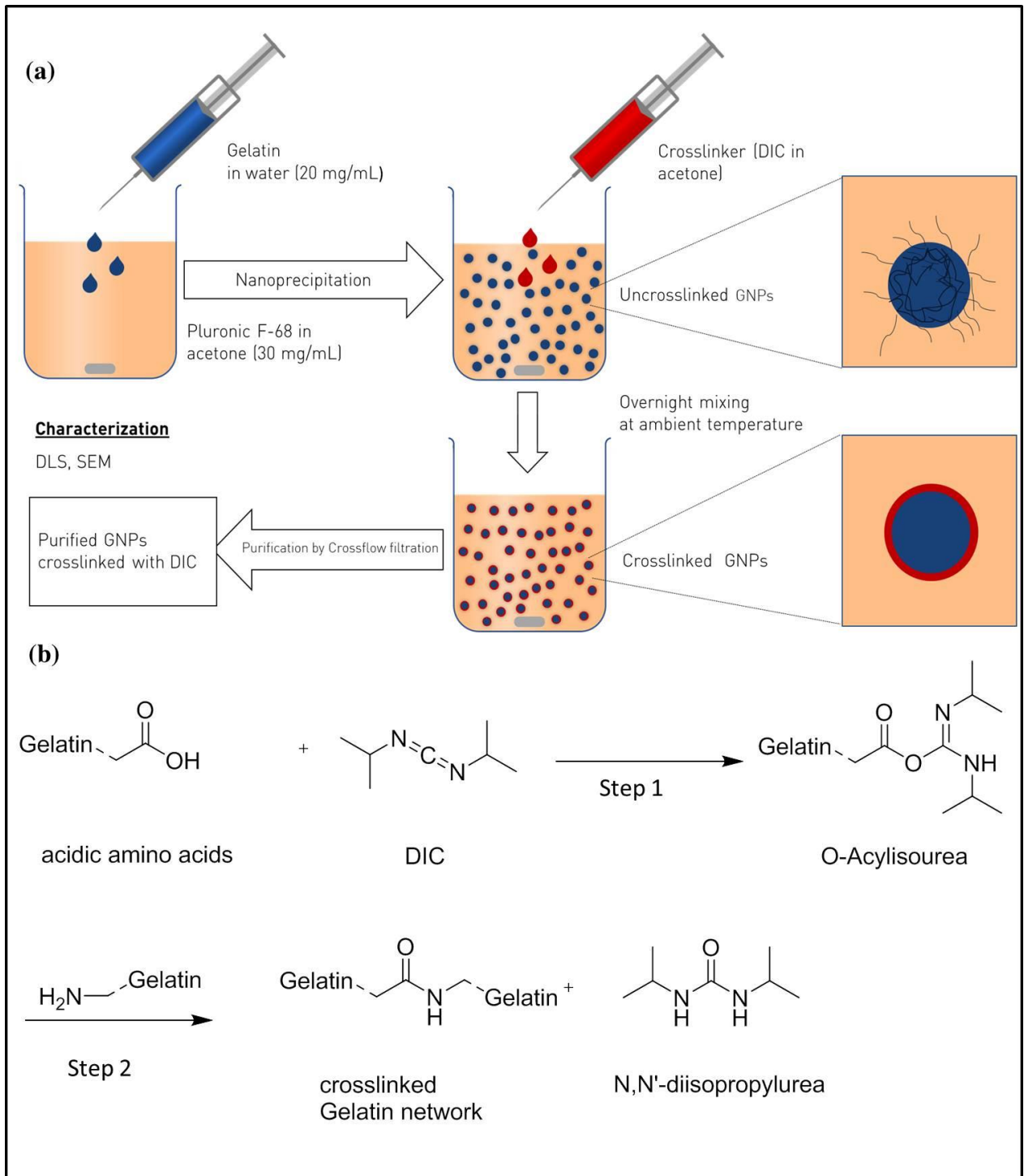


Figure 3-3. (a) Schematic representation of the procedure to form GNP nanoparticles via nanoprecipitation and crosslinking the particles by DIC. (b) Schematic representation of DIC-mediated crosslinking mechanism. Step 1: Formation of diisopropylcarbodiimide-mediated activation of (-COOH) to form an unstable intermediate O-Acylisourea. Step 2: Secondary reaction with nucleophilic substitution of free primary amino groups presented by lysine into the formerly formed DIC activated ester leading to formation amide crosslink at GNP interface [131-137].

3.4.1. Optimization of crosslinking conditions

3.4.1.1. Type B GNPs

Optimization of crosslinker concentration

Gelatin-B of bloom number 75 g was used in this experiment. Type B gelatin contains approximately 126×10^{-5} moles carboxylic acid groups/g on glutamic and aspartic acids and approximately 33×10^{-5} moles ϵ -amino groups/g on the lysine and hydroxy-lysine residues [138]. Due to the predominance of free carboxylic groups, type B gelatin possesses an acidic isoelectric point (IEP) of 4.5-5.5 [54, 139]. Due to its hydrophilicity, it readily dissolves in water. Therefore chemical crosslinking is indispensable for the physicochemical stabilization in water. In our case, the hydrophobic crosslinker (diisopropylcarbodiimide) activates the carboxylic functional groups present in the protein matrix of GNPs thus forming a transition unstable product called as *O*-acylisourea. This intermediate product readily reacts with a nucleophile, *e.g.*, primary amino groups present in the gelatin polypeptide chains. This reaction leads to the formation of a stable amide bond which acts as a crosslink (Figure 3-3-(b)). The crosslinked GNPs after crosslinking with DIC in the concentration range (0.99 mg/mL to 3.98 mg/mL) have a mean size of 250 nm with an in-homogeneous size distribution ($PDI > 0.2$) (Figure 3-4). Further increase of DIC concentration ≥ 4.98 mg/mL, monodisperse nanosuspensions with $PDI < 0.2$ were obtained while measuring in water. This is an indication that the particles are sufficiently crosslinked and are not getting dissolved in aqueous environment. The formulation can be considered as physicochemically stable. Larger crosslinker concentrations from 4.98 mg/mL – 15 mg/mL has no influence on the particle size (Figure 3-4). The physicochemical stability of crosslinked GNPs in aqueous environment can also be measured in terms of a physical parameter of the dynamic light scattering device (DLS) known as attenuator index. According to DLS measurements, attenuator index is a

DLS parameter which is dependent on nanoparticles' concentration in a given sample. The higher the concentration of particles in a given sample, the lower will be the attenuator index and vice versa. There are 11 attenuator positions in the ZetaSizer ranging from 100% to 0.0003% [140-142]. The relationship between the attenuator and the transmission value is shown in Table 3-2. The transmission value is the percentage of laser light that is transmitted through the sample cuvette.

Table 3-2. Relationship between attenuator index and transmission value [141]

Attenuator index	Transmission (% Nominal)	Attenuator index	Transmission (% Nominal)
1	0.0003	7	1
2	0.003	8	3
3	0.01	9	10
4	0.03	10	30
5	0.1	11	100
6	0.3		

The attenuator index of crosslinked GNPs formulations crosslinked with DIC concentration below 4.98 mg/mL is higher than 9 which is a clear indication for a low concentration of nanoparticles (see Table 3-3, Figure 3-4). It means that the nanoparticles cannot maintain their integrity in water and are getting dissolved on contact with aqueous environment. The attenuator index shifts to 8 using a crosslinker concentration above 4.98 mg/mL. At these concentrations of DIC, the nanoparticles maintain their particulate nature with PDI less than 0.2 in aqueous environment (see Table 3-3 and Figure 3-4).

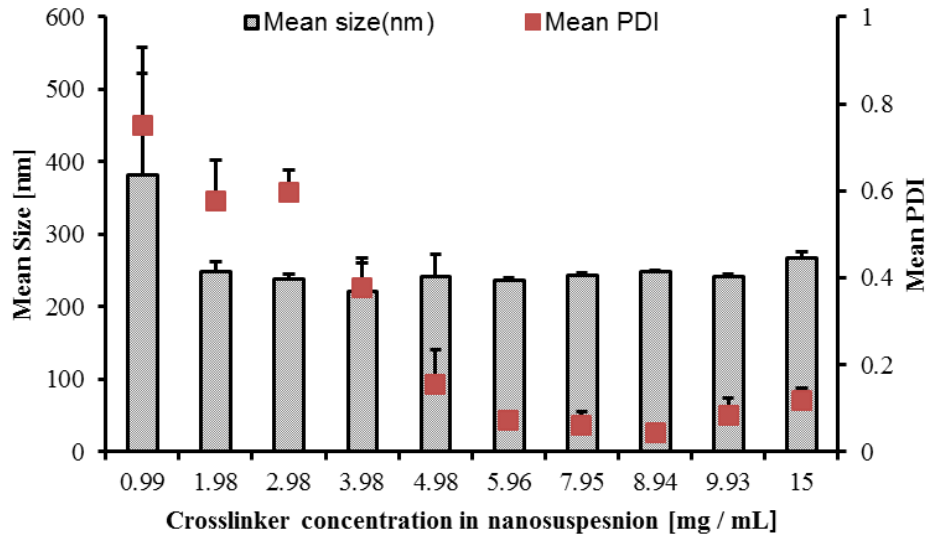


Figure 3-4. Effect of crosslinker concentration (DIC) on particle size and size distribution. The nanoparticles were measured in water after 10 times dilution before purification with three independent experiments (n = 3).

Table 3-3. Mean size and size distribution of DIC-crosslinked GNPs crosslinked at different concentrations of crosslinker (DIC) at room temperature. (Crosslinking time: 24 - 48 h).

DIC Concentration [mg / mL]	Mean size [nm] ± S.D.	Mean PDI ± S.D.	Attenuator index
0.99	382.00 ± 175.42	0.75 ± 0.12	11
1.98	248.48 ± 13.53	0.58 ± 0.09	11
2.98	237.98 ± 6.50	0.60 ± 0.05	11
3.98	221.88 ± 38.36	0.38 ± 0.07	10
4.98	241.80 ± 30.07	0.16* ± 0.08	8*
5.96	237.18 ± 3.63	0.07* ± 0.02	8*
7.95	243.33 ± 3.16	0.06* ± 0.03	8*
8.94	248.28 ± 2.50	0.04* ± 0.02	8*
9.93	241.78 ± 2.82	0.08* ± 0.04	8*
15	268.40 ± 7.75	0.12* ± 0.03	8*

* represents stabilized nanoparticles with PDI < 0.2

A crosslinker concentration above 4.98 mg/mL has also no relevant impact on the mean size of the nanoparticles. This experiment was performed at crosslinking times of 24 - 48 h but crosslinking time was also found to have an impact on particle stabilization kinetics. Therefore, it is important to investigate the effect of crosslinking time on mean size and size distribution.

Optimum crosslinking time

Effect of crosslinker concentration

In this experiment, the minimum crosslinking time was studied for two concentrations of DIC, *i.e.*, 5 mg/mL and 15 mg/mL at ambient temperature. The crosslinking under these conditions produced stable nanoparticles in aqueous environment with lowest size distribution (PDI < 0.1) after 25 – 30 h at 5 mg/mL and 15 - 20 h at 15 mg/mL (see Figure 3-5). At these crosslinking times, the mean size of particles in water is between 230 - 250 nm with PDI less than 0.2. The physicochemical stability of crosslinked GNPs in aqueous environment at different time points can also be correlated to the corresponding attenuator index value of the measurements. As explained in section 3.4.1, that attenuator index value is dependent on nanoparticles concentration. The larger the value of attenuator index, the lower will be the particles concentration in a given sample volume and vice versa. The attenuator index range of 6 - 9 is a representation of enough concentration of sufficiently crosslinked, stable GNPs in the sample. The attenuator value > 9 is an indication of unstable or slowly dissolving GNPs system. The respective attenuator indices at different crosslinking times with corresponding mean sizes and PDIs are presented in Table 3-4. It was observed that the attenuator index range of 8 - 9 was achieved after crosslinking time of 15 h at crosslinker concentration of 15 mg/mL while for crosslinker concentration of 5 mg/mL, the desired attenuator index (8 - 9) was achieved after crosslinking time of 25-28 h. The mean size of crosslinked GNPs at these conditions was observed to be 241.80 nm and 231.72 with PDI values of less than 0.2. Hence, increasing the crosslinker concentration to 15 mg/mL reduced the optimum crosslinking time (see Figure 3-5 and Table 3-4).

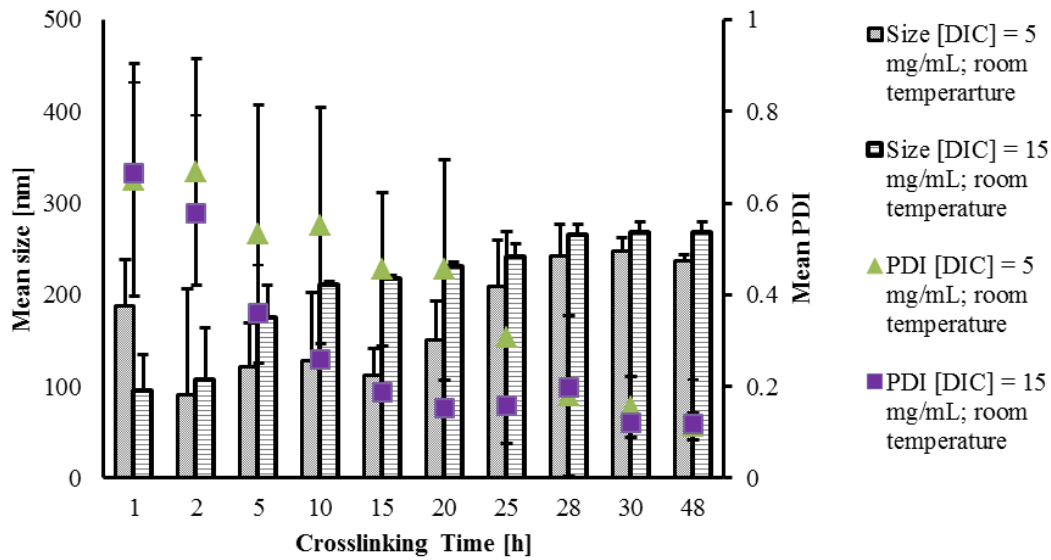


Figure 3-5. Mean size and size distribution analysis at different incubation times at room temperature (concentration of DIC in nanosuspension. (a) 5 mg/mL (b) 15 mg/mL).

Table 3-4. Relationship between mean particle size, size distribution and attenuator index of ZetaSizer at two concentrations of DIC. The attenuator index range (6-9) is an indicator of enough concentration of stable crosslinked GNPs due to sufficient crosslinking.

^(a) CT [h]	Mean size [nm] ± S.D. (PDI), [Attenuator index]	
	C _{DIC} [5 mg/mL]	C _{DIC} [15 mg/mL]
1	188.31 ± 50.07 (0.65),[11]	95.83 ± 39.00 (0.66),[11]
2	91.26 ± 115.57 (0.67),[11]	107.43 ± 56.84 (0.58),[10]
5	121.41 ± 48.21(0.53),[11]	175.78 ± 34.07 (0.36),[10]
10	128.20 ± 74.06 (0.55),[10]	211.28 ± 3.63 (0.26), [10]
15	113.10 ± 28.37 (0.46),[10]	217.98 ± 3.50 (0.19),[9]*
20	150.66 ± 41.96 (0.45),[10]	231.72 ± 4.29 (0.15),[9]*
25	209.33 ± 50.20 (0.31),[9]*	242.76 ± 13.07 (0.16),[8]*
28	242.66 ± 33.69 (0.18),[8]*	266.82 ± 10.30 (0.20),[8]*
30	247.70 ± 14.16 (0.15),[8]*	268.22 ± 11.65 (0.12),[7]*
48	236.98 ± 6.93 (0.11),[8]*	268.40 ± 11.24 (0.12),[7]*

* represents stabilized nanoparticles with PDI <0.2; ^(a) CT: Crosslinking time

Effect of Temperature

Since the rate of endothermic chemical reactions enhances with elevation in temperature, the crosslinking of GNPs with DIC with might also be activated. The crosslinking was carried out at three different temperatures, *i.e.*, room temperature, 30°C and 50°C in an incubator keeping the concentration of DIC constant (*i.e.*, 15 mg/mL). It was observed that the optimum crosslinking time is decreased with increase in temperature of the crosslinking mixture, demonstrating that rate of chemical crosslinking with DIC is enhanced at high temperatures. This behaviour was already expected. While performing the crosslinking of GNPs at room temperature, 30°C and 50°C, the optimum crosslinking time of GNPs at which the PDI was also observed to be less than 0.2 was 16 h, 2 h and 1 h, respectively as can be seen in Figure 3-6 and Table 3-5. This means that the DIC-crosslinked GNPs after being crosslinked with these crosslinking times at respective temperatures possess sufficient colloidal stability in aqueous environments. Moreover, the phenomenon of acceleration of DIC-mediated stabilization kinetics with increasing temperature was also supported by the apparent drop in the attenuator values of each formulation in DLS measurements. As explained previously the attenuator value 6 - 9 is a representation of sufficient concentration of stable, crosslinked GNPs suspension in DLS measurements. In fact, the crosslinked gelatin nanoparticles have the tendency of undergoing dissolution on contact with water due to insufficient crosslinking and consequently, the attenuator value increases (> 9). In this experiment, while performing the crosslinking at room temperature, 30°C and 50°C, the crosslinked GNPs suspensions attain the attenuator value of 8 - 9 after 16 h, 2 h and 1 h, respectively as shown in Table 3-5. The mean particle sizes of GNPs crosslinked under these conditions are between 230 and 270 nm and PDI less than 0.2. Hence, it can be inferred that temperature has a direct impact on DIC induced stabilization kinetics of GNPs.

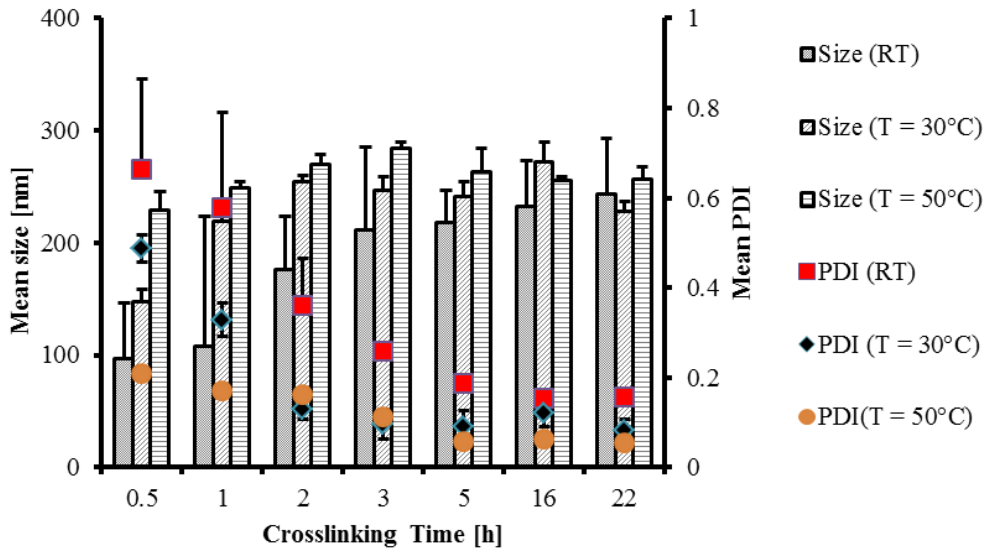


Figure 3-6. Mean size and size distribution analysis at different crosslinking reaction times at room temperature, 30°C and 50°C for DIC concentration of 15 mg/mL.

Table 3-5. Relationship between particle size and attenuator index of DLS machine for DIC concentration of 15 mg/mL at different crosslinking times at room temperature, 30°C and 50°C. The attenuator index range (6-9) is an indicator of enough concentration of stably crosslinked GNPs in aqueous medium due to sufficient crosslinking.

^(a) CT [h]	Mean size [nm] ± S.D. (PDI), [Attenuator index]		
	Room Temperature	30°C	50°C
0.5	95.83 ± 50.07 (0.66), [11]	146.83 ± 16.27 (0.49), [11]	228.86 ± 16.27 (0.21), [10]
1	107.43 ± 115.57 (0.58), [10]	218.54 ± 6.44 (0.33), [10]	248.43 ± 6.44 (0.17)*[9]
2	175.78 ± 48.21 (0.36), [10]	253.55 ± 9.21 (0.13)*[9]	269.45 ± 9.21 (0.16)*[8]
3	211.28 ± 74.06 (0.26), [10]	246.61 ± 6.66 (0.10)*[8]	283.41 ± 6.66 (0.11)*[7]
5	217.98 ± 28.37 (0.19), [10]	240.93 ± 22.29 (0.09)*[7]	262.31 ± 22.29 (0.06)*[7]
16	231.72 ± 41.96 (0.15)* [8]	271.33 ± 4.77 (0.12)*[7]	254.47 ± 4.77 (0.06)*[7]
22	242.76 ± 50.19 (0.16)*[8]	227.30 ± 11.82 (0.08)*[7]	256.31 ± 11.82 (0.05)*[7]

* represents stabilized nanoparticles with PDI < 0.2; ^(a) CT: Crosslinking time

In summary, with increasing the concentration of crosslinker and temperature of crosslinking mixture, the optimum crosslinking time at which the DIC-crosslinked GNPs possess the lowest PDI in aqueous environment, is reduced. The summary of crosslinking times at different crosslinker concentrations and temperature is summarized in Table 3-6.

Table 3-6. Summary of the optimum crosslinking times of DIC-crosslinked GNPs at different crosslinker concentration and temperatures.

^(a) C _{DIC} [mg/mL]	Crosslinking Temperature [°C]	Optimum *CT [h]	Mean size [nm] ± S.D	Mean PDI ± S.D	** AI
5	Room temperature	48	241.80 ± 30.07	0.16 ± 0.08	8
5	30	25	252.92 ± 16.80	0.14 ± 0.05	8
5	50	5	250.54 ± 11.53	0.11 ± 0.07	8
15	Room temperature	20	231.72 ± 4.29	0.15 ± 0.02	8
15	30	2	253.55 ± 9.21	0.13 ± 0.02	8
15	50	1	269.45 ± 9.21	0.16 ± 0.03	8

*Crosslinking time at which PDI is <0.2; **AI: Attenuator index; ^(a) Concentration of DIC

3.4.1.2. Type A GNPs

The formulation development of surface-crosslinked gelatin A nanoparticles was also in focus in this chapter due to some special advantages of type A gelatin. Due to its high isoelectric point (IEP of 7 - 9), type A gelatin exists as a cationic polymer at neutral pH [19, 139]. Therefore, GNPs fabricated from type A gelatin would have cationic surface at neutral pH (7). Due to this cationic character, it can be exploited as a delivery vehicle for negatively charged hydrophilic macromolecules which includes nucleic acid-based macromolecules, *e.g.*, oligonucleotides, plasmid DNA, locked nucleic acid nucleotide and small interfering RNA [98] as well as peptide-based drugs with isoelectric points (IEP < 7). The cationic surface is also advantageous in context of higher uptake rates for positively charged nanoparticles than negatively charged particles [143]. Accordingly, a larger *in vitro* uptake has been demonstrated for cationic gelatin A NPs in comparison to negatively charged gelatin B nanoparticles [143]. A good *in vitro* safety profile of gelatin A NPs has already been reported [144]. In contrast, in order to get positively charged gelatin particles, sometimes cytotoxic

cationic agents, *e.g.*, PEI, have also been employed [98, 145]. Hence, the GNPs fabricated from type A gelatin would be a promising delivery system in the context of enhanced cellular uptake avoiding the surface cationization procedures while using toxic poly-cations by covalent attachment to the surface of GNPs.

Optimum crosslinking time

Since, the isoelectric point of type A is between 7 and 9 [139] it is intrinsically a cationic molecule at neutral pH. This high isoelectric point of type A gelatin is attributed to a high density of free amino groups offered by basic amino acids (*e.g.*, L-lysine, hydroxylysine, asparagine and glutamine) as compared to acidic amino acids.

Just like gelatin B nanoparticles, the nanoparticles fabricated from gelatin A are not able to maintain their particulate nature in aqueous environments without crosslinking, therefore crosslinking is indispensable to make them physicochemically stable in aqueous environments. Using the zero-length hydrophobic crosslinker (DIC) renders a stable solid structure to the particles. Due to the difference of isoelectric points between the two types of gelatin, the DIC-mediated stabilization kinetics using gelatin A was also found to be different from gelatin B.

Together with the crosslinking time for particles stabilization the effect of molecular weight or better the bloom number was studied. Bloom number of gelatin is proportional to its mean molecular mass. It is an indication of the strength of a gel formed from a solution of known concentration. The bloom number is defined as the force (weight) required to depress a given sample area of gel a distance of 4 mm. The higher the bloom number, the stronger the gel strength. The relationship between bloom number & average molecular mass is given in the following Table 3-7.

Table 3-7. Relationship between bloom number and molecular mass [139].

Bloom Number	Average molecular mass (Dalton)
50-125 (Low Bloom)	20,000-25,000
175-225 (Medium Bloom)	40,000-50,000
225-325 (High Bloom)	50,000-100,000

Therefore, we conducted a crosslinking of type A GNPs with the three blooms mentioned above with DIC for different crosslinking times with parallel measurements using DLS to check the impact on mean size of so produced nanoparticles. The concentration of DIC used was 15 mg/mL which was optimized for gelatin B GNPs as was discussed in section 3.4.1.1.

As evident from DLS measurements in Table 3-8, the stabilization kinetics of GNPs produced from type A with different blooms is different using a constant gelatin concentration in solvent phase (20 mg/mL) and crosslinking with a constant concentration of crosslinker (DIC), *i.e.*, 15 mg/mL. It was observed that crosslinked GNPs prepared from gelatin type A bloom 90-100 and 300 attain a mean size of 400 - 500 nm and PDIs below 0.2 when measuring after crosslinking for 144 h in water. After long crosslinking times (144 h), the particles possess the lowest PDI in water. The colloidal stability was also characterized in terms of the attenuator value displayed by DLS measurements as explained in section 3.4.1. The attenuator index >10 indicates low particle concentrations present in a given sample volume. In the case of gelatin nanoparticles, it can be assumed that due to insufficient crosslinking the particles have the tendency to get dissolved in water, consequently converting the sample into gelatin solution. Hence, the solution state of GNPs would exhibit high attenuator index (>9). The attenuator value from 6 – 9 generally represents enough concentration of stable, crosslinked GNPs in water. In the above example, attenuator 9 is achieved after crosslinking time of 144 h for bloom 90 and 300 (see Table 3-8). At this crosslinking time, the PDI was also found to be below 0.2. Hence, the optimum crosslinking time for gelatin A for both bloom 90 and 300 at room temperature is regarded as 144 h. On the other hand, the GNPs produced from gelatin A (bloom 175) attains mean size 300 - 350 nm with PDI less than 0.2 after crosslinking the

dispersion for approximately 48 h. The GNPs dispersion system crosslinked for approximately 48 h possess already colloidal stability in water also depicted by low attenuator value (value of 9 after 48 h crosslinking). Therefore, the minimum crosslinking time needed for stabilization in aqueous media for gelatin A (bloom 175) is 48 h at room temperature (see Table 3-8).

After comparing the optimum crosslinking times of type A GNPs (bloom 90, 175 and 300) with type B GNPs (bloom 75) (see Table 3-4), it is clear that GNPs fabricated from gelatin B are crosslinked faster as compared to GNPs fabricated from gelatin A. The possible reason for this variability may be the difference of amino acid composition and isoelectric points of both types of gelatin. Type B gelatin has 100 - 115 millimoles of free carboxylic groups per 100 g of protein and an isoelectric point (IEP) of 4.7 - 5.2 [139]. On the other hand type A gelatin contains 78 - 80 millimoles of free carboxylic groups per 100 g of protein and an isoelectric point of 7 - 9 [139, 146]. Thus, the relative proportion of free carboxylic groups found in gelatin B is higher than gelatin A. So, this different distribution of acidic and basic functional groups in two types of gelatin might be a driving force for the variability of DIC-based crosslinking kinetics of the two gelatin types. As it was explained in section 3.4 (Figure 3-3) that the crosslinker (DIC) activates the free (un-bonded) carboxylic groups which is an initiation step in the crosslinking process. Since, gelatin B offers more free carboxylic groups for the formation of crosslinks, the particles get stabilized faster. In contrast, gelatin A contains comparatively low proportion of free carboxylates, and hence the crosslinking process mediated by DIC will be slower. This could explain the variability of crosslinking kinetics of both types of gelatin.

Table 3-8. Relationship between mean particle size/size distribution of DIC-crosslinked type A GNPs of different blooms and attenuator index. The crosslinker concentration was 15 mg/mL at room temperature. The attenuator indices (6-9) is an indicator enough nanoparticles concentration of stable crosslinked GNPs in aqueous media due to sufficient crosslinking.

CT ^a [h]	Mean size [nm] ± S.D. (PDI), [Attenuator index]		
	Type A (bloom 90-110)	Type A (bloom 175)	Type A (bloom 300)
0.5	134.78 ± 51.68 (0.3), [11]	105.47 ± 31.50 (0.33), [11]	101.55 ± 52.11 (0.29), [11]
1	116.46 ± 34.64 (0.32), [11]	85.98 ± 36.30 (0.57), [11]	85.81 ± 36.26 (0.21), [11]
2	122.80 ± 44.55 (0.31), [11]	97.86 ± 18.71 (0.88), [11]	57.95 ± 6.28 (0.28), [11]
4	174.39 ± 106.86 (0.39), [11]	332.72 ± 61.06 (0.72), [11]	276.11 ± 279.55 (0.5), [11]
8	114.54 ± 16.97 (0.35), [11]	381.97 ± 48.48 (0.58), [10]	82.01 ± 24.45 (0.32), [11]
16	384.75 ± 68.60 (0.52), [11]	357.53 ± 39.22 (0.2), [10]	174.64 ± 98.96 (0.94), [11]
48	484.03 ± 35.91 (0.26), [11]	321.80 ± 28.79 (0.05), [9]*	486.10 ± 15.41 (0.36), [11]
96	479.20 ± 3.55 (0.24), [9]	334.94 ± 8.13 (0.09), [8]*	483.65 ± 62.34 (0.26), [10]
144	479.73 ± 15.56 (0.11), [8]*	317.27 ± 4.68 (0.05), [7]*	501.23 ± 5.87 (0.14), [9]*

* represents stabilized nanoparticles with PDI < 0.2, CT^a: crosslinking time

Effect of gelatin concentration

After optimization of crosslinking time for gelatin A nanoparticles of different blooms at a constant concentration of diisopropylcarbodiimide, *i.e.*, 15 mg/mL, it was necessary to study the effect of gelatin concentration in the solvent phase on the mean size and size distribution of nanoparticles. The DIC-crosslinked particles were measured both in acetone as well as water as dispersion media. For comparison of DLS measurements, the measurements in acetone were considered which are presented in Figure 3-7 and Table 3-9. It was observed that the mean size of nanoparticles slightly increases with increasing the gelatin concentration from 10 mg/mL to 20 mg/mL in the solvent phase for all blooms. With further increase in gelatin concentration up to 30 mg/mL, the mean size of particles also increases significantly. The mean size was increased around 210 nm, 252 and 264 nm for bloom 90 - 110, bloom 175 and bloom 300 respectively (Figure 3-7 and Table 3-9).

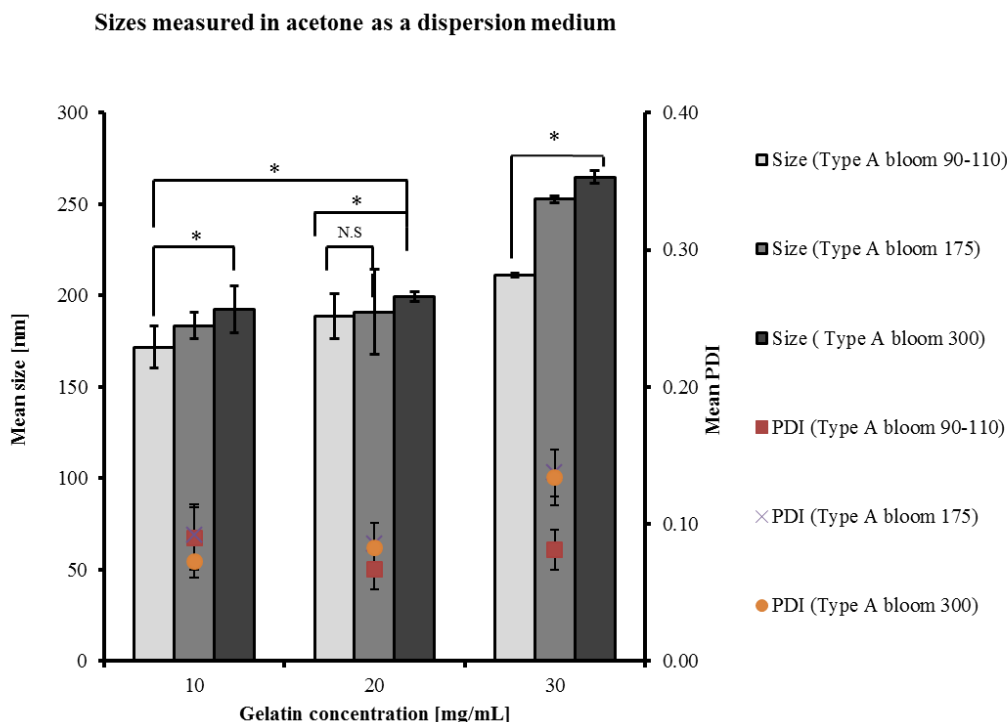


Figure 3-7. Effect of gelatin concentration on mean size and polydispersity index of GNPs. The samples were measured in triplicates for three independent experiments. Acetone was used as dispersion medium and samples were diluted 10 times with acetone before DLS measurements. *Statistics* (N.S: statistically non-significant on the basis of $p > 0.05$ as per one-way ANOVA). * statistically significant $p < 0.05$ as per one-way ANOVA.

However, using concentrations above 30 mg/mL almost for all studied blooms resulted in visible bigger precipitates formation of gelatin which cannot be re-dispersed easily (Table 3-9). The phenomenon of increase in mean hydrodynamic diameter and visible precipitates formation (phase separation) can be attributed to an increase in viscosity with increasing gelatin concentration in the solvent phase. The higher the viscosity of the solvent phase due to higher polymer concentration the lower would be the rate of diffusion of the solvent towards the non-solvent [99, 147]. Consequently, the bigger would be the particle sizes of so produced GNPs. In fact, there is always an optimum polymer concentration range in the solvent phase for particles formation, beyond which there is irreversible polymer aggregation leading to phase separation. So, for type A GNPs, the maximum permissible gelatin concentration for

optimum particles formation was observed to be 30 mg/mL. These observations are in close agreement with the results of other investigators regarding other polymers [147, 148].

Table 3-9. Effect of gelatin type, bloom number and concentration on particle size and size distribution. All samples were measured in acetone as dispersion medium before particles purification and diluted 10 times with acetone before DLS analysis.

Gelatin concentration [mg/mL]	Mean size \pm SD [nm] (PDI)		
	Type A (bloom 90-110 g)	Type A (bloom 175 g)	Type-A (bloom 300 g)
10	171.88 \pm 11.73 (0.09)	183.61 \pm 7.19 (0.09)	192.37 \pm 12.91(0.07)
20	188.78 \pm 12.08 (0.07)	191.10 \pm 23.08 (0.09)	199.38 \pm 2.78 (0.08)
30	211.02 \pm 1.14 (0.08)	252.66 \pm 1.79 (0.14)	264.82 \pm 3.34 (0.13)
40	ND ^a	ND ^a	ND ^a

ND^a: Not determined due to formation of bigger visible precipitates

After measuring the same samples in water as a dispersion medium before purification, it was observed that using gelatin concentration of 10 mg/mL in the solvent phase, the mean sizes of GNPs of all blooms were almost similar. The mean size of crosslinked GNPs for all blooms was in the range of 200 - 300 nm. With increasing gelatin concentration to 20 mg/mL, the mean size of GNPs produced by bloom 90 and 175 is increased up to 300 nm and 330 nm respectively, with PDIs below 0.2. The mean size of gelatin A (bloom 300) is increased up to 400 nm using a gelatin concentration of 20 mg/mL. Increasing the gelatin concentration further to 30 mg/mL, the mean size of GNPs produced from gelatin A bloom 90 and bloom 175 possess a mean size in the range 348 - 367 nm with PDI lower than 0.2. For gelatin A (bloom 300) in concentration of 30 mg/mL, the mean size is increased up to approximately 530 nm with PDI less than 0.2 (see Table 3-10).

Table 3-10. Effect of gelatin type, bloom number and concentration on mean particle size and size distribution. All samples were measured in water as dispersion medium before particles purification and diluted 10 times with water before DLS measurements.

Gelatin concentration [mg/mL]	Mean size \pm SD [nm] (PDI)		
	Type A (bloom 90-110 g)	Type A (bloom 175 g)	Type-A (bloom 300 g)
10	242.43 \pm 28.32 (0.09)	233.10 \pm 35.31(0.09)	240.28 \pm 12.57 (0.28)
20	329.50 \pm 17.82 (0.05)	303.28 \pm 7.30 (0.18)	414.18 \pm 3.83 (0.24)
30	348.71 \pm 7.40 (0.08)	359.65 \pm 2.81(0.13)	530.20 \pm 18.74(0.06)
40	ND ^a	ND ^a	ND ^a

ND^a: Not determined due to formation of bigger visible precipitates

In summary, the mean size of DIC-crosslinked GNPs increases with increasing the bloom number and concentration of gelatin in the solvent phase. The increase in hydrodynamic diameter can be attributed to high viscosity of gelatin solution in the solvent phase. The molecular weight of gelatin is a direct function of bloom number of gelatin used as shown in Table 3-7. The larger the bloom number of the gelatin used, the higher will be the molecular weight. In turn, the viscosity of gelatin solution increases with increasing the bloom number. Therefore, the higher the bloom number of gelatin used, the higher the viscosity of the solvent phase (*i.e.*, aqueous solution of gelatin) and the lower will be the diffusion rate of the solvent phase to the non-solvent phase during nanoprecipitation. This retardation of diffusion of solvent phase results in the formation of bigger particles.

It was also observed that the mean hydrodynamic diameter of particles while using water as a dispersion medium is higher than the sizes measured in acetone as can be seen in Figure 3-8, Table 3-9 and Table 3-10. This can be attributed to swelling of the crosslinked gelatin nanoparticles which behaves as a nano-hydrogel system following dispersion in aqueous media.

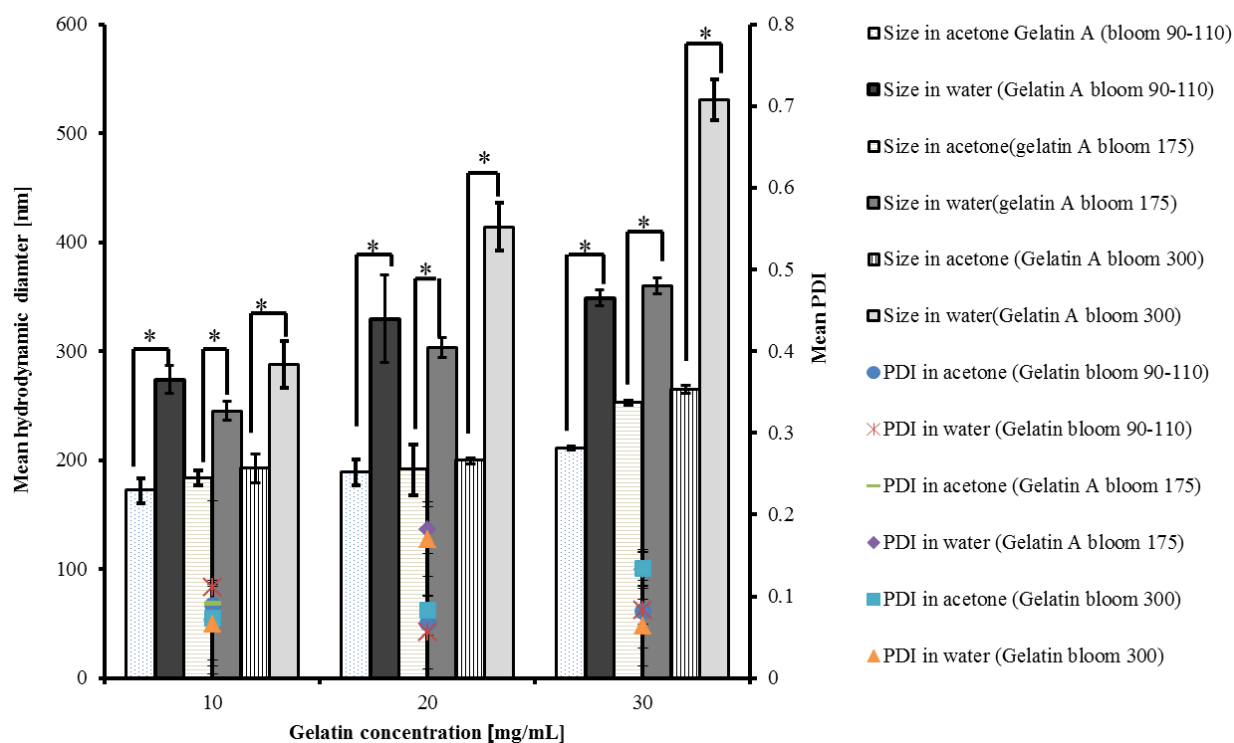


Figure 3-8. Comparison between mean sizes of DIC-crosslinked gelatin A NPs measured in acetone and water as dispersion media. $*p < 0.05$: statistically significant according to paired two-tailed t -test.

3.4.2. Investigation of crosslinking

3.4.2.1. Determination of crosslinking degree – TNBS Assay

The crosslinking degree of diisopropylcarbodiimide-mediated crosslinked gelatin nanoparticles was quantified using the already established protocols of trinitro benzenesulphonic acid (TNBS) assay [127]. This assay is a spectrophotometry based determination of primary amino groups in both crosslinked and un-crosslinked gelatin nanoparticles. From the absorbance values of both un-crosslinked and crosslinked gelatin nanoparticles, the numbers of un-crosslinked primary amino groups in crosslinked gelatin nanoparticles were calculated using the equation mentioned in section 3.3.5. It was observed that % crosslinking extent of gelatin nanoparticles increases with increasing the crosslinker concentration until an equilibrium crosslinking or plateau is obtained (see Figure 3-9). It can

be seen that the plateau is achieved around 3.98 mg/mL. Further increase in crosslinker concentration (>3.98 mg/mL) has no influence on crosslinking extent of GNPs. It is also evident from the statistical analysis (One-Way ANOVA) that the respective crosslinking extent for crosslinker concentrations from 3.98 mg/mL up to 18.4 mg/mL were non-significant statistically. Therefore, increasing the concentration of crosslinker above 3.98 mg/mL does not affect the % crosslinking extent of GNPs. This supports the idea of crosslinking saturation. It can also be speculated that the crosslinker (DIC) has no access to more free primary amino groups which are assumed to be present in the core of particles.

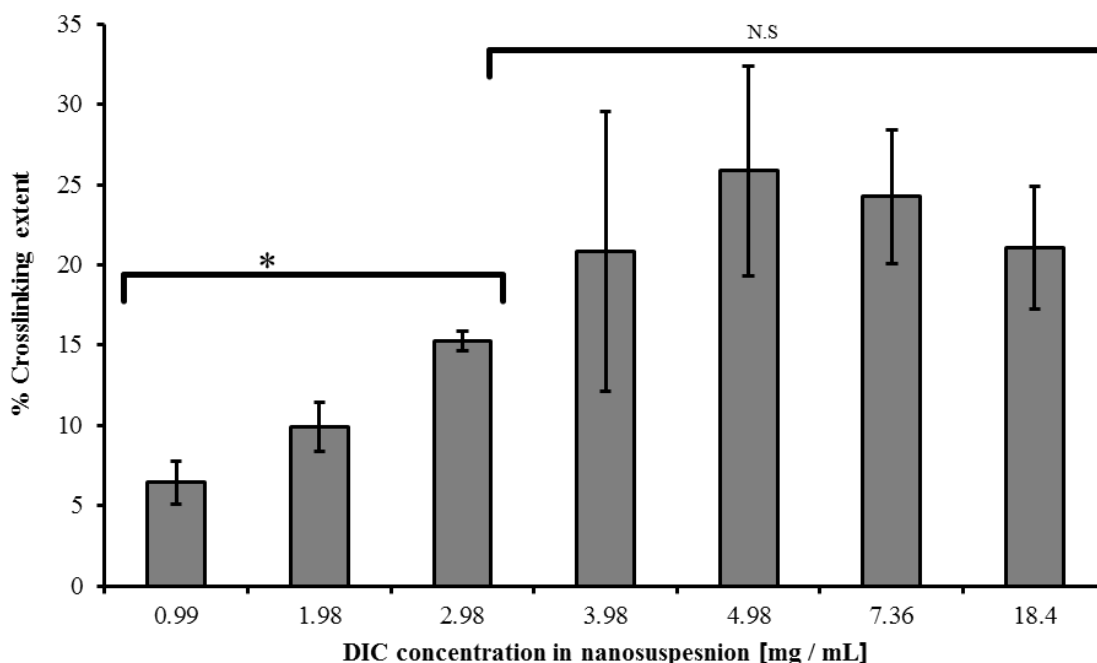


Figure 3-9. Relationship between % crosslinking extent and concentrations of crosslinker (DIC) for 18 h crosslinking reaction time. The volumes were kept constant during the preparations. Values determined from TNBS assay by using the absorption maximum of $\lambda_{\max} = 349$ nm, $n = 3$. *Statistics* (N.S: Non-significant statistically on the basis of $p > 0.05$ as per one-way ANOVA). * Statistically significant $p < 0.05$ as per one-way ANOVA.

To investigate the influence of crosslinking time on crosslinking extent, crosslinking of GNPs was performed at 48 h and the crosslinking extent was calculated (Figure 3-10). It was observed that increasing the crosslinking time from 18 h to 48 has no significant impact on %

crosslinking degree. After statistical evaluation of data (one-way ANOVA, $p > 0.05$), it can be inferred that the corresponding crosslinking extents at respective DIC concentrations were statistically not significant. Therefore, increasing the crosslinking time of above 18 h, the crosslinking degree is not affected no matter how much concentration of DIC is used. The highest crosslinking extent achieved was ~25 - 30 %. This low crosslinking extent might be correlated with the hydrophobicity of diisopropylcarbodiimide. Due to the hydrophobic nature of DIC, the accessibility of the crosslinker into the aqueous core is very limited. Therefore, it can be assumed that the un-crosslinked amino groups should be located in the core of the nanoparticles which have no exposure with the crosslinker. Consequently, the core of the particles is free from the crosslinker. This idea is supported by the DLS measurements as discussed previously, which demonstrated that the crosslinked particles are physicochemically stable in aqueous environments. If the interface of the GNPs is not crosslinked, the un-crosslinked core would get dissolved in water thus forming no particulates.

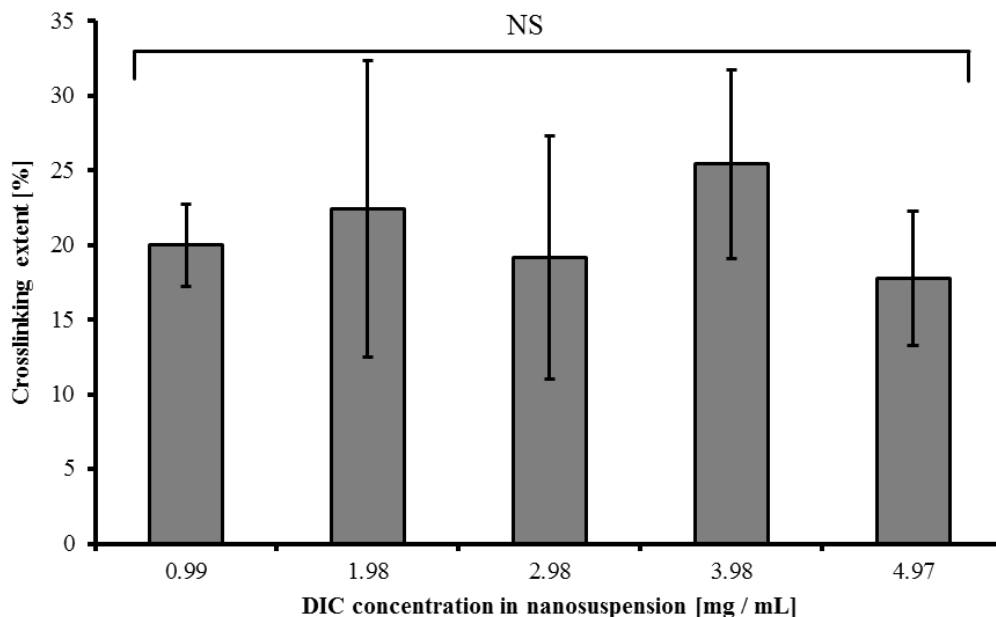


Figure 3-10. Relationship between % crosslinking degree and concentration of crosslinker for 48 h crosslinking reaction time. Values determined by TNBS assay using an absorption maximum of $\lambda_{\max} = 349$ nm, $n = 3$. *Statistics* (NS: Non-significant on the basis of $p > 0.05$ as per one-way ANOVA).

On the basis of results extracted from TNBS assay we can construct a hypothesized model of DIC surface crosslinked GNPs. This model is called as surface-crosslinked GNPs which is characterized by an un-crosslinked core surrounded by a crosslinked outer layer (see Figure 3-11). This model is based on the assumption that the crosslinked functional groups are located on the outside while the un-crosslinked functional groups are located in the interior of GNPs. Moreover, based on the principal that all crosslinkable groups are homogeneously distributed throughout the GNPs matrix, a core-shell GNP sphere is the possible structure which can explain this model. This core-shell structure is composed of an inner sphere of approximately 111 nm radius surrounded by a crosslinked edge of approximately 14 nm (see Figure 3-11).

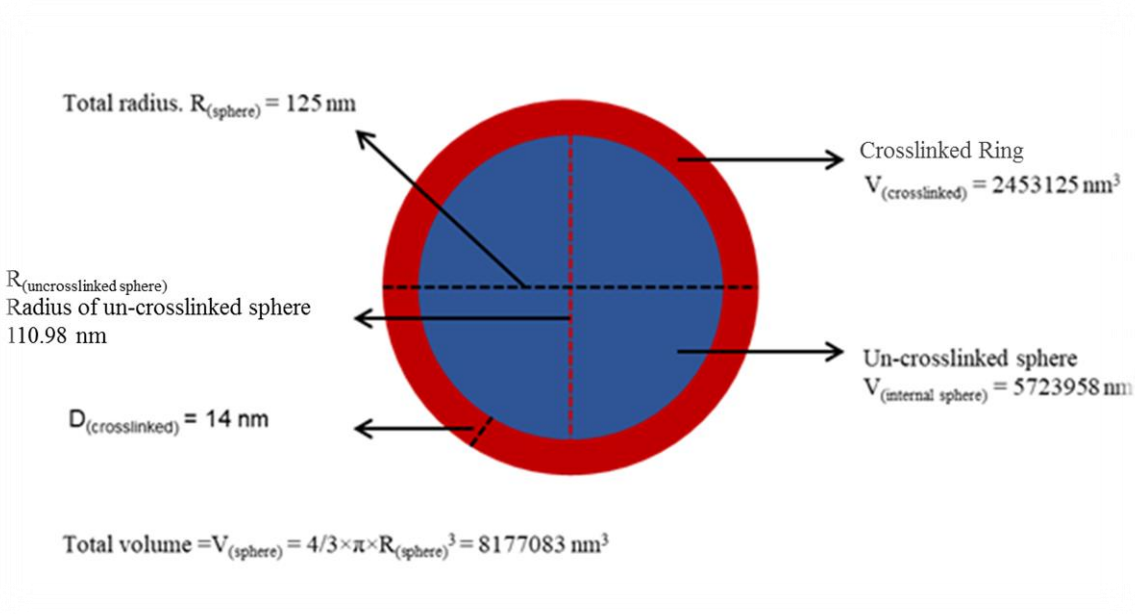


Figure 3-11. Proposed hypothetical model of DIC-crosslinked GNP based on TNBS assay. $V_{(sphere)}$: Total volume of GNP sphere. $V_{(internal \text{ sphere})}$: Volume of non-crosslinked sphere, $V_{(crosslinked)}$: Volume of crosslinked part of GNP, $R_{(un-crosslinked \text{ sphere})}$: Radius of uncross linked part of GNP which is the interior of GNP. $R_{(sphere)}$: Total radius of GNP. $D_{(crosslinked)}$: Thickness of the crosslinked edge (nm).

3.4.2.2. Monitoring of crosslinking

Measurement of un-reacted DIC

The crosslinker (DIC) which remains unreacted during crosslinking was quantified employing gas chromatography (GC) method connected with flame ionization detector (GC-FID). Prior to analysis of actual samples of DIC-crosslinked GNPs, calibration curve was made after plotting peak areas under each GC chromatogram versus corresponding standard concentrations of diisopropylcarbodiimide in acetone. For this study, three different formulations of GNPs with different amounts of crosslinker were analyzed. Briefly, these GNPs suspensions were centrifuged at $20,000 \times g$ for 25 minutes. The supernatant was isolated and analyzed for the amount of un-reacted DIC present in each formulation.

Table 3-11. Relationship between crosslinker amounts (mg) used initially for crosslinking and amounts of DIC consumed in crosslinking of GNPs

Mass of DIC used for crosslinking (mg)	Un-reacted mass of DIC (mg) \pm SD	Reacted mass of DIC ^a (mg) \pm SD	
32.4	26.36 \pm 3.03	6.04 \pm 3.03	} N.S.
48.6	44.40 \pm 0.21	4.20 \pm 0.21	
64.8	57.38 \pm 0.01	6.97 \pm 0.01	

^a: The reacted amounts were found statistically insignificant on the basis of $p > 0.05$ as per one-way ANOVA

From the data in Table 3-11, we can conclude that the converted amounts of DIC are similar regardless of whatever amount of crosslinker being used for crosslinking. As the gelatin concentration and thus the particles concentration is more or less the same, this behaviour is complementary to the TNBS assay results. The summary is that the amount of DIC in the crosslinking process is extremely low. Furthermore, specific amount of crosslinker is participating in the crosslinking of GNPs irrespective of the initial amount of DIC used. This is an indication that the crosslinking process is saturable (see Table 3-11). It can be inferred, the crosslinker (DIC) due to its hydrophobicity has only access to the functional groups which are present at the GNPs interface. Therefore, the crosslinking process ceases when all the functional groups present on the colloidal interface are conjugated.

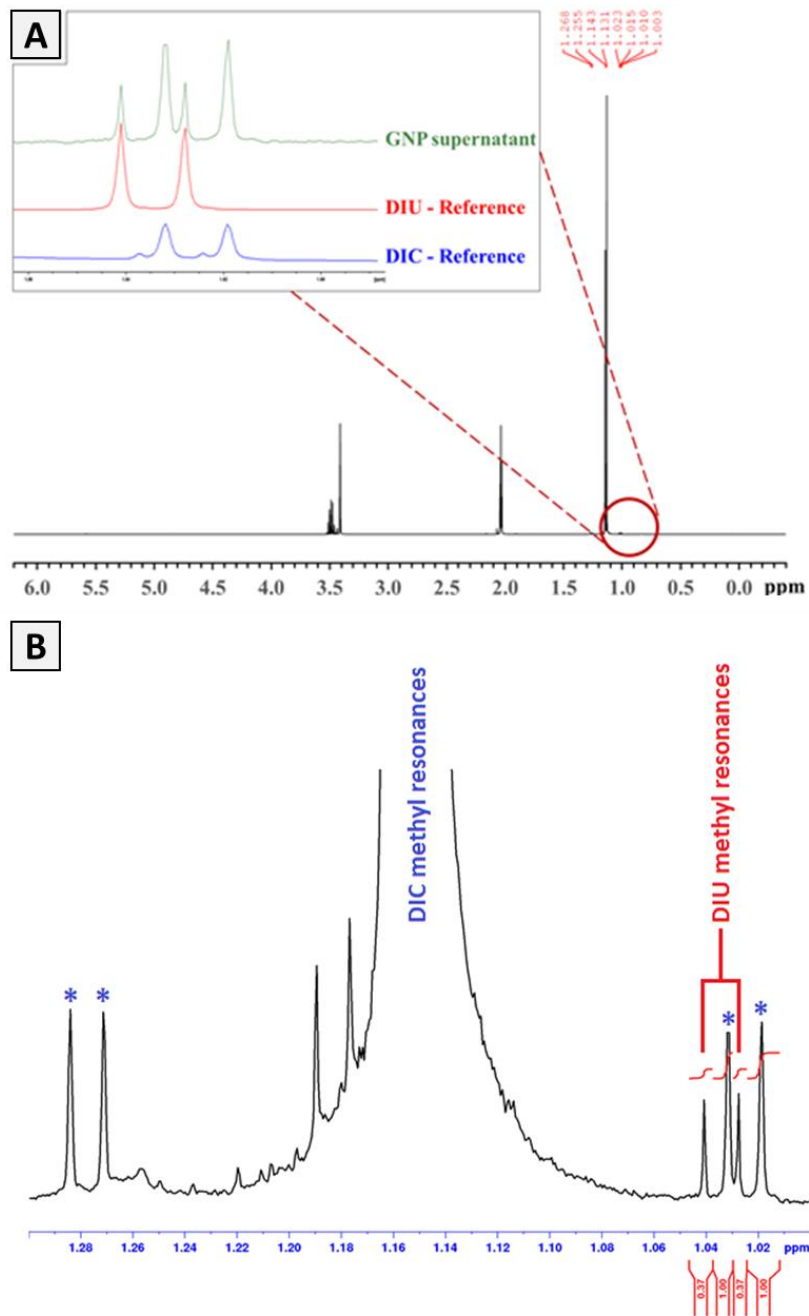
Measurement of diisopropylurea

It is already explained in section 3.4 (Figure 3-3) b) of this chapter, that diisopropylcarbodiimide covalently couples the carboxylic acid groups with the primary amino groups which are present in the GNPs peptidal matrix. This leads to the formation of amide bond which acts as a crosslink. These crosslinks are the foundations of physicochemical and mechanical stability gelatin nanoparticles in hydrophilic media. As a result, DIC is converted into its side-product which is called as diisopropylurea (DIU) that is soluble in organic solvents, *e.g.*, acetone. For the qualitative and quantitative analysis of DIU, ¹H-NMR spectroscopy was employed. For the quantification of DIU in the GNPs

nanosuspension, the supernatant was analyzed using proton NMR spectrometer. For this purpose, DIC-crosslinked GNPs suspension was centrifuged ($24,000 \times g$, for 30 minutes), and so isolating the supernatant and discarding the pellet. Subsequently, the supernatant was analyzed using ^1H - NMR spectroscopy.

The proton NMR spectrum of the crosslinking mixtures showed resonances for DIC together with tiny signals for the by-product DIU providing the methyl resonances for quantification (Figure 3-12 A). In contrast to DIC, the methyl protons of DIU were slightly shifted to higher field appearing almost free of superimposition in the region of the high field carbon-13 satellite of the DIC methyl resonances (Figure 3-12 A, close-up). Therefore, integration of the separate DIU methyl doublet lines as well as the DIC methyl carbon-13 satellite lines could easily be performed (Figure 3-12 B). These integration values were taken to establish the relationship between the amount of DIC and DIU, taken into account that a carbon-13 satellite resonance represented only 0.55 % of the complete peak intensity. This way of quantification provided much more accurate results than a direct integration of the methyl resonances of the main compound DIC. The following equation (4) can be employed to calculate the % DIU amount formed relative to the total amount of DIC present in the reaction mixture.

$$\frac{DIU}{DIC} = \frac{\int DIU \text{ (methyl resonance)}}{\int DIC \text{ high field satellite signal (methyl resonance)} \times 0.55\%} \times 100 \dots\dots\dots(4)$$



*DIC methyl carbon-13 satellites

Figure 3-12. Quantification of the reaction by-product (DIU). (A) ^1H -NMR-spectrum of the supernatant of the crosslinked GNPs. The close-up in green shows the spectrum of the supernatant between 1.00 and 1.06 ppm; in red the signal of DIU methyl protons and in blue the high field satellite peak of DIC. (B) Shows the integration of the DIU methyl resonances and of the DIC methyl carbon-13 satellites.

Formulation Optimization for the Design of Surface-Crosslinked Gelatin Nanoparticles

It is evident from the calculated % relative amounts of DIU measured for each formulation using ^1H NMR spectroscopy (Figure 3-13), that a very low amount of by-product is obtained during the crosslinking of GNPs with diisopropylcarbodiimide. It is also clear that using a fixed mass of gelatin (20 mg), the % relative amount of DIU formed during crosslinking is not dependent on initial amount of DIC being used for crosslinking of GNPs. In summary, it is evident from NMR and GC based measurements that only a certain number of amino and carboxylic functional groups are participating in the crosslinking process of GNPs which is not increasing with increasing the initial amount of crosslinking. Moreover, after comparing these results with TNBS experiments, it can also be concluded that the GNPs are crosslinked to a very low extent using DIC.

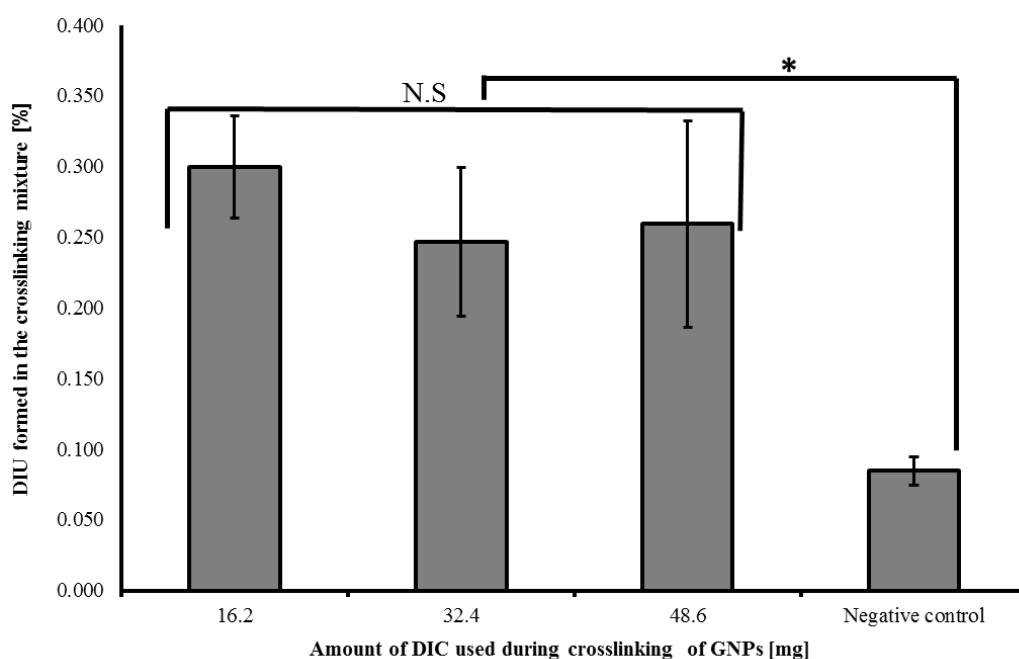


Figure 3-13. Quantification of the reaction by-product DIU. The diagram shows the results of the DIU quantification, calculated by the integral of the corresponding peaks for different amounts of crosslinker. Negative control: sample without gelatin. Statistics (* $p < 0.05$ as per one-way ANOVA, N.S: Non-significant statistically)

In summary, the TNBS assay, gas chromatography and ^1H NMR spectroscopy support the hypothesis of surface crosslinking. Presumably, this is due to the access of crosslinker to a certain number of amino and carboxylic groups which are present in the colloidal interface of GNPs. While, the diffusion of the crosslinker (DIC) into the hydrophilic core of GNPs is very limited or restricted.

3.4.3. Zeta potential of DIC-crosslinked GNPs

The zeta potential of DIC induced-crosslinked gelatin nanoparticles was determined at pH range of 6-10. Due to the fact that gelatin is a poly-ampholyte biopolymer, it contains both cationic and anionic functionalities. Therefore, the net charge of gelatin is dependent on the pH of nanosuspension. Since gelatin-B contains high amount of acidic functional groups (*e.g.*, free carboxylates), therefore it possess an acidic isoelectric point (IEP) of 4.7 - 5.4 [146, 149]. Hence, it can be expected that the GNPs formulated from type B gelatin should have neutral surface charge at pH 4.7 - 5.4 while it should be negative at pH above the 5.4 provided that the isoelectric point is not being altered during crosslinking of gelatin. On the other hand, type A gelatin is basic biopolymer possessing an isoelectric point of 7 - 9 [139, 150]. Therefore, it can be expected that gelatin A nanoparticles should be positively charged at pH below its isoelectric point (pH 7 - 9) and negatively charged at pH >9 provided that the isoelectric point is not being altered during crosslinking of GNPs. The pH dependent zeta potential profile for both types of gelatin can be theoretically represented as shown in Figure 3-14.

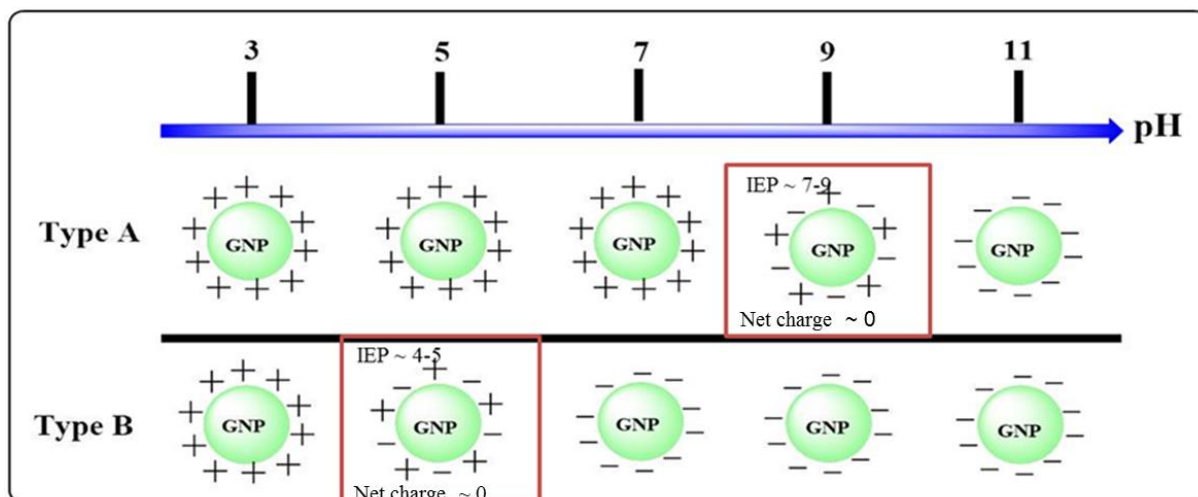


Figure 3-14. Theoretical scheme of pH dependent surface charge of type A and Type B GNPs.

After measuring the zeta potential of DIC-crosslinked GNPs, it is clear (see Figure 3-15) that the zeta potential of gelatin B nanoparticles is slightly positive (\sim between +7 and +11 mV) at pH 5 (isoelectric point of type B gelatin). The surface charge becomes negative at $\text{pH} \geq 7$. The zeta potential approaches to zero at pH range of 6-7. It means that the isoelectric point of gelatin B is increasing up to a value of 6 and 7 as can be seen in Figure 3-15.

Likewise, type A GNPs possess positive zeta potential (approximately +20 mV) at its isoelectric point, *i.e.*, pH 7 - 9. The zeta potential approaches to zero around pH 9.5, hence a slight shifting of IEP towards 9.5. Therefore, it can be inferred that there is slight increase of isoelectric points in both gelatin A as well as gelatin B nanoparticles following crosslinking with diisopropylcarbodiimide.

Looking at the amino acid composition of gelatin B, it contains 2.7% L-lysine and 5% arginine [151]. Assuming that all lysine residues are engaged in the crosslinking leaving behind 5% arginine residues which are un-crosslinked. The pKa value of arginine (12.1) [152] is higher than the pKa value of L-lysine (10.3). Due to the consumption of acidic groups (carbonic acid groups having pKa value of ~ 4) due to crosslinking, the isoelectric point is

shifted to a high pH value (~6.5-7) as can be seen in Figure 3-15 due to the predominance of basic amino acids.

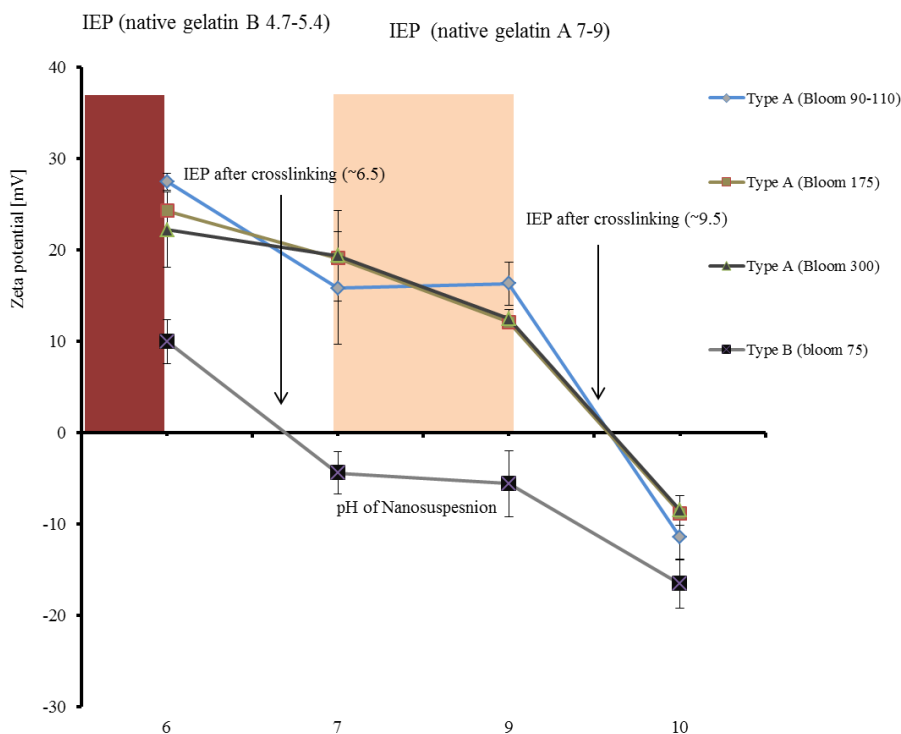


Figure 3-15. Zeta potential of type A and type B GNPs crosslinked with DIC [15 mg/mL] measured at different pH values.

Similarly, the isoelectric point of type A gelatin shifts to pH ~ 9.5. Due to this shift of isoelectric point to higher pH value, the zeta potential of type A GNPs is positive at its native IEP (*i.e.*, pH 7-9) due to the presence of predominantly protonated amino groups on the surface of GNPs.

3.4.4. Morphology of nanoparticles – Scanning Electron Microscopy

The visualization of DIC-induced crosslinked GNPs using scanning electron microscopy (SEM) revealed that they have spherical morphology (Figure 3-16). The mean sizes of particles were also calculated from SEM image using image J[®] (see Table 3-12). It can be observed that the mean size calculated from SEM image is lower than the corresponding mean size measured on DLS. Possibly, this can attributed to drying of dispersion medium

Formulation Optimization for the Design of Surface-Crosslinked Gelatin Nanoparticles

(water) from GNPs droplets before SEM analysis. On the other hand, the particles in aqueous dispersion also include the solvent while measuring the mean diameter which is known as the hydrodynamic diameter in DLS measurements. The same observation has also been reported by other investigators [98, 153].

Table 3-12. Size characterization of DIC crosslinked Type-B GNPs purified *via* tangential flow filtration (TFF)

Formulation name	Mode of purification	Size \pm S.D. [nm]	
		DLS ^{a)}	SEM ^{b)}
DIC crosslinked GNPs	TFF ^{d)} filtration (RC ^{c)} membrane of 100 kDa)	224.5 \pm 1.87 (0.12)	145.33 \pm 58.12

^{a)} terms in parenthesis represent polydispersity index. ^{b)}100 particles analysed using image J software. RC^{c)}: Regenerated cellulose, TFF^{d)}: Tangential flow filtration

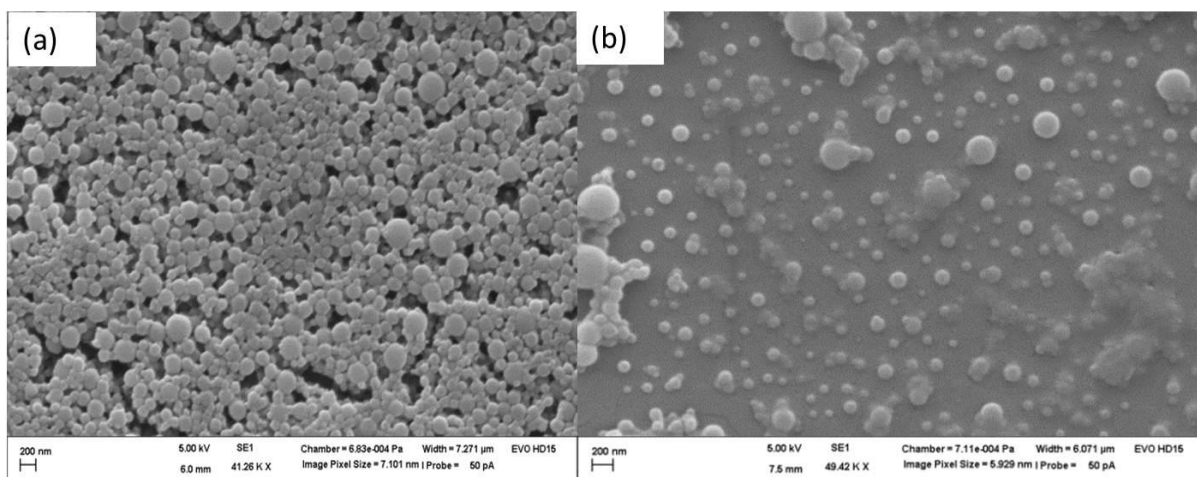


Figure 3-16. SEM images of DIC-crosslinked type B GNPs washed via tangential flow filtration (TFF) set-up containing modified regenerated cellulose membrane (Hydrosart) of 100 kDa pore size. (a) concentrated sample. (b) Diluted sample

3.4.5. Cytotoxicity Evaluation

In order to evaluate the cytotoxicity of DIC-crosslinked GNPs, MTT assay was used. MTT test was performed on four different concentrations of gelatin nanoparticles. The results show no significant cytotoxicity on adenocarcinoma human alveolar basal epithelium cells (A549) incubated with gelatin nanoparticles for 4 hours (Figure 3-17). Thus, it can be concluded that the DIC-crosslinked nanoparticles are biocompatible and do not possess any pronounced *in vitro* toxicity up to 1 mg/mL GNP. Although, the crosslinker diisopropylcarbodiimide (DIC) possesses certain biological toxicity profile, the GNPs crosslinked with DIC show no significant *in vitro* cytotoxicity on A549 cells. The crosslinking of GNPs with DIC involves the formation of only intra-and intermolecular amide or ester bonds which are being established within the gelatin molecules. These newly established amide bonds caused by DIC works as crosslinks. Besides this crosslinking, the crosslinked does not induce any noticeable toxicity in the gelatin matrix. The DIC is converted to its by product, known as diisopropylurea (DIU) which is efficiently removed during the purification process. For a more generalized statement more different cell lines need to be investigated.

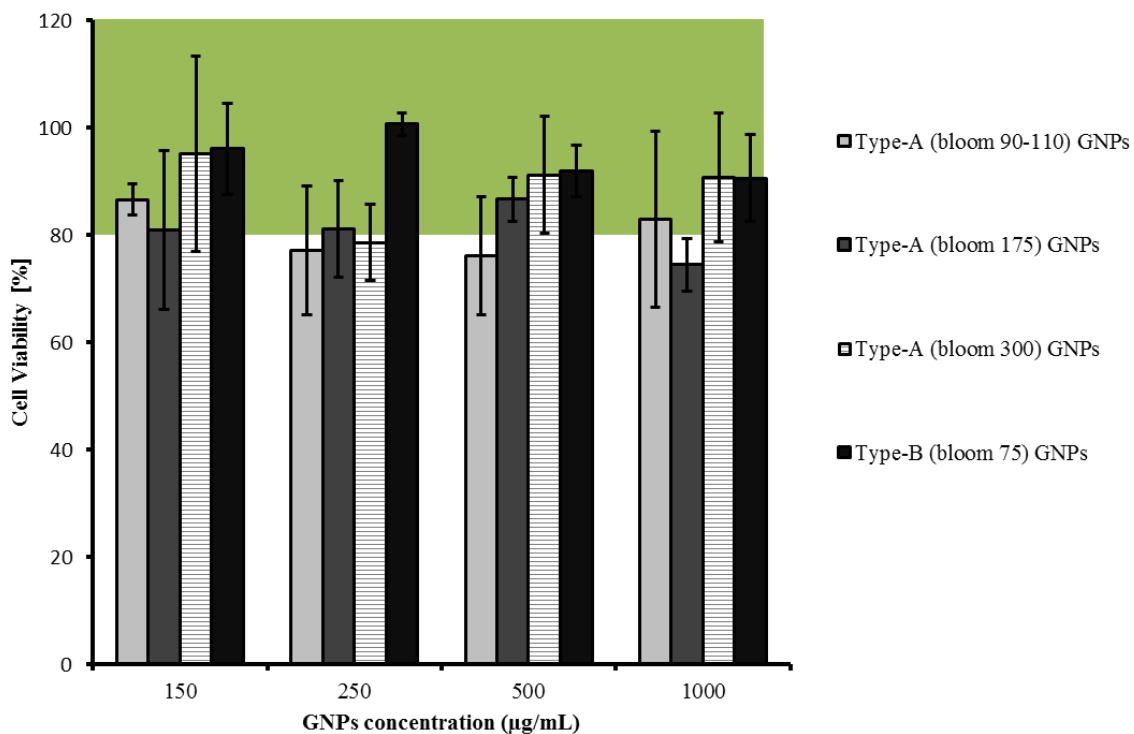


Figure 3-17. Cell viability analysis of DIC-crosslinked GNPs by MTT assay after 4 h incubation on A549 cells. The % viability for all concentrations of GNPs is above 80 %. MTT assay was performed in triplicates and data is average of three independent experiments.

3.5. Conclusions

This research work is focused on efforts to stabilize gelatin nanoparticles after selectively crosslinking the colloidal interface of GNPs produced from both type B and type A gelatin using hydrophobic zero length crosslinker, *i.e.*, diisopropylcarbodiimide (DIC). Crosslinking of GNPs produced as a result of nanoprecipitation resulted in the formation of GNPs of 200 - 300 nm using type B gelatin and 300 - 500 using type A gelatin. The physicochemical stability of crosslinked gelatin nanoparticles in aqueous medium was highly dependent on optimum crosslinker concentration, crosslinking time and temperature of crosslinking mixture. The surface crosslinking phenomenon was supported by saturation of crosslinking degree and the limited utilization of crosslinker during crosslinking reaction. The crosslinking degree of particles increased proportionally with increasing crosslinker concentration until an equilibrium crosslinking degree was achieved (approximately 25 - 30 %) which was not affected further by increasing the crosslinker concentration and crosslinking time. This showed a saturation of the crosslinking process. Assuming a homogenous distribution of primary amino groups within the GNPs matrix, it can be speculated that DIC exhibits reactivity with 25 - 30 % amino groups which are located at the GNPs interface. The rest of 70-75 % amino groups are believed to be located in the core of GNPs which are still un-crosslinked. The morphology of these surface crosslinked gelatin nanoparticles indicates spherical geometry as confirmed by SEM analysis. No cytotoxicity was observed on A549 cell lines. Therefore, it can be concluded that the apolar zero length crosslinker (DIC) only crosslinks the colloidal interface of GNPs dispersed in acetone. These DIC-surface crosslinked gelatin nanomaterials provide a new nanotechnology-based platform thus providing an excellent biodegradable and biocompatible delivery system for hydrophilic macromolecules especially for protein-based APIs.

4 Optimization of Purification Procedures for Surface-Crosslinked Gelatin Nanoparticles

Parts of this chapter have been published in:

Abdul Baseer, Aljoscha Koenneke, Joseph Zapp, Saeed A. Khan, Marc Schneider, Design and Characterization of Surface Crosslinked Gelatin Nanoparticles for the Delivery of Hydrophilic Macromolecular Drugs. *Macromolecular Chemistry and Physics*. 2019. **220**(18): p. 1900260.

4.1. Abstract

This chapter is focused on comparative evaluation of different techniques employed for the purification of diisopropylcarbodiimide-induced surface-crosslinked gelatin nanoparticles. These methods include centrifugation, dialysis and crossflow filtration. In this chapter, the purification efficiency of the two purification techniques, *i.e.* dialysis and tangential flow filtration in terms of removing excess stabilizer (poloxamer 188), un-reacted crosslinker and its by-product from the crude crosslinked GNPs suspension was investigated. Moreover, the effect of certain critical process parameters, *e.g.*, membrane type, pore size of membrane and amount of washing water used on the purification performance and physicochemical properties of nanoparticles were evaluated. According to this comparative evaluation, the tangential flow filtration was found to be comparatively efficient and straightforward method than dialysis and centrifugation.

4.2. Introduction

As discussed in detail in chapter 1 (section 1.5.1.1), gelatin nanoparticles can be prepared using different formulation techniques. During particles' formulation there are certain formulation additives and side products whose removal from the nanoparticles suspensions is indispensable. These additives and side products include the excess amounts of stabilizers, polymerizations initiators, chemical crosslinkers and their by-products, etc. In general, different approaches have been reported for the purification of polymeric nanoparticles to get rid of these impurities. These include micro-filtration [154, 155], centrifugation and ultracentrifugation [154, 156, 157], gel-filtration [158], dialysis [159], diafiltration [160, 161] and cross-flow microfiltration [154, 162]. The most commonly used approaches are centrifugation and ultracentrifugation which are comparatively advantageous in removing large quantities of impurities from the crude nanosuspensions [163, 164]. Although, centrifugation is a simple, straightforward and highly reported purification approach, it has some serious demerits. Amongst these demerits, the centrifugation at high speed sometimes produces hard pellets of nanoparticles which are very difficult to re-disperse in water [165]. The problem of re-dispersibility becomes more pronounced when organic solvents, *e.g.*, acetone and alcohol are used as dispersion media [99]. In order to avoid this problem, low speed centrifugation is used but this leads to a significant loss of nanoparticles and consequently low yield of nanoparticles. While using dialysis as a purification tool, it results in the release of drug loaded in nanoparticle due to lengthy duration of operation. While using size exclusion chromatography (SEC), very low amounts of nanoparticles can be processed. During formulation of DIC-crosslinked gelatin nanoparticles following nanoprecipitation, there are certain undesired hazardous substances present in the final crude nanosuspension system. These include excessive amounts of stabilizers such as poloxamer 188, the un-reacted crosslinker (DIC) and its by-product, *i.e.*, diisopropylurea (DIU). To remove these impurities

from the crude nanosuspensions, an effective purification methodology of nanoparticles is highly demanding.

In our application, while employing the centrifugation as a purification tool, the surface-crosslinked nano-formulation consisting of DIC-crosslinked GNPs also suffer from non-redispersibility. The pellet obtained after centrifugation cannot be re-dispersed in water despite vigorous mechanical shaking. Even, application of ultra-sonication assisted sheer stress did not solve the problem of re-dispersibility.

Therefore, in order to avoid the formation of non-dispersible pellet and loss of particles, we attempted to use tangential flow filtration (TFF) and dialysis membrane filtration as a purification tools for washing of these DIC-mediated surface-crosslinked gelatin nanoparticles.

In the work discussed in this chapter, we optimized the tangential flow filtration for the purification of DIC-crosslinked gelatin nanoparticles. For comparative evaluation, the particles were also purified using low speed centrifugation and dialysis. For the assessment of purification performance of TFF and dialysis-based purification, the residual amounts of poloxamer 188, unreacted crosslinker and its by-product in the final product were determined employing cobalt-thiocyanate colorimetric assay, gas chromatography (GC) and $^1\text{H-NMR}$ spectroscopy, respectively. The ultra-filtration (TFF, dialysis) and centrifugation-based purified surface-crosslinked gelatin nanoparticles (scGNPs) were characterized in terms of mean size and size distribution using dynamic light scattering. For morphological characterization of purified GNPs, scanning electron microscopy (SEM) was used.

4.3. Experimental

4.3.1. Materials

Gelatin B bloom75 from bovine skin, was obtained from Sigma-Aldrich, Munich, Germany. Acetone was obtained from VWR-International, Darmstadt, Germany. Tangential flow filtration (TFF) cassettes (Vivaflow 50 R) fitted with modified regenerated cellulose material (hydrosart) with a pore size of 30 kDa and 100 kDa were purchased from Sartorius Stedim Biotech Ltd., Goettingen. Another TFF setup (MinimateTM TFF capsule) with a pore size of 300 kDa, composed of polyethersulfone was purchased from VWR international Ltd., Darmstadt, Germany. Dialysis membranes (spectra/por7 flat trial kit having flat width of 28 mm, diameter of 18 mm, volume of 2.5 mL/min) composed of regenerated cellulose was purchased from Spectrum Laboratories, Europe B.V., Breda, Netherland). Milli-Q water with a resistivity of 18.2 M Ω ·cm was used throughout the experiments.

4.3.2. Preparation of DIC-crosslinked gelatin nanoparticles

The DIC-crosslinked gelatin nanoparticles were prepared following the standard protocols mentioned in chapter 3, section 3.3.2.

4.3.3. Purification of DIC-crosslinked GNPs

For the purification of crude nanosuspension, the purification tools, *i.e.*, centrifugation, dialysis and cross-flow filtration were employed and evaluated in terms of removal effectiveness from impurities, *i.e.*, the stabilizer (poloxamer), the crosslinker (DIC) and its side product, diisopropylurea (DIU).

4.3.3.1. Centrifugation

Since, high speed centrifugation leads to formation of hard pellet of NPs which cannot be re-dispersed in water, the DIC-surface linked GNPs suspension system was purified with three different sets of centrifugation conditions followed by re-dispersion in water. The centrifugation conditions included a speed of 3000×g for 10 minutes, 5000×g for 15 minutes, 3000×g for 25 minutes and speed of 3000×g for 30 minutes. The crude nanosuspensions were purified with one time centrifugation.

4.3.3.2. Dialysis

The dialysis membrane composed of regenerated cellulose (RC) with a pore size of 50 kDa was employed for purification. Regenerated cellulose was used because of its compatibility to a wide range of organic solvents including acetone. In our application scenario, as all the impurities of the crude dispersion system are soluble in acetone, hence dialysis was performed in acetone as a dialysate reservoir for 24 h. The dialysate was re-freshed after 1 h, 2h and 24 h. For dialysis experiment, a sample volume of 16 mL crude nanosuspension was filled in pre-washed regenerated cellulose membrane tube of 5 cm in length. Afterwards, the dialysis tube filled with crude nanosuspension was immersed in 600 mL acetone as a dialysate reservoir. The dialysis process was continued for 24 h sufficient time to completely remove all the impurities from the nanosuspension.

4.3.3.3. Tangential flow filtration (TFF)

Two types of TFF assemblies with different membranes types and pore size were employed. The vivaflow TFF cassettes (Vivaflow 50R, Sartorius, Goettingen) and Minimate™ TFF capsule (Omega™ 300 kDa, VWR international Ltd., Darmstadt, Germany) were used for the purification of DIC-crosslinked GNPs crude suspension. The membranes with three molecular weight cut-offs, *i.e.*, 30, 100 and 300 kDa were used. The construction material of vivaflow

Optimization of Purification Procedures for Surface-Crosslinked Gelatin Nanoparticles

50 R was modified regenerated cellulose which is also known as hydrosart. According to specifications of manufacturer (Sartorius), the material, hydrosart, demonstrates highest degree of resistance to organic solvents. Another TFF device, *i.e.*, Minimate™ TFF capsule fitted with polyethersulfone (PES) membrane having pore size of 300 kDa was also employed. Since, the material PES is not completely compatible to acetone, therefore, the nanosuspension containing acetone as a main dispersion medium was diluted 10 times with water before starting TFF operation. With acetone concentration less than 10 % v/v, PES membrane showed compatibility. In terms of compatibility, the TFF device used here is not 100 % compatible to acetone. Some parts of the device, *e.g.*, the casing and tubings are composed of polycarbonate and nylon, respectively, which are not compatible to acetone. For this purpose, prior to starting TFF based washing, the crude nanosuspension was diluted with sufficient water to make the fraction of acetone below 10 % (v/v) for making the device components acetone compatible.

The purification of crude nanodispersion using TFF involves passing the formulation parallel to the membrane surface (see Figure 4-1 a). The crude nano-suspension is then divided into two streams. One stream known as filtrate or permeate is composed of impurities having molecular weights smaller than the pore size of membrane. The other part known as retentate is the washed nanoparticles which is retained and re-circulated back into the initial container holding the crude nanosuspension. The working principal of TFF based purification of surface-crosslinked gelatin nanoparticles is shown schematically in Figure 4-1 (b).

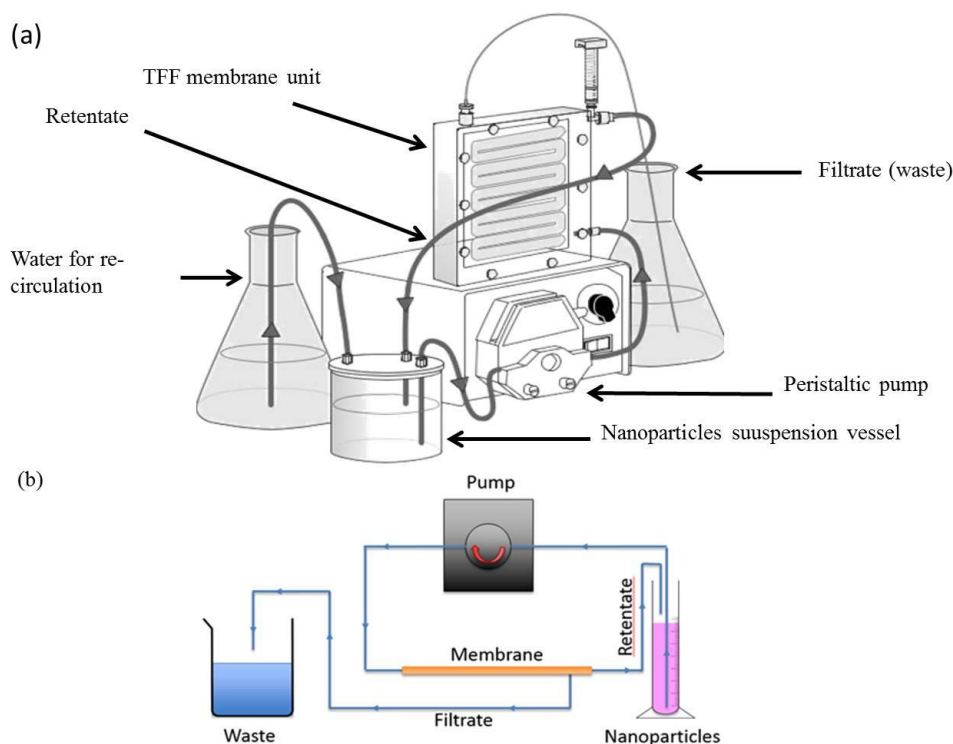


Figure 4-1. Schematic representation of TFF assembly used for the purification of sc-GNPs. (a). External overview of TFF assembly. (adapted from product operational manual provided by Sartorius) (b). Scheme of the working principal of TFF assembly.

4.3.4. Evaluation of purification performance

The purification efficiency of dialysis and TFF-based ultra-filtration was evaluated in terms of % clearance of stabilizer (Poloxamer P-188), unreacted crosslinker (DIC) and its by-product (DIU) from the DIC-crosslinked gelatin nanosuspension.

4.3.4.1. Quantification of poloxamer

For the quantification of poloxamer-188, a colorimetric assay known as cobalt thiocyanate method was used [166-168]. This assay is based on the formation of a water insoluble complex between poloxamer molecules and a dye known as cobalt thiocyanate. For the solubilization of this water insoluble complex, acetone was used, and subsequently quantified spectrophotometrically using 624 nm as the absorption maximum. The poloxamer content in the samples is proportional to poloxamer-complex formation. Briefly, the cobalt thiocyanate

Optimization of Purification Procedures for Surface-Crosslinked Gelatin Nanoparticles

solution was made after dissolving 3 g of cobalt (II) nitrate and 20 g of ammonium thiocyanate in Milli-Q water (100mL). Afterwards 1 mL from cobalt-thiocyanate solution was transferred to 10 mL falcon tube. To this solution, 2 mL of poloxamer solution and 2 mL of ethyl acetate was added followed by vigorous mixing. After mixing, the mixture was centrifuged (Thermo Fisher Scientific, Osterode am Harz, Germany) at $1000 \times g$ for 5 minutes [168]. After centrifugation, the poloxamer-cobalt complex was sedimented and the upper two layers formed by aqueous solution and ethyl acetate was discarded. The sedimented pellet was washed with 2 mL ethyl acetate followed by re-centrifugation at $1000 \times g$ or 5 minutes. The centrifugation and redispersion in ethyl acetate was repeated several times till the upper layer consisting of ethyl acetate solution became colourless. After washing thoroughly with ethyl acetate, 10 mL of acetone was added to the falcon tube followed by vigorous mixing until the pellet was completely dissolved in acetone. The calibration as well as the unknown samples (supernatants of GNPs formulation) were prepared in the same way. The absorbance at 624 nm was recorded using UV-Vis Spectrophotometer (Perkin-Elmer Lambda 35, Rodgau, Germany) against a blank. Calibration curve was constructed based on the above mentioned colorimetric assay. In order to quantify the poloxamer present in the TFF-based washed suspension containing surface-crosslinked GNPs, the suspension was centrifuged at $20000 \times g$ for 20 minutes. The supernatant was extracted and analysed for the amounts of poloxamer using the calibration curve based on the cobalt thiocyanate assay and subsequently, the corresponding amounts of poloxamer present in the supernatants of dialysis and TFF washed crosslinked GNPs were calculated. For the quantification of residual amounts poloxamers in dialyzed samples, the acetone of the extracted supernatant was evaporated at room temperature and reconstituted with similar amount of Milli-Q water and then following the same procedure as was discussed for TFF washed samples.

4.3.4.2. Quantification of un-reacted crosslinker (DIC)

For the measurement of residual amounts of DIC in the purified nanosuspension, the lyophilized DIC-crosslinked GNPs were re-dispersed in acetone to re-dissolve the residues of DIC if present in the purified nanoparticles. The dispersion was then centrifuged at $20,000 \times g$ for 20 min. The supernatant was withdrawn for the quantification of residues of DIC using the validated gas chromatography method (Shimadzu GC-2010, Japan) connected with flame ionization detector (FID) (Shimadzu GC-2010, Japan). The procedure of gas chromatography-based quantification has been described in chapter 3 (section 3.3.6). Briefly, Supreme 5-MS column with a length of 25 mm and inner diameter (ID) of 0.25 mm was used which contained 5% phenylpolysilphenylsiloxane as a packing material with a film thickness of 0.25 μm . The carrier gas used was a mixture of nitrogen and air. The flow rate of carrier gas was 1.24 mL/min. The injection mode selected was split with a split ratio of 1:10. The total run time was 28 minutes. During the elution process, the temperature of column oven was raised up to 40°C followed by warming to 220°C with a heating rate of 10°C/min. The temperature of 220°C was hold for 5 minutes. For the detection and quantification of DIC, flame ionization detector (FID) was used.

For the quantification of DIC, a calibration curve was constructed by plotting the corresponding peak areas in the GC chromatograms versus different DIC concentration (mg/mL) in acetone.

4.3.4.3. Quantification of crosslinking by product (DIU)

For the measurements of traces of by-products (DIU) present in the purified GNPs, the lyophilized GNPs samples were dispersed in deuterated acetone (NMR grade acetone) to re-dissolve the residual DIU if present in the washed gelatin nanoparticles. Subsequently, the suspension was centrifuged at $20,000 \times g$ for 20 minutes. The supernatant was isolated for quantification of traces of DIU present in the dialysis/TFF washed nanoparticles using ^1H -

NMR spectroscopy. For this purpose, ^1H -NMR spectra were recorded at 298 K in acetone- d_6 with a Bruker Avance 500 spectrometer (Bruker, BioSpin GmbH, Rheinstetten, Germany) equipped with a 5 mm BBO probe. The chemical shifts were reported in parts per million (ppm) relative to the solvent peak at δH 2.05.

4.3.4.4. Fourier Transform-Infrared (FT-IR) analysis of crosslinked GNPs

As explained in the mechanism of DIC-based crosslinking of gelatin nanoparticulates (see chapter 3, section 3.4.1) that DIC establishes amide bonds within the gelatin molecules, and is itself transformed into diisopropylurea. Nevertheless, for the experimental confirmation that the crosslinker (DIC) does not become a part of gelatin molecule during crosslinking reaction, the lyophilized samples of TFF-washed GNPs being crosslinked with different amounts of DIC were analysed using Fourier transform infrared spectrometer (FT-IR spectrometer (Tensor 27, Bruker, Ettlingen, Germany)). The FT-IR spectra were recorded in transmittance mode over a wavenumber range of 400-5000 cm^{-1} . Each spectrum was the accumulation of 32 scans. The software used was OPUS V4.

4.3.5. Measurement of particle size

The size (z-average mean) and size distribution of centrifugation, TFF and dialysis-based washed surface crosslinked gelatin nanoparticles was analysed using dynamic light scattering using a Zetasizer nano-ZS (Malvern Instruments Ltd., Worcestershire, UK). The nanoparticles suspension was 10 times diluted with Milli-Q water at 25°C before measurement. Each sample was analysed in triplicates for three independent experiments.

4.3.6. Morphological Characterization

4.3.6.1. Scanning Electron Microscopy (SEM)

For SEM imaging, a drop of 20 μL of purified nanosuspension was dropped onto a silicon wafer already mounted on a metal hub using carbon adhesive tape. Afterward, the samples were allowed to dry overnight by evaporation at room temperature. Before SEM imaging, samples were coated with gold layer of approximately 15 nm, in an atmosphere of argon using sputter coater Q150 RES (Quorum Technologies Ltd. Laughton, UK). SEM images were recorded using EVO HDI5 microscope (Carl Zeiss Microimaging, GmbH, Jena, Germany).

4.4. Results and Discussion

After the production of nanoparticles, a crucial step is the purification of nanoparticles from the undesired impurities. The subsequent characterization of nanoparticles, *e.g.*, the *in vitro* and *in vivo* evaluation and imaging, *e.g.*, SEM, SPM and TEM measurements are mostly conducted with washed nanoparticles. In this context, numerous methods have been reported for the purification of nanoparticles. These include centrifugation, ultra-centrifugation, dialysis, tangential flow filtration, *etc.* The nanoparticles are necessarily purified from impurities such as the un-reacted crosslinker, its by-products and excessive amounts of stabilizers. Centrifugation is the most commonly used method for the purification of polymeric nanoparticles. However, when the particles are dispersed in organic solvents (*e.g.*, acetone, alcohol *etc.*), then centrifugation at higher speeds leads to formation of strong pellets which are not easily re-dispersible in water [99]. On the other hand, centrifugation at a low speed results in low nanoparticles yield.

In our scenario, the DIC-crosslinked GNPs cannot be purified with centrifugation-based washing due to the formation of non-dispersible pellet. Therefore, it was necessary to use alternative purification methods.

In this context, we optimized the ultra-filtration in tangential flow filtration (TFF) mode for the purification of DIC-induced gelatin nanoparticles. The effect of different pore sizes of membrane and its possible impact on purification performance and the physicochemical properties of nanoparticles will be investigated to get a highly purified and stable nano-formulation of DIC surface crosslinked GNPs.

4.4.1. Nanoparticles preparation

The formation of gelatin nanoparticles (GNPs) was carried out following the standard formulation as described in chapter 3 section 3.4.1.

4.4.2. Optimization of purification

4.4.2.1. Centrifugation

After getting DIC-induced crosslinked GNPs suspension, it was purified with centrifugation followed by re-dispersion in water. The centrifugation was carried out at different speed and time. The mean size and size distribution of purified gelatin nanoparticles corresponding to each parameter is shown in Table 4-1. The DLS measurements indicate that increasing the speed of centrifugation and time, the mean size is also increased. Besides, the nano-dispersion is also showing in-homogeneous distribution at high centrifugation speeds and longer times of centrifugation. This is because the GNPs are converted to a strong pellet which is very difficult to re-disperse in water.

Table 4-1. Effect of centrifugation speed and time on mean size and size distribution. (*) Particles were centrifuged once.

S.No.	Time [min]	*Centrifugation speed (\times g)	Mean size [nm] \pm S.D.	PDI \pm S.D.
1	10	3000	277.58 \pm 0.14	0.18 \pm 0.06
2	15	5000	307.20 \pm 11.93	0.27 \pm 0.03
3	25	3000	310.23 \pm 11.70	0.24 \pm 0.01
4	30	3000	277.19 \pm 7.15	0.26 \pm 0.03

So, the appropriate centrifugation speed and time at which the pellet can be re-dispersed in water is 3000 \times g for 10 minutes. These nanoparticles possess the desired characteristics in terms of particle size (200 - 300 nm with PDI less than 0.2). But using centrifugation-based purification has two demerits. Firstly, the lower centrifugation speed leads to significant loss of particles (the data regarding the yield is not shown). Secondly, the particles cannot be purified completely from the impurities using one time centrifugation. So, in order to get stable nanoparticles with desired mean size and PDI with maximum particles recovery, it is necessary to purify the DIC-crosslinked GNPs suspension using alternate methods of purification.

4.4.2.2. Dialysis and cross-flow filtration

In order to by-pass the formation of non-redispersible pellet, dialysis and tangential flow filtration fitted with ultra-filtration membranes of different pore sizes were employed. The selection of membrane type and pore size was based on compatibility with acetone and molecular weights of impurities which need to be removed from the GNPs suspension. The physicochemical properties of these impurities are summarized in Table 4-2. For the effective removal of unwanted impurities as listed in Table 4-2 from the nanosuspension, the selected pore sizes of membrane used, *i.e.*, 30, 50, 100 and 300 kDa are bigger than the molecular weights of impurities listed in Table 4-2.

Table 4-2. Impurities of DIC crosslinked GNPs

Impurities	Molecular weight (g/mol)	Solubility
Poloxamer 188	8400	Soluble both in water and acetone
Diisopropylcarbodiimide	126.20	Soluble in acetone and water insoluble
Diisopropylurea	144.22	Soluble in acetone and water insoluble

4.4.3. Evaluation of purification performance

4.4.3.1. Removal of Poloxamer-188

The pore size of filtration membrane and amount of washing water used was found to be the rate limiting factors in purification efficiency in removing the poloxamer 188 having the molecular weight of ~ 8400 g/mol from the crude suspension of scGNPs. After quantitative determination of poloxamer 188 concentrations in the supernatant of dialyzed as well as TFF washed nanoparticles, it was observed that the purification efficiency is high while using higher pore size ultra-filtration membrane. The purification efficiency was expressed as % removal of poloxamer 188 from the nanosuspension (see Figure 4-2 a). The maximum pore size suitable for removal of poloxamer was found to be 300 kDa. Similarly, the amount of water in the washing cycle results in enhanced permeation of poloxamer across the membrane (see Figure 4-2 b). Therefore, the rate limiting factor of purification efficiency is both pore size of ultra-filtration membrane (maximum pore size of 300 kDa) and water utilization (> 2000 mL for a volume of 16 mL crude nanosuspension).

The pore size of dialysis membrane was smaller than the pore size of TFF membrane, and the comparison of purification efficiencies of the two purification methodologies using membranes of different pore sizes is not rational. But, the main disadvantage of dialysis-based purification is the non-flexibility of exchange of dispersion medium, *i.e.*, the dialysis cannot be performed in water as a dialysate if the crosslinked GNPs are dispersed in acetone. While

Optimization of Purification Procedures for Surface-Crosslinked Gelatin Nanoparticles

using water as a dialysate for purifying the particles dispersed in acetone, it leads to an extensive agglomeration of particles inside the dialysis bag which cannot be re-dispersed. Secondly, the dialysis cannot be performed in water due to the insolubility of crosslinker (DIC) and its by product in water. Due to these demerits, dialysis is not a good choice for the purification.

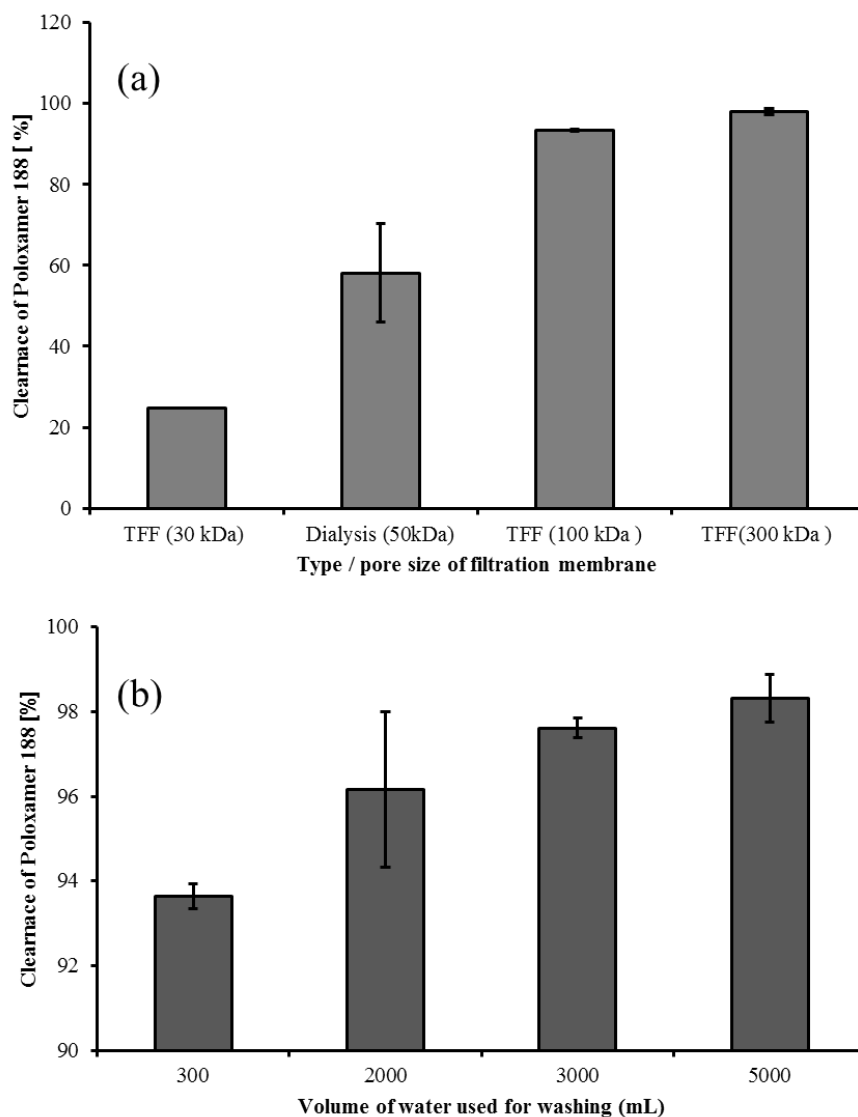


Figure 4-2. Purification efficiency of TFF and dialysis-based purification in terms of % clearance of poloxamer and effect of critical parameters. (a) Effect of membrane pore size, and (b) effect of water amounts used in re-circulation using 100 kDa membrane using TFF based purification.

4.4.3.2. Removal of un-reacted crosslinker (DIC)

After analysis of supernatant of redispersed lyophilized GNP in acetone using a validated gas chromatography method, it was observed that the un-reacted crosslinker can be effectively removed from the suspension to approximately 100 % after purification with both dialysis (50 kDa pore size) for 24 h and TFF filtration (pore size of 100 kDa and 300 kDa) for 8 h. There is no peak for any residual amount of DIC observed in the gas chromatogram of dialysis- and TFF-purified samples (see the GC chromatograms of washed samples in Figure 4-3).

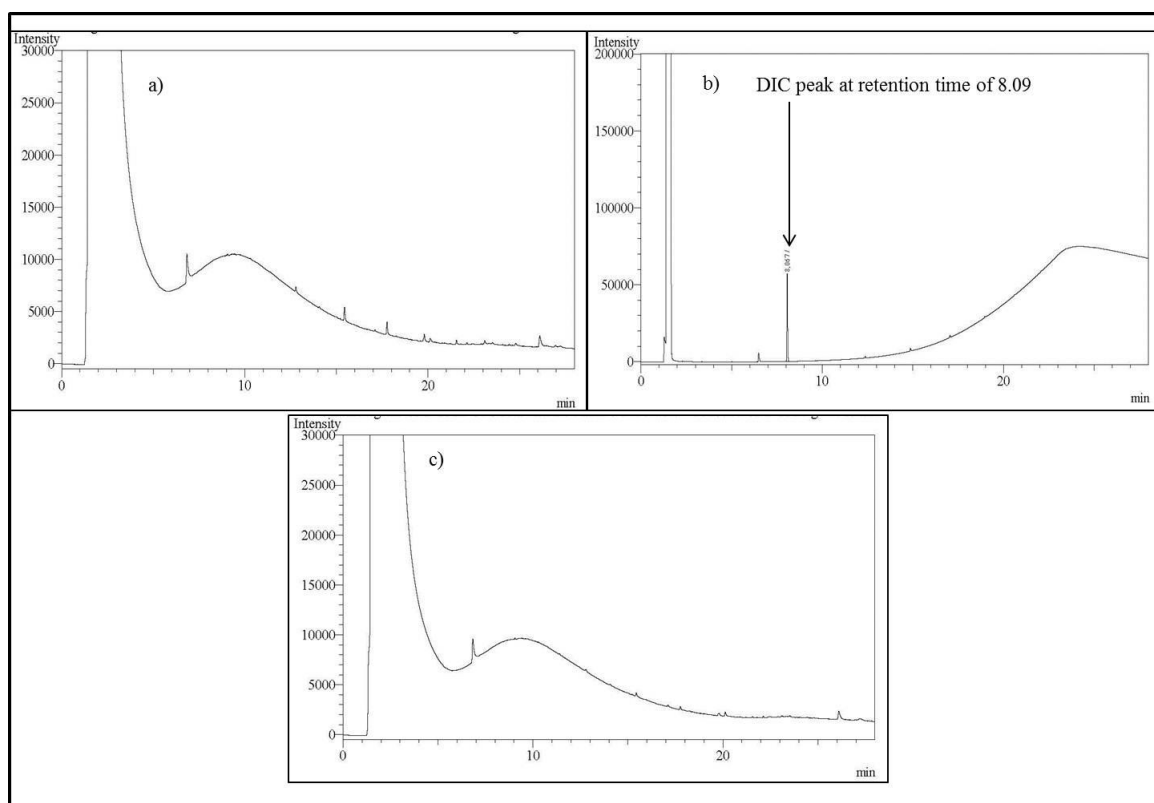


Figure 4-3. GC chromatograms. (a). DIC-crosslinked GNPs washed with dialysis. (b) Reference compound of DIC. (c). DIC-crosslinked GNPs washed with TFF filtration.

4.4.3.3. Removal of crosslinking by product (DIU)

For the detection and quantification of the by-product *i.e.*, diisopropylurea (DIU) in the dialysis and TFF purified samples, the supernatant of both dialysis and TFF washed crosslinked GNPs was isolated after centrifugation at $20,000 \times g$ for 20 min. In $^1\text{H-NMR}$

spectra of supernatant, no NMR signals corresponding to DIU were observed in the mixture (see Figure 4-4 for the ^1H NMR spectra of washed NPs).

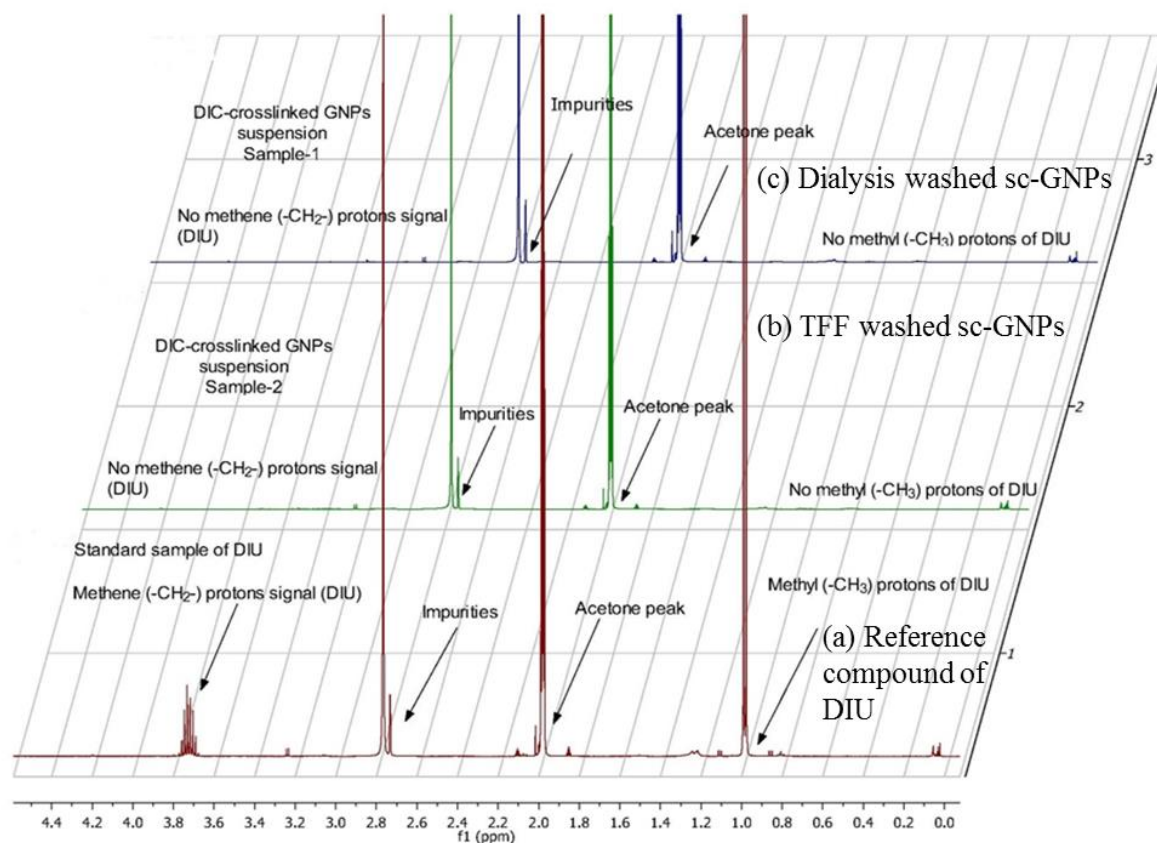


Figure 4-4. Proton NMR (^1H -NMR) spectra of supernatant of washed nanoparticles taken in deuterated acetone. (a) ^1H -NMR spectrum of standard compound of DIU. (b) ^1H -NMR spectrum of TFF purified scGNPs samples. (c) ^1H -NMR spectrum of dialysis washed scGNPs sample.

4.4.3.4. Fourier Transform-Infrared (FT-IR) analysis of crosslinked GNPs

The FT-IR spectrum of native gelatin is characterized in terms of 5 types of infra-red (IR) absorption bands, known as amide bands. These are 5 sub-types of amide bands which are termed as amide A, amide B, amide I, II and III. The corresponding IR frequencies and functional groups representing these amide bands are elaborated in Table 4-3. FTIR spectra taken for both un-cross-linked as well as cross-linked gelatin are almost superimposed on

each other indicating that no structural change is induced by the crosslinker (see Figure 4-5). Besides, there is no significant change in the position of already present absorption bands.

Table 4-3. IR absorptions bands of gelatin and corresponding vibrational frequencies and functional groups

IR band	Wavenumber (cm ⁻¹)	Functional group
Amide-A	3200-3400	N-H stretching
Amide-B	2800-3100	C-H stretching
Amide I	1660-1600	C=O stretching
Amide II	1565-1500	C-N stretching and N-H bending
Amide III	1240	C-N stretching

Moreover, the FTIR spectra also demonstrated that no additional peak for the crosslinker DIC and its degradation product (diisopropylurea) was observed which reveals that DIC does not become a part of the peptidal structure of gelatin. It is clear from the crosslinking mechanistic explained in section 3.4.1, that the DIC conjugates only the free carboxylic and free amino groups constituting amide bond which acts as a crosslink which stabilizes the gelatin nanoparticles. Due to these stabilization bonds, the DIC-crosslinked gelatin do not dissolve in aqueous environments.

In summary, the stabilizer (poloxamer), the un-reacted crosslinker (DIC) and its by-product (DIU) are efficiently removed from the nanosuspension using TFF based purification as compared to dialysis, as explained in Table 4-4.

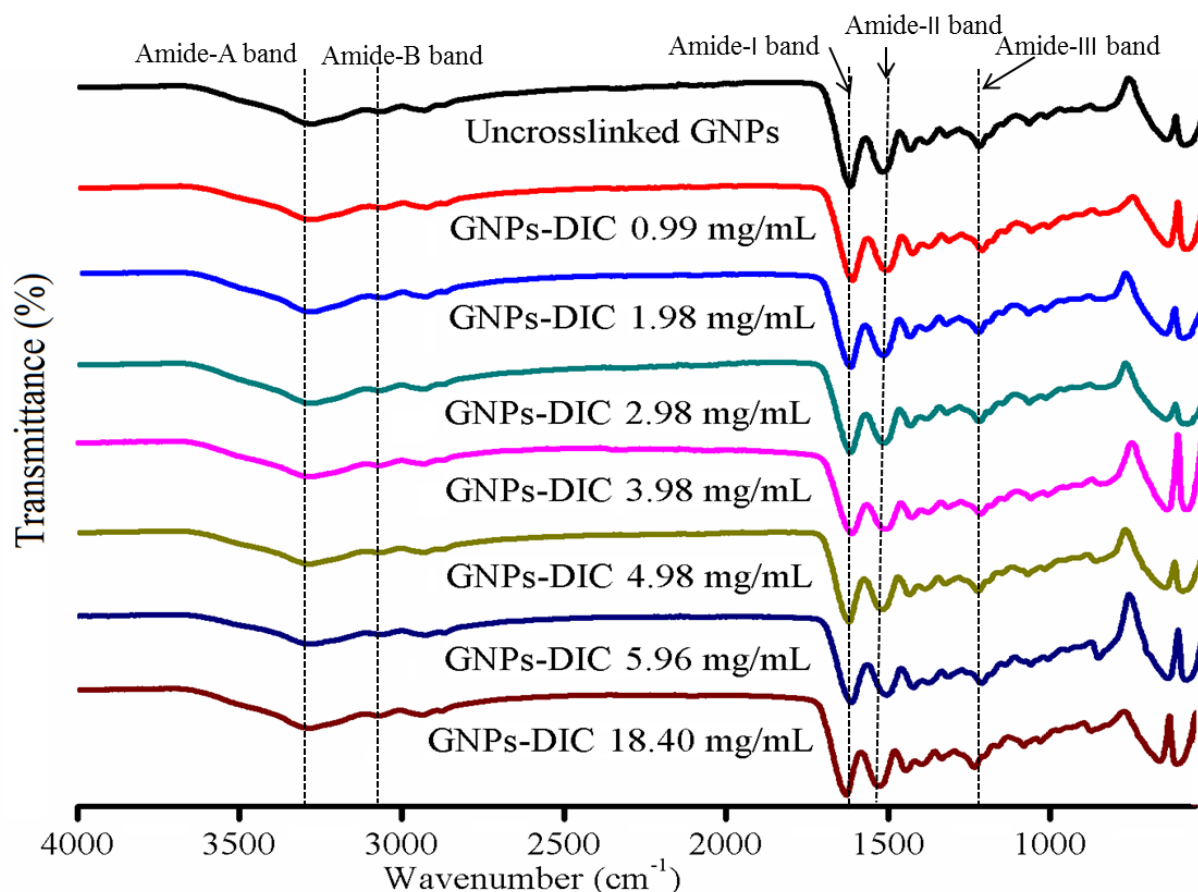


Figure 4-5. FT-IR spectra of GNPs crosslinked with different amounts of crosslinker (DIC) purified with tangential flow filtration.

Table 4-4. Comparison of TFF and dialysis in terms of removal of poloxamer 188, DIC and DIU from crude nanosuspension of DIC-crosslinked GNPs.

Impurities	Purification efficiency (%)	
	Dialysis ^a	TFF ^b
Poloxamer -188	58.10 ± 12	98.3 ± 0.56
Diisopropylcarbodiimide (DIC)	100	100
Diisopropylurea (DIU)	100	100

^a50 kDa pore size; ^b100 kDa pore size

4.4.4. Measurement of particle size and size distribution

4.4.4.1. Effect of membrane type and pore size

All TFF and dialysis-based washed samples of DIC-crosslinked GNPs possess nearly the same size and size distribution irrespective of membrane type and its pore size. All the

Optimization of Purification Procedures for Surface-Crosslinked Gelatin Nanoparticles

samples are statistically insignificant (according to one-way ANOVA, $p > 0.05$). There is no significant impact of pore size on the physicochemical properties of DIC-crosslinked gelatin nanoparticles as can be seen in Figure 4-6.

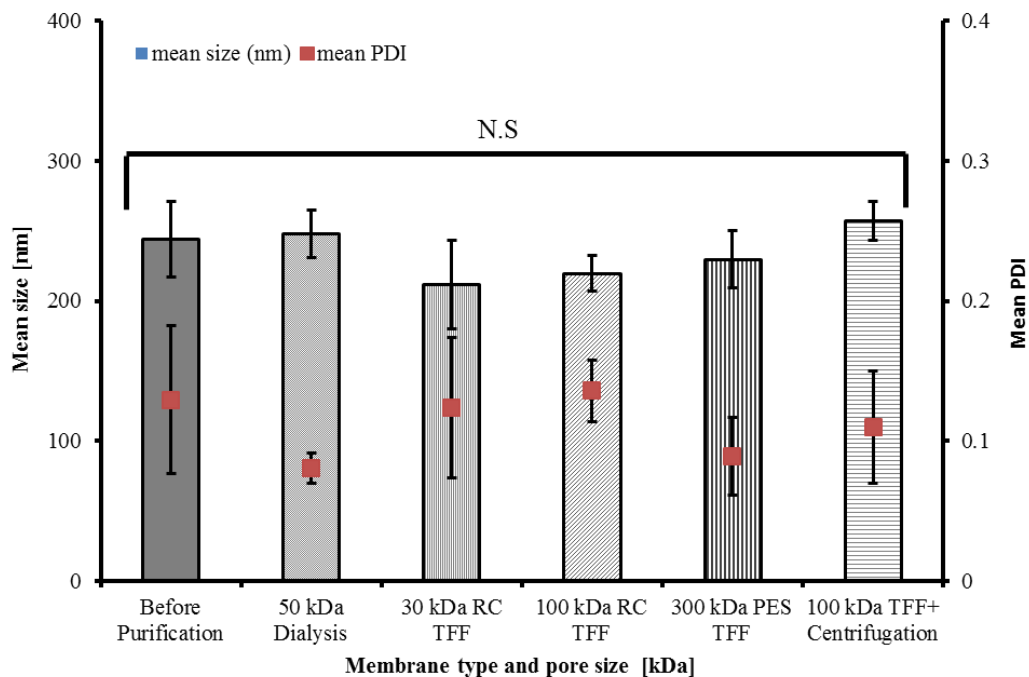


Figure 4-6. Mean size and size distribution of DIC-crosslinked GNPs purified with dialysis and TFF-based purification, using membranes of different pore sizes and type (RC: regenerated cellulose; PES: polyethersulfone). *Statistics*: N.S: statistically non-significant on the basis of $p > 0.05$ as per one-way ANOVA

4.4.4.2. Effect of amount of water in re-circulation

During TFF washing of crude nanosuspension, different amounts of water were recirculated across the TFF membrane. After the DLS measurements of nanoparticles washed with different amounts of water, it was observed that the size and size distribution was not changed. The mean size was always between 241 - 250 nm with PDI lower than 0.2 (See Figure 4-7).

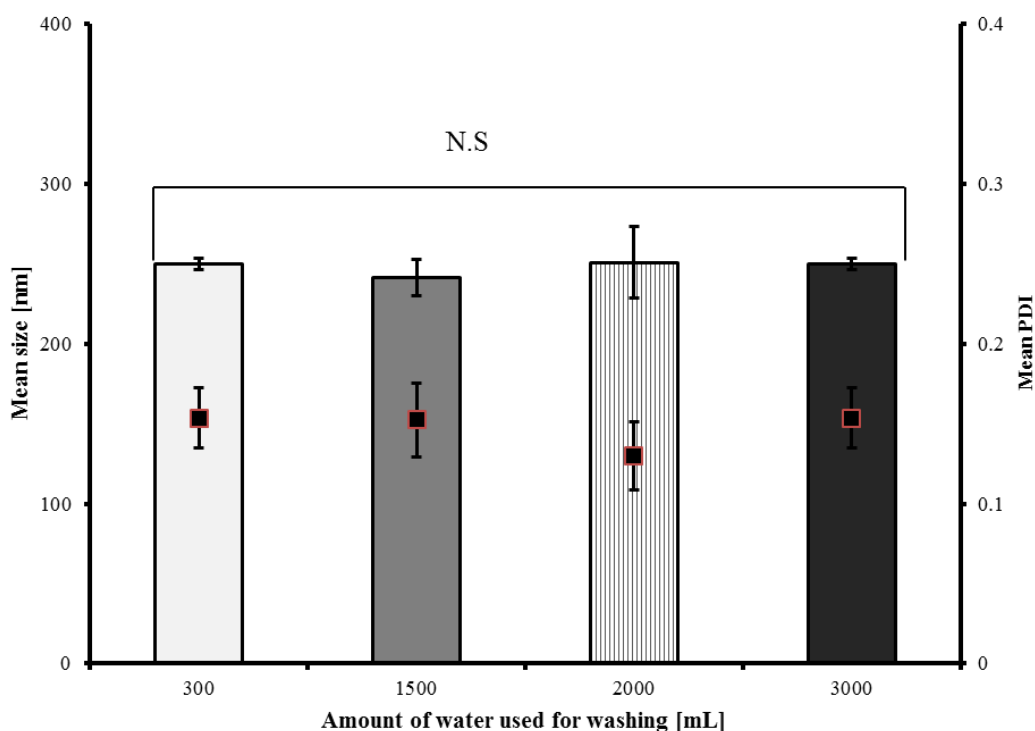


Figure 4-7. Particle size & size distribution versus volume of water used for TFF washing. *Statistics:* N.S: statistically non-significant on the basis of $p > 0.05$ using one-way ANOVA.

4.4.5. Morphological Characterization

4.4.5.1. Scanning Electron Microscopy (SEM)

The SEM analysis of DIC-crosslinked GNPs revealed that the nanoparticles have spherical morphology (Figure 4-8). The mean size calculated from SEM image using image J® is summarized in Table 4-5. As can be seen that the mean size of gelatin nanoparticles calculated from SEM image is lower than that of DLS analysis. Presumably, this is due to drying of

Optimization of Purification Procedures for Surface-Crosslinked Gelatin Nanoparticles

samples before SEM imaging. On the other hand, the particles in aqueous dispersion are associated with a water shell which is termed as hydrodynamic radii in DLS measurements. The same observation has also been reported by other investigators [113, 130].

Table 4-5. Size characterization of DIC-crosslinked GNPs purified via different purification techniques

S.No	Mode of purification	¹ Mean size DLS (PDI)	² Geometric mean size (SEM)
1	Centrifugation (3000 ×g for 10 minutes)	277.58 ± 14 (0.18)	125.25 ± 16.30
2	Dialysis membrane filtration (50 kDa pore size)	211.87 ± 31.71 (0.12)	166.97 ± 52.85
3	Tangential flow filtration (100 kDa pore size)	224.5 ± 1.87 (0.12)	145.33 ± 58.12

¹terms in parenthesis represent polydispersity index. ²100 particles analysed using image J software

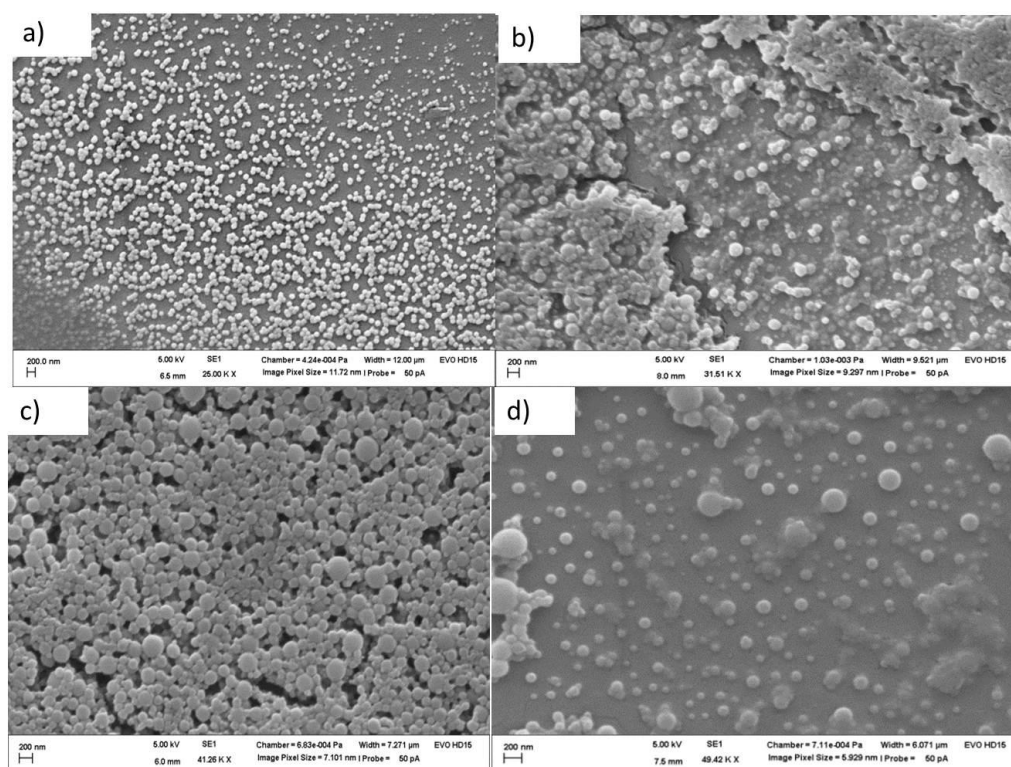


Figure 4-8. SEM micrographs of GNPs suspension purified with different techniques (a) DIC-crosslinked GNPs purified with centrifugation (3000 × g; t = 10 min), (b) DIC-crosslinked GNPs purified with dialysis (regenerated cellulose membrane of 50 kDa), (c) DIC-crosslinked GNPs purified with tangential flow filtration (membrane 100 kDa pore size, concentrated sample), (d) same formulation with diluted sample.

4.5. Conclusions

This research work demonstrated the possibility of tangential flow filtration for the purification of DIC surface-crosslinked gelatin nanoparticles which was proven to be comparatively more effective and efficient than dialysis and centrifugation having a couple of advantages. It was found to be effective in terms of removing the hazardous substances of formulation, *i.e.*, the un-reacted crosslinker (DIC) and its by product diisopropyl urea (DIU) and excess amounts of stabilizer (poloxamer 188). The parameters influencing the purification efficiency of the TFF-based purification were membrane pore size and amount of water consumed in re-circulation cycles during washing treatment. The molecular weight cut-off range 100 - 300 kDa of TFF membrane was promising in removing these impurities effectively. Likewise, increasing the amount of water in re-circulation cycles enhances the purification efficiency. The physicochemical properties of purified crosslinked nanoparticles, *e.g.*, mean size, size distribution and morphology of gelatin nanoparticles are not affected using a pore size of 100 kDa irrespective of whatever amount of water is being used for the purification. The mean particle size of purified nanoparticles was found to be between 200 - 300 nm with PDI less than 0.2 and possessing spherical morphology. In comparison to dialysis and centrifugation, TFF-based purification was found promising option. The final formulation of surface-crosslinked GNPs was found to be free from the residual amounts of crosslinker, its by products and excess amounts of poloxamer 188. Therefore, it can be concluded that tangential flow filtration is more easy, straightforward and efficient approach for the purification of DIC-induced surface crosslinked GNPs.

5 Characterization and loading of Surface -Crosslinked Gelatin Nanoparticles with Hydrophilic Macromolecules

Parts of this chapter have been published in:

Abdul Baseer, Aljoscha Koenneke, Joseph Zapp, Saeed A. Khan, Marc Schneider, Design and Characterization of Surface Crosslinked Gelatin Nanoparticles for the Delivery of Hydrophilic Macromolecular Drugs. *Macromolecular Chemistry and Physics*. 2019. **220**(18): p. 1900260.

5.1. Abstract

This chapter is focused on further investigating and proving our working hypothesis of colloidal interfacial crosslinking of gelatin nanoparticles in terms of loading a model hydrophilic peptide-based drug substance. Furthermore, a hydrophilic non-peptidal compound, *i.e.*, fluorescein isothiocyanate labelled dextran with different molecular weights was also loaded into these surface-crosslinked GNPs for the assessment of entrapment and loading potential and *in vitro* release kinetics of these surface-crosslinked GNPs and comparing the observations with glutaraldehyde crosslinked GNPs. The entrapment potential and release kinetics of fluorescein isothiocyanate-dextran was dependent on the molecular weight of FITC-dextran. The release of small molecular weight FITC-dextran was faster as compared to high molecular weight FITC-dextran.

The surface crosslinking behaviour by DIC was evaluated in terms of loading therapeutic protein-based cargo, *i.e.*, lysozyme. For comparison with a water soluble crosslinker, lysozyme loaded glutaraldehyde crosslinked GNPs were also produced with homogeneously crosslinked GNPs matrix. The lysozyme-loaded gelatin nanoparticles possess mean sizes between 200 - 300 nm and a size distribution of PDI < 0.2. The DIC-surface crosslinked GNPs demonstrated nearly complete release of lysozyme. The lysozyme released in the release medium maintains its enzymatic activity with a negligible loss of activity. In contrast, the GTA-crosslinked GNPs showed a hindered *in vitro* release. These observations revealed that the hydrophobic zero length crosslinker (DIC) demonstrates negligible interference in the release of lysozyme from gelatin nanoparticulate matrix. In contrast, the hydrophilic crosslinker glutaraldehyde shows a strong influence on release of lysozyme and hence a significant amount of lysozyme is believed to be permanently entrapped in the gelatin matrix.

5.2. Introduction

In the past few decades, gelatin nanoparticles have been found as interesting nanocarriers for different hydrophilic compounds, *e.g.*, nucleic acids, proteins and peptides [169, 170]. Numerous researchers have observed many fascinating advantages in gelatin nanoparticles (GNPs) such as modifiable distribution in the body, tunable drug release and nano-sized dimension of particles [171, 172]. The majority of the preparation methods reported for the formulation of GNPs are dependent on the chemical crosslinking as a stabilization strategy. The main disadvantage of these crosslinkers is that they also crosslink the entrapped protein-based cargo with the gelatin matrix due to their hydrophilic properties. Consequently, the release and biological activity of the encapsulated protein-based hydrophilic macromolecule is interfered with.

Keeping in view this challenge, a stable and optimized formulation consisting of surface linked GNPs was established which has been discussed in chapter 3 of this thesis. This was possible due to the application of a hydrophobic crosslinker, *i.e.*, diisopropylcarbodiimide. The theory of surface-crosslinking was partially supported by TNBS assay, gas chromatography and ¹H-NMR spectroscopic measurements revealing a saturated crosslinking process. This saturated crosslinking degree independent of crosslinker concentration and crosslinking times was regarded as the first evidence of surface crosslinking. To experimentally prove that the hydrophobic zero length crosslinker (DIC) does not crosslink the entrapped protein-based payload and preferentially crosslink the GNPs colloidal interface, it was necessary to load these surface-crosslinked GNPs with a protein-based macromolecule following pre-nanoparticles formation loading procedure and subsequently crosslinking the protein loaded GNPs with diisopropylcarbodiimide.

Therefore, the basic objective of the current chapter is to prove the second part of our working hypothesis which can be stated as that hydrophobic crosslinker would not crosslink the

Characterization and loading of Surface-Crosslinked Gelatin Nanoparticles with Hydrophilic Macromolecules

hydrophilic protein-based payload entrapped in the GNPs matrix; rather it would only crosslink the colloidal interface of dispersed GNPs which is necessary for the stabilization of GNPs in hydrophilic environments.

For this purpose, lysozyme was selected as a model peptide-based macromolecule. The polypeptide chain of lysozyme contains a total of 129 amino acids having a molecular weight of 14.4 kDa with an isoelectric point (IEP) between 10 and 11 [173-175]. Lysozyme was loaded to the gelatin polymer matrix prior to nanoparticle formation. The loaded GNPs were prepared employing nanoprecipitation followed by crosslinking with crosslinker (DIC) using an already optimized concentration (*i.e.*, $C_{DIC} = 15 \text{ mg/mL}$). After re-optimization of crosslinking conditions for lysozyme-loaded GNPs, the loaded GNPs crosslinked with DIC were characterized in terms of particle size, size distribution and zeta potential measurements, quantification of entrapment and loading potential, *in vitro* enzyme release evaluation and determination of biological activity. The *in vitro* release profile and biological assay of the encapsulated lysozyme were the major supporting experiments to prove the hypothesis of surface crosslinking. Furthermore, a non-peptidal hydrophilic macromolecule, *i.e.*, FITC-dextran with different molecular weights was also loaded to these surface-crosslinked GNPs in order to investigate the loading potential and *in vitro* release behaviour of these surface crosslinked GNPs for non-peptidal substances. The physicochemical properties of loaded GNPs crosslinked with DIC were compared with glutaraldehyde crosslinked GNPs.

5.3. Experimental

5.3.1. Materials

Gelatin type B Bloom 75 from bovine skin, poloxamer 188 and diisopropylcarbodiimide (reagent grade) were purchased from Sigma-Aldrich (Steinheim, Germany). Acetone (HPLC grade) was obtained from Fischer Chemicals Ltd. (Loughborough, U.K.). Milli-Q water with a resistivity of 18.2 M Ω .cm was used throughout the experiments. Hen egg white lysozyme was purchased from Sigma-Aldrich, Steinheim, Germany. The lyophilized powder of *Micrococcus lysodeikitus* ATCC 4698 cells used a substrate for lysozyme and glutaraldehyde aqueous solution (25% w/w, grade II) were purchased from Sigma-Aldrich, Steinheim, Germany. FITC-dextran was purchased from TdB Consultancy AB, Uppsala, Sweden. All reagents and chemicals used in this research work were of analytical grade and were used as received.

5.3.2. Preparation of loaded gelatin nanoparticles

Gelatin nanoparticles were prepared using the nanoprecipitation technique (see chapter 3, section 3.4.1). Two model hydrophilic macromolecules, *i.e.*, FITC-dextran and lysozyme were added to the solvent phase consisting of gelatin solution in water (gelatin concentration in water: 20 mg/mL).

5.3.2.1. Loading with FITC-dextran

Briefly, 20 mg of gelatin B was dissolved in water and heated up to 50°C. Afterwards, FITC-dextran (1 mg) with different molecular weights, *i.e.*, 20 kDa, 70 kDa, 150 kDa and 2000 kDa was added to gelatin solution. Subsequently, the solvent phase containing gelatin and FITC-dextran with different molecular weights was added dropwise to the non-solvent phase consisting of acetone containing poloxamer 188 (3 % w/v). Afterwards, the FITC-dextran

Characterization and loading of Surface-Crosslinked Gelatin Nanoparticles with Hydrophilic Macromolecules

loaded GNPs were crosslinked with 0.347 mL of diisopropylcarbodiimide solution in acetone from its stock solution (69.16 % [w/v] for 24 h (see chapter 3 for optimized DIC concentration and crosslinking time)).

5.3.2.2. Loading with lysozyme

The lysozyme loaded gelatin nanoparticles (GNPs) were prepared following the same protocols as mentioned for FITC-dextran loading (section 5.3.2.1). The molecular structure of lysozyme contains both primary amino as well as non-bonded carboxylic groups [176] so there is maximum probability for chemical crosslinking caused by any crosslinker including diisopropylcarbodiimide (see Figure 5-1).

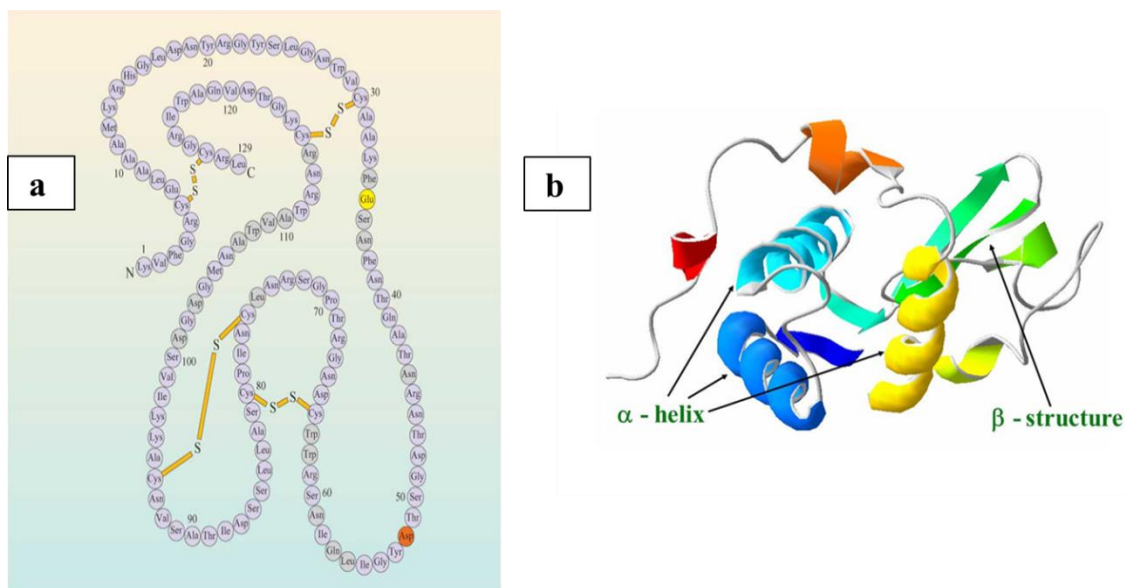


Figure 5-1. Chemical structure of lysozyme. (a) Primary structure. (b) Secondary structure. (Reprinted from Phillips *et al.* (1966) [177].

Briefly, 20 mg of gelatin was dissolved in 1 mL Milli-Q water at 50°C. Subsequently, lysozyme in different drug/polymer ratio was added to the gelatin solution. The drug to polymer mass ratios ranged from 2.5 to 40 %. Afterwards, the solvent phase containing both gelatin and lysozyme were added dropwise to the non-solvent phase (15 mL acetone

Characterization and loading of Surface-Crosslinked Gelatin Nanoparticles with Hydrophilic Macromolecules

containing poloxamer 188 (3% w/v). Following this co-nanoprecipitation, lysozyme loaded GNPs are produced which were subsequently crosslinked with an already optimized amount of DIC in acetone, *i.e.*, 0.347 mL of diisopropylcarbodiimide solution in acetone from its stock solution (69.16 % [w/v]) was added dropwise to the nanosuspension and stirred for varying crosslinking times with intermittent DLS measurements in water thus monitoring the optimum crosslinking time of lysozyme-loaded GNPs with DIC. In parallel, the same samples were also analysed for DLS in acetone as a dispersion medium to investigate the possible impact of loading on mean size and size distribution of lysozyme loaded particles. The crude nanosuspension of DIC-crosslinked lysozyme loaded GNPs was purified using our pre-established SOP of tangential flow filtration (TFF) as discussed in previous chapter (see section 4.3.3.3). Briefly, the TFF assembly fitted with modified regenerated cellulose (Hydrosart) with a pore size of 100 kDa was employed for washing of loaded nanoparticles. The preparation procedure is shown schematically in Figure 5-2.

Characterization and loading of Surface-Crosslinked Gelatin Nanoparticles with Hydrophilic Macromolecules

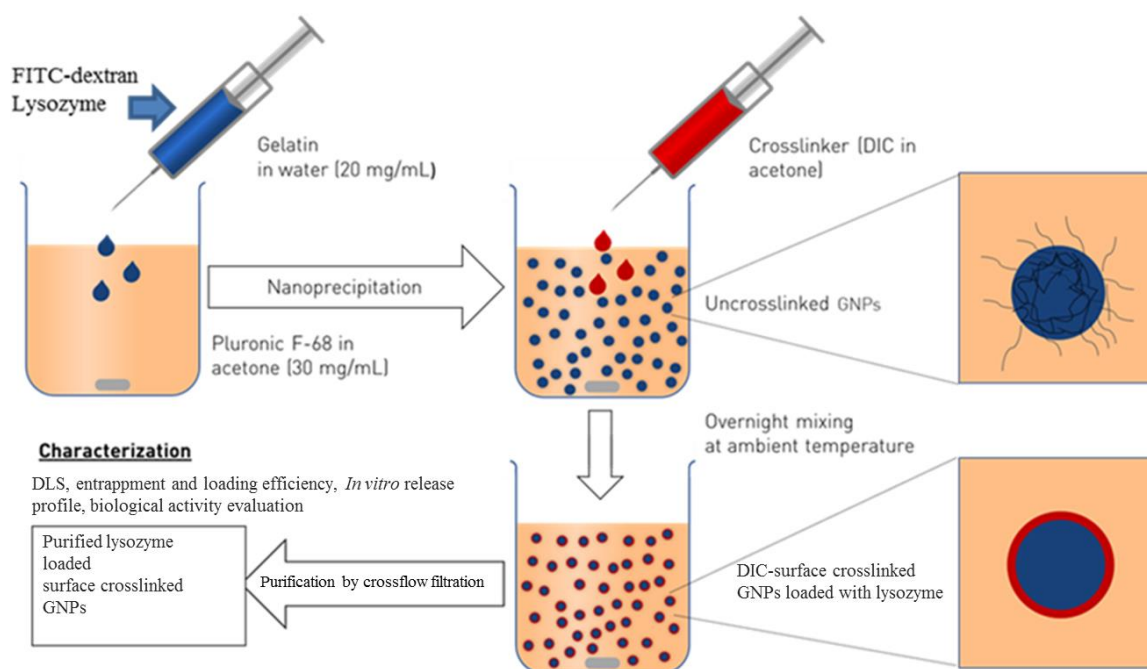


Figure 5-2. Schematic representation of the procedure lysozyme and FITC-dextran loaded GNPs via nanoprecipitation and crosslinking the particles by DIC.

Optimization of lysozyme loading and crosslinking

In order to investigate the effect of lysozyme loading on optimum crosslinking time which was validated for un-loaded GNPs discussed in chapter 3, section 3.4.1, the GNPs suspension loaded with varying amounts of lysozyme were incubated for different crosslinking times with a fixed concentration of DIC (*i.e.*, 15 mg/mL (already optimized in chapter 3, section 3.4.1)). The aim was to get lysozyme-loaded GNPs which maintain the particulate integrity in aqueous environments with a homogeneous size distribution ($PDI < 0.2$). The crosslinking incubation time was studied for three time points, *i.e.*, 24, 72 and 96 h. In parallel, the DIC crosslinked GNPs loaded with different lysozyme amounts were prepared and evaluated using DLS measurements to determine the maximum loadable mass of lysozyme.

5.3.3. Physicochemical Characterization

5.3.3.1. Determination of size and size distribution

After crosslinking for varying crosslinking times, samples of DIC-crosslinked gelatin nanoparticles were measured both in acetone and water before purification. The mean size (z-average mean) and size distribution (PDI) were measured in triplicates for each batch by dynamic light scattering (DLS), using the Zetasizer nano-ZS (Malvern instruments, Ltd., Malvern, UK). The nano-suspension samples were 10 times diluted with respective dispersion media *e.g.*, Milli-Q water and acetone before measurements.

5.3.3.2. Determination of zeta potential

Zeta potential of DIC-crosslinked gelatin nanoparticles loaded with varying amounts of lysozyme after washing with tangential flow filtration was measured by Laser Doppler Anemometry (LDA) at pH 6 using Zetasizer nano-ZS (Malvern Instruments Ltd., Worcestershire, UK). All nanoparticles suspensions were 10 times diluted with Milli-Q water at 25°C before measurements. Each sample was measured in triplicate.

5.3.4. Entrapment and loading efficiency

5.3.4.1. FITC-dextran

For the determination of entrapment efficiency (% EE), 5 mg of lyophilized nanoparticles were dispersed in 5 mL phosphate buffer saline (PBS) at pH 7.4 at room temperature ($23 \pm 2^\circ\text{C}$). To this mixture, trypsin (0.5 mg/mg of polymer) was added to digest the gelatin nanoparticles (digestion for 6 h). Subsequently, the digested particles were filtered using 0.2 μm filter. The samples were analysed using Tecan infinite[®]M200 plate reader (Tecan group

Characterization and loading of Surface-Crosslinked Gelatin Nanoparticles with Hydrophilic Macromolecules

Ltd., Männedorf, Switzerland) for the measurement of fluorescence intensity. The fluorescence emission intensity was recorded at 520 nm using 485 nm as excitation wavelength. For FITC-dextran of each molecular weight, a calibration curve was constructed after plotting the fluorescence intensities versus different FITC-dextran concentrations ($\mu\text{g/mL}$). The entrapment efficiency (% EE) was determined using the following equation (5).

$$\% \text{ Entrapment Efficiency} = \frac{\text{Mass of FITC-dextran determined in the formulation (mg)}}{\text{Mass FITC-dextran used for the formulation (mg)}} \times 100 \dots(5)$$

5.3.4.2. Lysozyme

In order to avoid the trypsin induced digestion of entrapped lysozyme, un-crosslinked GNPs loaded with lysozyme were considered for the determination of entrapment as well as loading efficiency. The entrapment and loading efficiencies calculated for un-crosslinked GNPs will be regarded as representative for DIC-and GTA crosslinked GNPs. Before quantification of lysozyme entrapped in the nanoparticulate matrix, a procedure for isolating the free lysozyme from loaded GNPs was optimized. For this purpose, aqueous solution of lysozyme (1 mg/mL) was precipitated in acetone (non-solvent) and measured the sizes of precipitated free lysozyme without gelatin. Afterwards, the micro-dispersion system of free lysozyme was filtered through syringeable micro-filter units consisting of polytetrafluoroethylene (PTFE) membrane of 0.45 μm (Millex[®]-FH, Millipore Corporation, City, France). The filtrate was analysed for the presence of filtered lysozyme using a validated method of RP-HPLC (discussed in the next paragraph). The mass of lysozyme found in the filtrate was subtracted from the total amount to calculate the amount of lysozyme retained on the surface of PTFE membrane. Likewise, the crude nanosuspension consisting of lysozyme loaded GNPs was filtered using the same syringeable PTFE filters 0.45 μm . For the determination of entrapment and loading efficiencies, the filtered nano-suspension containing un-crosslinked GNPs loaded

Characterization and loading of Surface-Crosslinked Gelatin Nanoparticles with Hydrophilic Macromolecules

with lysozyme were washed with acetone after three times centrifugation (20,000 g for 20 min) and re-dispersing in acetone. After the third centrifugation, the purified pellet of lysozyme-loaded GNPs was isolated followed by air-drying at room temperature. Subsequently, 5 mg of un-crosslinked lysozyme loaded nanoparticles pellet was dissolved in 5 mL phosphate buffer saline (PBS) at pH 7.4 at room temperature ($23 \pm 2^\circ\text{C}$). After re-dissolution of the un-crosslinked gelatin nanoparticles pellet in PBS (pH 7.4), the samples were measured using reverse-phase (RP-HPLC) [178] after some necessary modifications in the previous method. A calibration curve was constructed after plotting the mean peak areas of the standard samples of lysozyme in PBS in the RP-HPLC chromatogram versus the corresponding lysozyme concentration ($\mu\text{g/mL}$).

In this context, the already reported method of RP-HPLC [178] was re-validated due to a few changes in the chromatographic conditions, *e.g.*, packing material of column, column dimensions, mobile phase composition and flow rate. For this purpose, an HPLC system (Ultimate 3000 series, Rapid Speed, Thermo Fisher Scientific, Waltham, MA, USA), equipped with a quaternary pump and a Dionex Ultimate 3000 UV/Vis detector was used. Furthermore, the system used an autosampler (ASI-100, Dionex, Sunnyvale, CA, USA), a column oven (STH 585, Dionex, Sunnyvale, CA, USA) and a LiChrosphere 100 RP-18e column (5 μm material, 4x125 mm, Merck KGaA, Darmstadt, Germany). The column oven was heated up to 25 $^\circ\text{C}$. The mobile phase was prepared with degassed and filtered acetonitrile and deionized water. The mobile phase used consisted of two solvent systems, *i.e.*, mobile phase A and B. Mobile phase-A consisted of 90 % water and 10 % acetonitrile acidified with 0.1 % [v/v] trifluoroacetic acid. Mobile phase B consisted of 90 % acetonitrile and 10 % Milli-Q water acidified with 0.1 % trifluoroacetic acid [v/v]. The gradient started with 100 % mobile phase A acetonitrile and decreased linearly up to 100 % mobile phase B in 15 min. Afterwards, from 15 to 20 min, the column was equilibrated with 100 % mobile phase A. The flow rate of mobile phase was adjusted to 0.8 mL/min. For the detection and

Characterization and loading of Surface-Crosslinked Gelatin Nanoparticles with Hydrophilic Macromolecules

quantification of lysozyme, the detector was fixed at 220 nm. The sample injection volume selected was 20 μ L. The retention time was 8.9 min. For data analysis, the chromatography software Chromeleon 6.8 Chromatography Data System (Thermo Fisher Scientific, Waltham, MA, USA) was used, and the quantification was based on peak integration with the help of software thus recording the area under the chromatographic peak appearing at a retention time of 8.9 min.

The encapsulation efficiency (% E.E) and the loading efficiency (% LE) of lysozyme-loaded crosslinked GNPs were calculated using the following equation (6) and (7).

$$\% \text{ Entrapment efficiency} = \frac{\text{Mass of lysozyme quantified in NPs [mg]}}{\text{Total mass of lysozyme added to NPs formulation [mg]}} \times 100 \dots\dots(6)$$

and;

$$\% \text{ Loading efficiency} = \frac{\text{Mass of lysozyme quantified in NPs [mg]}}{\text{Mass of GNPs formulation mg}} \times 100 \dots\dots\dots(7)$$

5.3.5. Investigation of *in vitro* release

5.3.5.1. FITC-dextran

For the determination of *in vitro* release profiles, 10 mg of lyophilized FITC-dextran-loaded GNPs were dispersed in 5 mL of PBS (pH 7.4) maintained at $37^{\circ}\text{C} \pm 0.5$. The release medium was stirred at 400 rpm using a mechanical shaker. At pre-determined time points, 1 mL supernatant was withdrawn and centrifuged at 20,000 g for 20 min. The pellets were re-dispersed in 1 mL fresh PBS and added to the original dissolution medium to keep the particles concentration constant. The supernatant (1 mL) was analysed for the quantification of released FITC-dextran using Infinite[®] M200 plate reader (Tecan group, Switzerland). For recording the fluorescence emission intensities, these excitation and emission wavelengths

Characterization and loading of Surface-Crosslinked Gelatin Nanoparticles with Hydrophilic Macromolecules

$[\lambda_{\text{ex}}/\lambda_{\text{em}}: 485/520 \text{ nm}]$ were used. The % cumulative mass of FITC-dextran released at time point (t) was calculated using the following equation (8).

$$\text{Cumulative amount of FITC-dextran released at time point (t) [\%]} = \frac{M_t}{\Sigma M} \times 100 \dots \dots \dots (8)$$

M_t : Mass of FITC (mg) released after time point (t).

ΣM : Total mass of FITC-dextran (mg) entrapped in crosslinked GNPs.

5.3.5.2. Lysozyme

For the determination of *in vitro* release profile of lysozyme, 10 mg of dried powder of lysozyme-loaded GNPs was dispersed in 5 mL of PBS (pH 7.4) maintained at $37^\circ\text{C} \pm 0.5$. The release medium was stirred at 400 rpm using a mechanical shaker. At pre-determined time points, 1 mL supernatant was withdrawn and centrifuged at 20,000 g for 20 min. Then 1 mL aliquots were withdrawn from the supernatant and the pellet was re-dispersed in 1 mL PBS and added to the original release medium to maintain the particles concentration constant in the release medium. The aliquots withdrawn (1mL) were analysed using a validated procedure of RP-HPLC mentioned in section 5.3.4.2 for the quantification of lysozyme concentration released at that particular time point. Afterwards, the % cumulative mass of lysozyme released from crosslinked GNPs at its corresponding time points was calculated using the following equation (9).

$$\text{Cumulative amount of lysozyme released [\%]} \text{ after time point (t)} = \frac{M_t}{\Sigma M} \times 100 \dots \dots \dots (9)$$

M_t : Mass of lysozyme (mg) released after time point (t).

ΣM : Total mass of lysozyme (mg) entrapped in crosslinked GNPs.

5.3.6. Determination of the biological activity

This is a turbidimetric bioassay which involves the measurement of turbidity clearance potential of lysozyme after incubating it with its substrate. This turbidimetric assay is based on the hydrolytic activity of lysozyme on the substrate which consisted of lyophilized powder of a gram positive bacterium called *Micrococcus lysodeikticus* ATCC No. 4698 cells. The measurement of enzymatic activity of lysozyme entrapped in DIC-crosslinked GNPs was performed using standard protocols of turbidimetric bioassay as provided by the manufacturer (Sigma-Aldrich) [179]. The objective was to determine whether the lysozyme after entrapment in DIC and GTA-crosslinked gelatin nanoparticles maintains its intended biological activity or not. The lysozyme digests the bacterial cell wall by hydrolysing the β (1,4)-glycosidic linkages between N-acetylmuramic acid (NAM) and N-acetyl glucose amine (NAG) [180, 181]. The following protocols of turbidimetric assay were used. Firstly, the substrate suspension in a concentration (0.015 % w/v) was prepared after dispersing a known amount of lyophilized powder of *Micrococcus lysodeiktitus* in phosphate buffer saline (PBS) at pH 7.4. Afterwards, 2.5 mL from this substrate suspension was transferred to quartz cuvette having path length of 1 cm. Subsequently, 100 μ L of lysozyme calibration standards or release samples of crosslinked GNPs was added to the substrate suspension in the cuvette and the mixture was homogeneously mixed by inversion. The decrease in absorption was recorded at 450 nm ($\Delta A_{450\text{nm}}$) for 5 minutes using a UV/VIS spectrophotometer at 25°C. The turbidity clearance potential of lysozyme expressed as absorption change per unit time represented by $\Delta A_{450\text{nm}}/\text{min}$ was considered as a quantification parameter for the lysozyme enzymatic activity. For the activity-based quantification of lysozyme, a calibration curve was constructed after plotting the absorption change per unit time [$\Delta A_{450\text{nm}}/\text{min}$] against the corresponding concentrations of lysozyme ($\mu\text{g/mL}$). Likewise, the supernatants of DIC- as well as GTA-crosslinked nanoparticles containing the released lysozyme in the release media were analysed in the same way as the calibration standards. Briefly, 8 mg of lyophilized

Characterization and loading of Surface-Crosslinked Gelatin Nanoparticles with Hydrophilic Macromolecules

crosslinked gelatin nanoparticles were dispersed in 4 mL PBS buffer at pH 7.4 at 37°C and incubated for 24 h with continuous stirring at 400 rpm. After 24 h, the release mixture was centrifuged at 15,000 g for 10 min. From the supernatant, a 0.1 mL aliquot was withdrawn and the activity was checked in the same way as described above for the calibration standards of lysozyme. Afterwards, the biological activity in terms of turbidity clearance potential expressed as absorption change per unit min (*i.e.*, $\Delta A_{450\text{nm}}/\text{min}$) was converted to corresponding mass of lysozyme which is biologically active using the turbidimetric bioassay-based calibration curve. The same samples were also analysed simultaneously using the validated RP-HPLC for the determination of total released mass of lysozyme in the release medium. Moreover, the biologically active mass of lysozyme measured with turbidimetric assay was compared with the amount calculated on the basis of reverse-phase HPLC. From this correlation, the biologically active mass of lysozyme was estimated.

5.4. Results and Discussion

Both FITC-dextran and lysozyme loaded GNPs were prepared following the standard protocols as already mentioned (section 5.3.2, Figure 5-2). Pre-nanoparticle formation loading procedure was employed for loading these hydrophilic macromolecules into GNPs. In the case of FITC-dextran loading, 1 mg of FITC dextran of different molecular weights (20 kDa, 70 kDa, 150 kDa and 2000 kDa) was loaded into GNPs, while in case of lysozyme loading, different % mass ratios of lysozyme-to-gelatin were used, *i.e.*, 2.5, 5, 10, 25, 30 and 40 %.

During nanoprecipitation, both the payloads, *i.e.*, FITC-dextran and lysozyme, are co-nanoprecipitated with gelatin during diffusion to non-solvent phase resulting in the formation of FITC-dextran loaded GNPs and lysozyme-loaded GNPs. Due to hydrophilicity, both the FITC-dextran and lysozyme diffuse to gelatin phase during the nanoprecipitation process leading to the entrapment of hydrophilic macromolecules in gelatin nanoparticulate matrix. Subsequently, the influence of loading of these hydrophilic macromolecules on

Characterization and loading of Surface-Crosslinked Gelatin Nanoparticles with Hydrophilic Macromolecules

physicochemical properties of GNPs, *e.g.*, mean particle size (*Z*-average), size distribution characterized by polydispersity index and zeta potential were evaluated.

5.4.1. Effect of loading on mean size and size distribution

5.4.1.1. FITC-dextran loaded GNPs

It was observed that the loading of FITC-dextran in a drug to polymer mass ratio of 1:20 has no influence on mean size of loaded gelatin nanoparticles irrespective of molecular weight of FITC-dextran (Figure 5-3, Table 5-1). The mean size of loaded and un-loaded GNPs is between 230 - 250 nm, but the polydispersity index (PDI) is increasing with loading of FITC dextran. The PDI of un-loaded GNPs was less than 0.2 while the loaded GNPs possess PDI from 0.2 - 0.3. Besides, the optimum crosslinking time of FITC-dextran loaded GNPs was found similar to un-loaded GNPs as can be seen in Table 5-1. For both loaded and un-loaded GNPs, the optimum crosslinking time is approximately 20 - 24 h. It means that the loading of FITC-dextran has no significant impact on optimum crosslinking times as optimized in chapter 3 for un-loaded nanoparticles (Figure 5-3).

Characterization and loading of Surface-Crosslinked Gelatin Nanoparticles with Hydrophilic Macromolecules

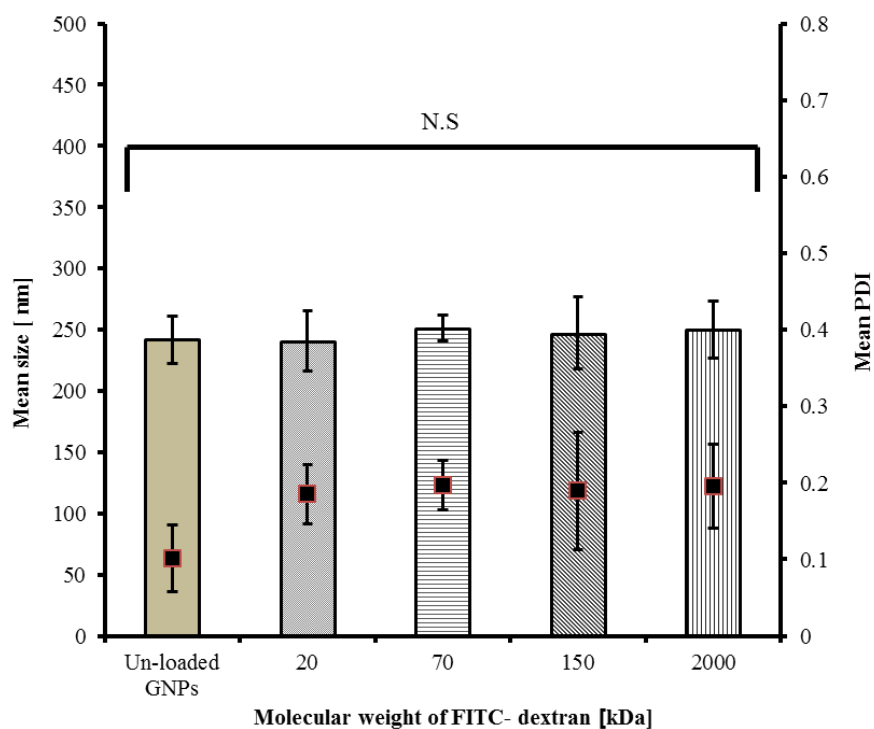


Figure 5-3. Effect of FITC-dextran (1mg) loading of different molecular weights on mean size and size distribution of produced gelatin nanoparticles. The FITC-dextran to gelatin mass ratio was 1:20. *Statistics:* (N.S: Not significant statistically as per one-way ANOVA ($p > 0.05$))

Table 5-1. Mean sizes and size distribution of FITC-dextran loaded GNPs crosslinked with DIC used in a concentration of 15 mg/mL in nanosuspension

FITC-dextran loaded GNPs	Mean size [nm] \pm S.D.	Mean PDI \pm S.D.	Crosslinking time (h)	
Unloaded (blank) GNPs	241.48 \pm 19.18	0.10 \pm 0.04	20-24	N.S. ^a
FITC-dextran 20 kDa	240.88 \pm 24.92	0.18 \pm 0.04	20-24	
FITC-dextran 70 kDa	251.08 \pm 10.41	0.20 \pm 0.03	20-24	
FITC-dextran 150 kDa	247.23 \pm 29.62	0.19 \pm 0.08	20-24	
FITC-dextran 2000 kDa	250.03 \pm 23.42	0.19 \pm 0.05	20-24	

N.S.^a: Not significant statistically as per one-way ANOVA ($p > 0.05$)

5.4.1.2. Lysozyme loaded GNPs

The lysozyme loaded gelatin nanoparticles prepared via nanoprecipitation as shown in Figure 5-2 were crosslinked with 0.347 mL diisopropylcarbodiimide solution (taken from stock solution of DIC in acetone having concentration of 69.16 % w/v) at room temperature. The concentration of DIC in total bulk of nanosuspension is 15 mg/mL which was optimized in chapter 3. It was observed that no apparent change in mean size was observed with lysozyme loading below 5 %. Increasing the mass ratio above 5 or 10 % slightly increased the mean size of GNPs as can be seen in Figure 5-4. However, the maximum loadable amount of lysozyme was found to be 25 % [lysozyme/gelatin]. Increasing the amount above 25 % resulted in the formation of bigger visible precipitates, which consequently leads to phase separation of the entire bulk dispersion system as can be seen in Figure 5-4.

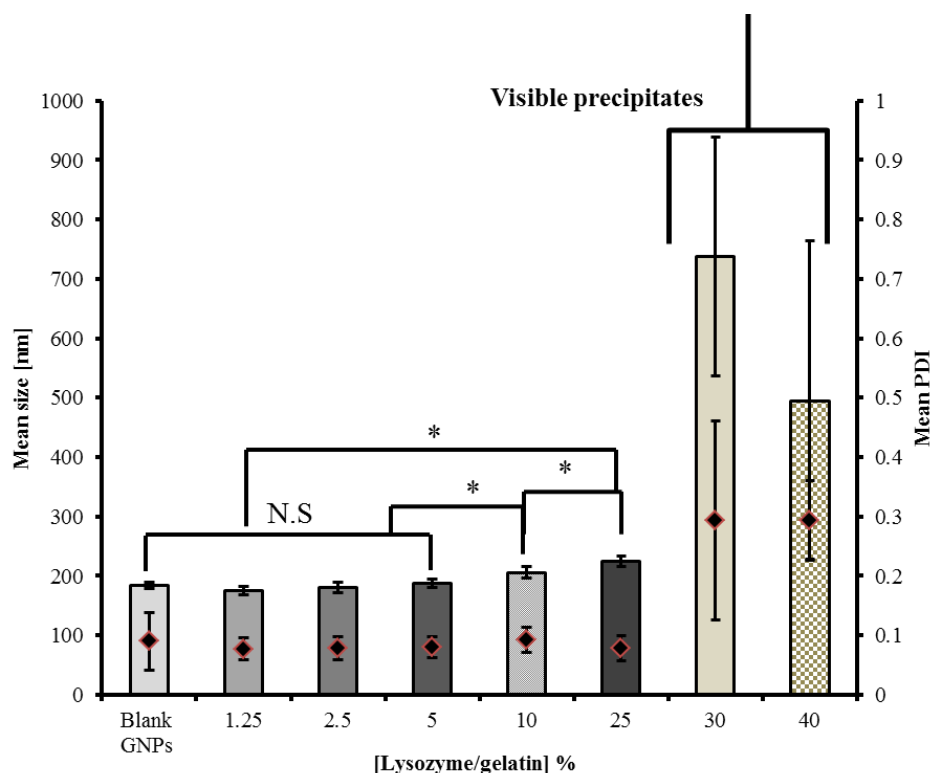


Figure 5-4. Mean size and size distribution analysis of DIC-crosslinked GNPs loaded with different drug to polymer mass ratio at room temperature for DIC concentration of 15 mg/mL. The samples were measured in acetone as a dispersant and were diluted 10 times with acetone before DLS measurements. *Statistics* (N.S.: statistically non-significant on the basis of $p > 0.05$ as per one-way ANOVA). (*) $p < 0.05$: Statistically significant as per one-way ANOVA.

Overall, the mean hydrodynamic diameter of lysozyme-loaded GNPs is increased by an increment of approximately 15 - 30 nm using lysozyme of 25 %. The increase in mean size of DIC-crosslinked GNPs loaded with lysozyme above 5 % may be attributed to an increase in viscosity of the solvent phase with higher lysozyme amounts. The higher the viscosity of solvent phase, the slower will be the diffusion rate of the solvent phase into the non-solvent phase during particles formation in nanoprecipitation [99]. This leads to formation of bigger particles.

During preparation of DIC-crosslinked lysozyme loaded gelatin nanoparticles, another observation was the pronounced impact on optimum crosslinking time. After loading

lysozyme above 5 %, the loaded particles were not stable in water for crosslinking time of 24 - 28 h. So, it needs re-optimization of the crosslinking time which is explained in the following section (see section 5.4.2).

5.4.2. Optimization of crosslinking time for lysozyme loading

The physicochemical integrity of DIC-crosslinked GNPs loaded with lysozyme in varying amounts in aqueous medium need to be re-evaluated. The optimization of crosslinking time for blank gelatin nanoparticles has been discussed in detail in chapter 3 sub-section 3.4.1. For the re-optimization of crosslinking time for lysozyme-loaded GNPs, the time interval after which the polydispersity index (PDI) was below 0.2 while measuring the DIC-GNPs in water was considered as optimum crosslinking time. In this experiment, the samples from DIC-crosslinked GNPs dispersion were taken after different time points and measured in water using DLS. It was observed that the optimum crosslinking time is also affected with increasing the amount of loaded lysozyme in the solvent phase. Using lysozyme amount up to 2.5 % does not affect the crosslinking time which is optimum for un-loaded GNPs (*i.e.*, approximately 16 - 24 h) keeping the crosslinker concentration constant (*i.e.*, 15 mg/mL) at room temperature. Increasing the amount of lysozyme in the solvent phase above 5 % leads to an increase in the optimum crosslinking time. In this way, the corresponding optimum crosslinking times for 2.5, 5, 10 and 25 % lysozyme were 24 h, 24 - 48 h, 72 h, and 96 h, respectively as can be seen in Table 5-2 and Figure 5-5. At these incubation times, the PDI was less than 0.2.

After optimizing the crosslinking times for the above lysozyme amounts, the mean size and size distribution of crosslinked GNPs loaded with lysozyme were measured both in acetone and water using DLS as shown in Figure 5-6 and Table 5-2. The mean sizes measured in acetone are smaller than the measured sizes in water. This might be due to swelling phenomenon which happens when the crosslinked gelatin nanoparticles are transferred from

Characterization and loading of Surface-Crosslinked Gelatin Nanoparticles with Hydrophilic Macromolecules

organic phase (acetone) to aqueous phase (water). In fact, the crosslinked GNPs act as a nano-hydrogel system. The same phenomenon was also observed for un-loaded DIC-crosslinked GNPs (see chapter 3, Figure 3-8, Table 3-9 and Table 3-10).

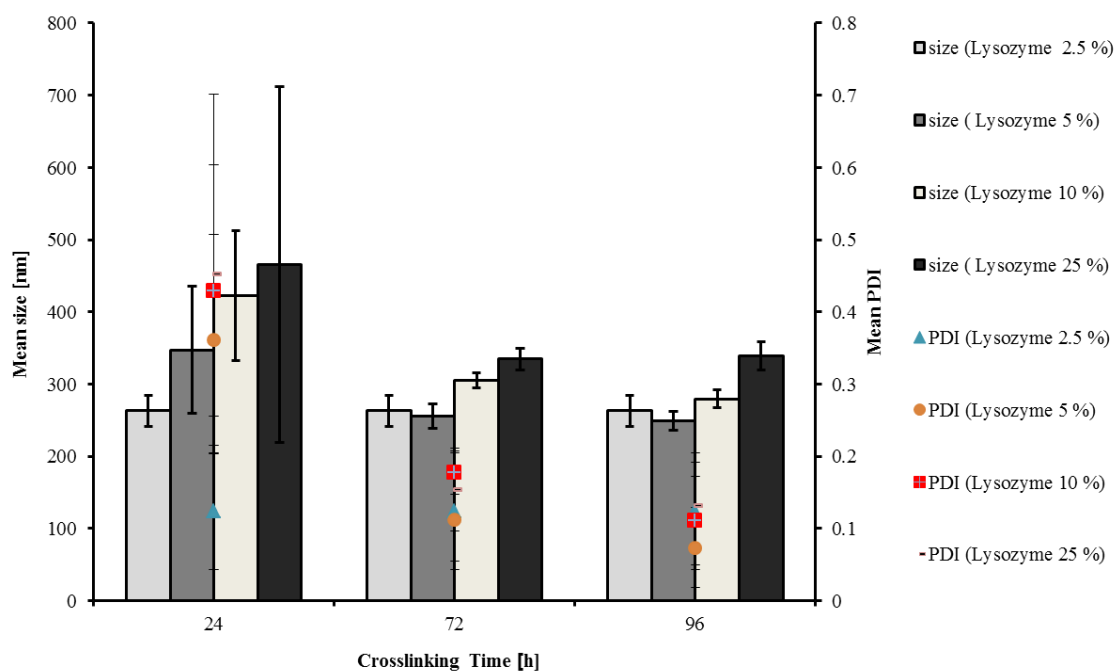


Figure 5-5. Mean size and size distribution analysis of lysozyme-loaded GNPs loaded with different amounts of lysozymes at different incubation times at room temperature (concentration of DIC was 15 mg/mL). Samples were measured in water as a dispersant for DLS measurements and each sample was diluted 10 times in water before measurements.

Table 5-2. Effect of lysozyme loading on mean size, size distribution and optimum crosslinking time (h) of DIC-crosslinked GNPs loaded with different amounts of lysozyme. The DIC concentration used for the crosslinking was 15 mg/mL.

[Lysozyme/gelatin] %	Optimum CT*	Mean size [nm] \pm SD (PDI)	
		Measured in acetone (before washing)	Measured in water (before washing)
Blank GNPs	24	184.20 \pm 5.18 (0.09)	268.40 \pm 7.75 (0.12)
2.5	24	180.15 \pm 9.49 (0.08)	262.79 \pm 20.98 (0.12)
5	72	186.83 \pm 7.27 (0.08)	255.88 \pm 16.65(0.11)
10	96	205.59 \pm 9.76 (0.09)	279.5 \pm 12.13(0.11)
25	96	223.86 \pm 8.84 (0.08)	338.62 \pm 19.76(0.13)
>25	-	ND ^a	ND ^a

ND^a: Not determined due to visible precipitates formation. CT*: crosslinking time

Characterization and loading of Surface-Crosslinked Gelatin Nanoparticles with Hydrophilic Macromolecules

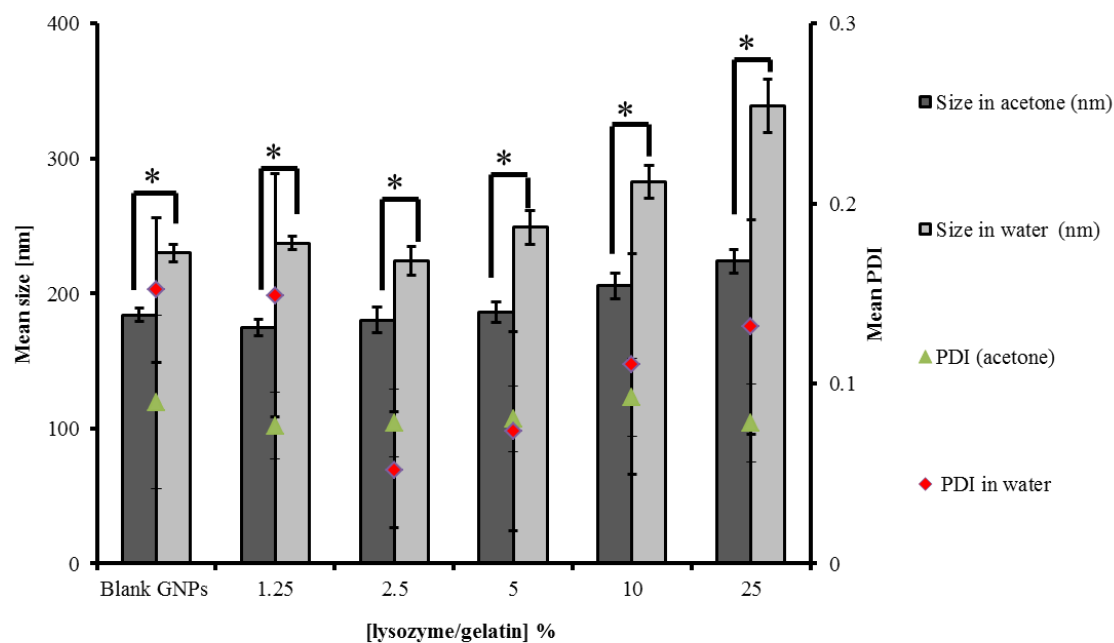


Figure 5-6. Mean size and size distribution analysis of DIC-crosslinked GNPs loaded with different lysozyme amounts. The DIC concentration used was 15 mg/mL. The samples were measured both in acetone and water as dispersion media and were diluted 10 times before DLS measurements. Each sample was measured in triplicates with three independent experiments. *Statistics:* (*) $p < 0.05$: Statistically significant according to paired two-tail t -test.

The increase in optimum crosslinking time can be explained in terms of electrostatic interaction between the negatively charged carrier molecule (gelatin B having IEP of 4.7-5.4) [54, 139] and positively charged cargo molecule (lysozyme, with IEP between 9 and 11) [19, 182]. Due to the difference of isoelectric points (IEPs) between gelatin B and lysozyme, the electrostatic interaction between the peptidal cargo (lysozyme) and carrier molecule (gelatin) would be dominant. This phenomenon is called poly-ionic complexation [183]. The electrostatic interaction between the negatively charged gelatin matrix and positively charged enzyme has also been investigated by other researchers [184]. From these literatures, it is apparent that the majority of negatively charged carboxylic groups are electrostatically connected with the positively charged amino groups of lysozyme. Consequently, a very low population of free carboxylic groups would be available for crosslinking at the colloidal

Characterization and loading of Surface-Crosslinked Gelatin Nanoparticles with Hydrophilic Macromolecules

interface, and hence, the process of crosslinking would be delayed. Since, the rate determining step in DIC-mediated crosslinking is the activation of carboxylic groups leading to the formation of an unstable transition complex, known as O-Acylisourea (see chapter 3, Figure 3-3 b). Subsequently, this intermediate is readily attacked by a nucleophile (*e.g.*, primary amino groups). Therefore, this delaying of crosslink formation is believed to be accountable for an increase in the crosslinking time with loading of lysozyme above 5 %. That is, the higher the amount of loaded lysozyme, the higher will be the degree of electrostatic interaction between gelatin and lysozyme, the more carboxylic groups would be engaged in the electrostatic interaction, and the slower will be the crosslinking rate with DIC. Besides, some fraction of lysozyme is also believed to be adsorbed onto the colloidal interface especially in higher lysozyme loads (*e.g.*, > 5 %), which will constitute a poly-ionic complex at the colloidal interface. In turn, this would interfere with the normal crosslinking chemistry caused by the DIC which may lead to an increase in the optimum crosslinking time. Therefore, the GNPs loaded with higher amounts of lysozyme need comparatively more time for stabilization.

In contrast, in the case of loading of lower amounts of lysozyme, low fraction of free carboxylic groups of gelatin would be engaged in the electrostatic interaction with lysozyme molecules, and hence more free carboxylic groups would be available on GNPs surface for DIC-mediated crosslinking. So, the electrostatic complexation between lysozyme and gelatin on the colloidal interface may affect the DIC crosslinking kinetics. The larger the extent of electrostatic interaction between lysozyme and gelatin the higher amounts of lysozyme, higher will be the optimum crosslinking times for the optimum stability of GNPs and vice versa.

5.4.3. Determination of zeta potential

As discussed previously, gelatin B is an acidic polymer having isoelectric point (IEP) of 4.7-5.4 [139], while the lysozyme is a basic polypeptide macromolecule having isoelectric point of between 10-11[173, 174, 182]. Due to the basic isoelectric point of lysozyme, the lysozyme will exist as predominantly cationic polypeptidal molecule. In this experiment, the zeta potential of DIC-crosslinked gelatin nanoparticles loaded with different amounts of lysozyme was measured at pH 6. It is evident from Figure 5-7 and Table 5-3 that the zeta potential of lysozyme-loaded GNPs is similar to the zeta potential of unloaded GNPs with lysozyme loading up to 5 %. The positive zeta potential increases proportionately with increasing the amount of loaded lysozyme above 5 %. This observation has also been reported in the literature [125]. The increase in positive zeta potential may be attributed to the surface adsorbed lysozyme while loading lysozyme above 5 %. In contrast, for the lysozyme loading below 5 %, there is low possibility of surface adsorbed lysozyme onto surface crosslinked GNPs, and possibly, a significant fraction of lysozyme is believed to be entrapped in the core of DIC crosslinked GNPs. Due to high isoelectric point of lysozyme (~ 11.4), the net charge of lysozyme at pH 6 will be positive due to the predominance of protonated amino groups (NH_3^+ groups) present on the molecule. Hence, it was expected that the zeta potential of lysozyme-loaded GNPs should be more positive as compared to blank GNPs due to the predominance of more protonated cationic groups (*e.g.*, $^+\text{NH}_3$ groups) contributed by the surface anchored/adsorbed lysozyme molecules.

Characterization and loading of Surface-Crosslinked Gelatin Nanoparticles with Hydrophilic Macromolecules

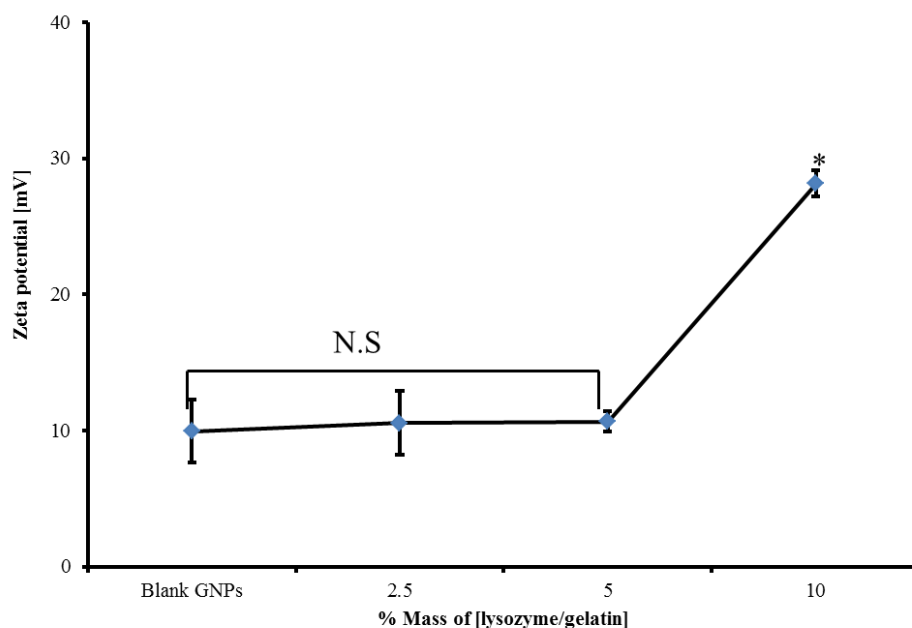


Figure 5-7. Zeta potential of DIC-crosslinked GNPs loaded with different amounts of lysozyme measured at pH 6. *Statistics* (N.S: non-significant statistically ($p > 0.05$), (*) $p < 0.05$: Statistically significant as per one-way ANOVA.

Table 5-3. Zeta potential profile of Lysozyme-loaded GNPs crosslinked with DIC at pH 6.

S.No.	Formulation	Mass ratio [Lysozyme/gelatin] %	Zeta potential [mV] ± SD
1	Unloaded GNPs	-	9.94 ± 2.30
2	Lysozyme-loaded GNPs	2.5	10.56 ± 2.35
3	Lysozyme-loaded GNPs	5	10.67 ± 0.76
4	Lysozyme-loaded GNPs	10	28.14 ± 0.97

5.4.4. Entrapment and loading efficiency

5.4.4.1. FITC-dextran

The entrapment efficiency of DIC-crosslinked GNPs increases with increase in molecular weight of FITC-dextran. For FITC dextran (20 kDa, 70 kDa, 150 kDa and 2000 kDa), the entrapment efficiency observed was approximately 3 %, 13.57 %, 36.14 % and 82.62 %, respectively, as can be seen in Figure 5-8. The possible reason for low entrapment efficiency of low molecular weight FITC-dextran is the pre-release of FITC-dextran molecules during purification step of nanoparticles. In contrast, FITC-dextran of high molecular weight is

Characterization and loading of Surface-Crosslinked Gelatin Nanoparticles with Hydrophilic Macromolecules

believed to be strongly embedded in the nanoparticulate matrix of gelatin, hence is not easily released during washing step. Consequently, this results in an apparent higher entrapment efficiency. This type of relationship between entrapment efficiency and molecular weight of FITC-dextran has also been reported by other researchers [123, 185].

It is also evident from this data that glutaraldehyde crosslinked GNPs loaded with FITC-dextran possess comparatively higher entrapment efficiency as compared to DIC-crosslinked GNPs as can be seen in Figure 5-8. This is probably due to a difference of swelling potential of two types of nano-hydrogel systems due to differences of crosslinking degrees between the two types of crosslinkers. The glutaraldehyde induced crosslinking of GNPs demonstrates a crosslinking degree of approximately 72 % as has been investigated previously in our group [123]. On the other hand, the DIC-crosslinked GNPs demonstrated approximately 25 % crosslinking degree (see chapter 3, section 3.4.2.1). Furthermore, the two types of crosslinkers establish different crosslinks within the gelatin peptide networks. Glutaraldehyde establish a Schiff's base within the gelatin peptide network [104] while DIC is believed to induce amide bonds within the gelatin peptide network just like other carbodiimides [131-134].

Therefore, the glutaraldehyde-crosslinked GNPs are homogenously crosslinked nanocarriers which are comparatively rigid nanostructures due to higher crosslinking degree as compared to DIC-crosslinked GNPs which have been hypothesized to be crosslinked only on the colloidal interface with a lower degree of crosslinking.

In summary, due to the difference of crosslinking degrees between the two types of crosslinked GNPs, the extent of pre-release or diffusion of FITC-dextran to the external aqueous environment during washing of nanoparticles is different. According to literature, the same phenomenon, *i.e.*, dependency of release or diffusion of encapsulated cargo in GNPs on crosslinking degree, has also been observed by other investigators [66, 71, 186]

Characterization and loading of Surface-Crosslinked Gelatin Nanoparticles with Hydrophilic Macromolecules

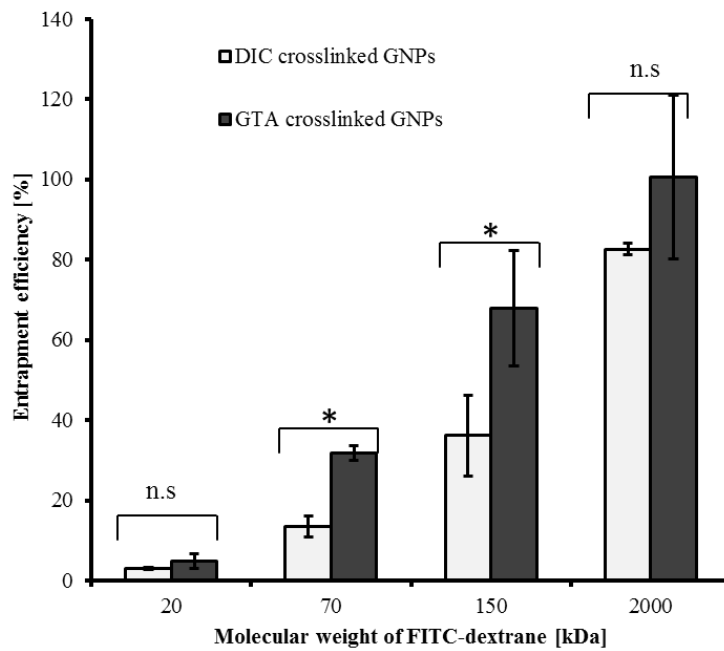


Figure 5-8. Comparison of entrapment efficiency between GTA-crosslinked and DIC-crosslinked GNP systems and effect of molecular weight of FITC-dextran on entrapment potential of both types of GNP systems. *Statistics* (n.s.: statistically non-significant on the basis of $p > 0.05$ using t-test. (*) Statistically significant $p < 0.05$)

Due to the differences in crosslinking degree and crosslink networks inside gelatin matrix, the entrapped FITC-dextran in glutaraldehyde crosslinked GNP are not easily washed with water during purification step in contrary to DIC-crosslinked GNP which show comparatively higher rate of leakage of entrapped FITC-dextran during particles purification step. Secondly, the FITC-dextran of lower molecular weight exhibits higher leakage as compared to high molecular weight FITC-dextran for both types of crosslinkers. Similar behaviour has also been previously reported for glutaraldehyde crosslinked gelatin nanoparticles encapsulated with FITC-dextran of different molecular weights [123].

5.4.4.2. Lysozyme

Before the measurement of the total mass of entrapped lysozyme in GNP matrix, the procedure for isolating the free (or un-entrapped) lysozyme from loaded GNP was validated. For this purpose, aqueous solution of lysozyme (1 mg/mL) without addition of gelatin was

Characterization and loading of Surface-Crosslinked Gelatin Nanoparticles with Hydrophilic Macromolecules

precipitated in acetone (15 mL) both with and without stabilizers (poloxamer 3% w/v). The DLS measurements demonstrated that the precipitated free lysozyme exists as visible macroscopic aggregates following precipitation in acetone as can be seen in Figure 5-9. These macroscopic aggregates can be separated using syringe filters composed of acetone resistant material, *i.e.*, polytetrafluoroethylene (PTFE) with a pore size of 0.45 μm . After microfiltration of the denatured free lysozyme, the filtrate was analysed for the amount of free lysozyme in filtrate fraction using reversed phase HPLC. From this amount, the fraction of lysozyme retained on top of the membrane was calculated after subtracting the filtered mass from total mass. It was observed that 100 percent of lysozyme is retained on top of the membrane because of the sizes of the macroscopic aggregates are larger than the pore size of the membrane (see Figure 5-10 (b)). Therefore, it can be concluded from this experiment that all free or un-entrapped fraction of lysozyme will be retained on top of the PTFE membrane having pore size of 0.45 μm during filtration. Likewise, after filtration of lysozyme-loaded GNPs suspension (un-crosslinked) using 0.45 μm PTFE filters, the quantity of entrapped lysozyme was analysed after centrifugation and subsequently dissolving the particles in PBS at pH 7.4. In another experiment, the un-filtered GNPs (un-crosslinked) loaded with similar amount of lysozyme were centrifuged and analysed after dissolving the pellet in PBS at pH 7.4. It was found that the entrapment efficiency of filtered GNPs was almost similar to non-filtered GNPs (see Figure 5-10 a and Table 5-4).

In summary, these validation experiments demonstrates that un-entrapped lysozyme exists in the form of micro-sized precipitates which can be isolated by micro-filtration from lysozyme-loaded GNPs. The lysozyme loaded GNPs will pass through the microfilters while free lysozyme micro-sized precipitates will be retained on the membrane surface. In accordance with the results of this validation experiment, the amount of lysozyme present in loaded GNPs after microfiltration was found almost equivalent to lysozyme amounts calculated for the non-filtered GNPs. This means that almost all the enzyme is entrapped in GNPs which is being

Characterization and loading of Surface-Crosslinked Gelatin Nanoparticles with Hydrophilic Macromolecules

filtered across the PTFE filter of 0.45 μm . The entrapment and loading efficiency of un-crosslinked GNPs loaded with different amounts of lysozyme are summarized in Figure 5-11 (a) and Figure 5-11 (b), respectively. The loaded GNPs without micro-filtration were analysed for entrapment and loading efficiencies. It can be observed that the entrapment efficiency is above 80 % for all amounts of lysozyme. The loading is constantly increasing and can be adjusted to 12 % (see Figure 5-11 (a) and (b)).

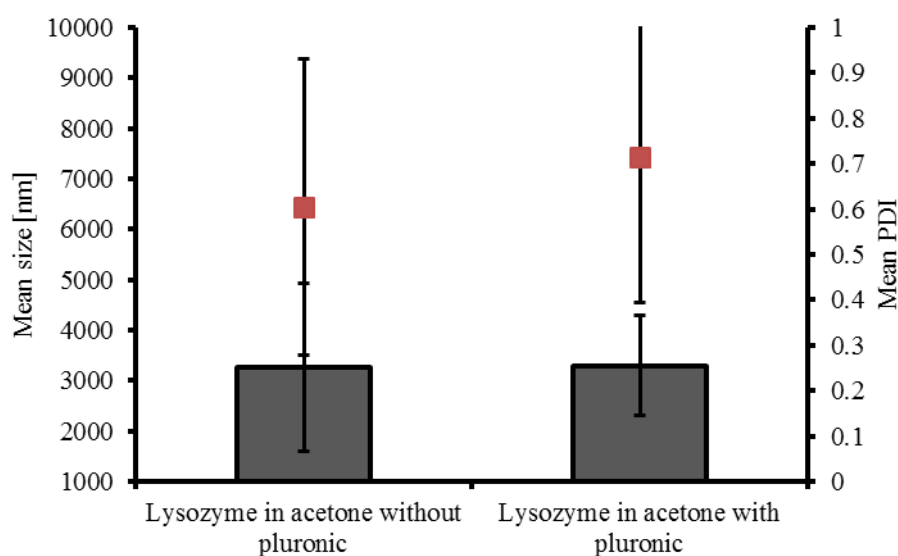


Figure 5-9. Mean sizes of free lysozyme having concentration of 2 mg/mL in water dispersed in acetone. The mean sizes are in the micro-range.

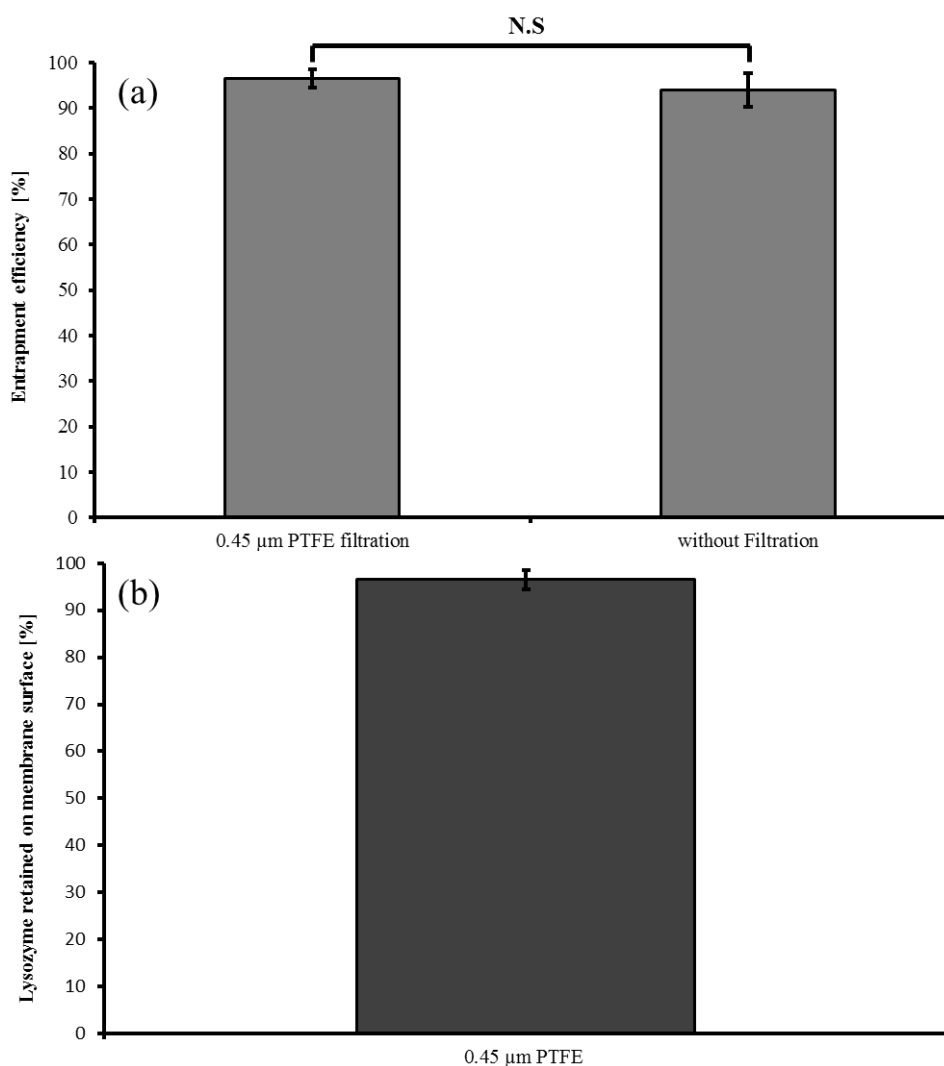


Figure 5-10. Microfiltration of free lysozyme dispersed in acetone and lysozyme-loaded GNPs. (a). Entrapment efficiency of lysozyme-loaded un-crosslinked GNPs with and without microfiltration of nanosuspension using PTFE syringe filters (0.45 µm pore size). (b) % lysozyme retained on membrane surface after microfiltration of free lysozyme dispersion in acetone using µm 0.45 PTFE filter. *Statistics* (N.S: statistically non-significant on the basis of of $p > 0.05$ using t-test).

Table 5-4. Comparison of entrapment efficiencies of lysozyme-loaded GNPs with and without microfiltration using PTFE syringe filters (0.45µm pore size).

S.No	Formulation	Entrapment efficiency [%]
1	Lysozyme loaded GNPs (without filtration)	96.53 ± 2.00
2	Lysozyme loaded GNPs (after filtration with 0.45 µm PTFE membrane)	93.97 ± 3.78

Characterization and loading of Surface-Crosslinked Gelatin Nanoparticles with Hydrophilic Macromolecules

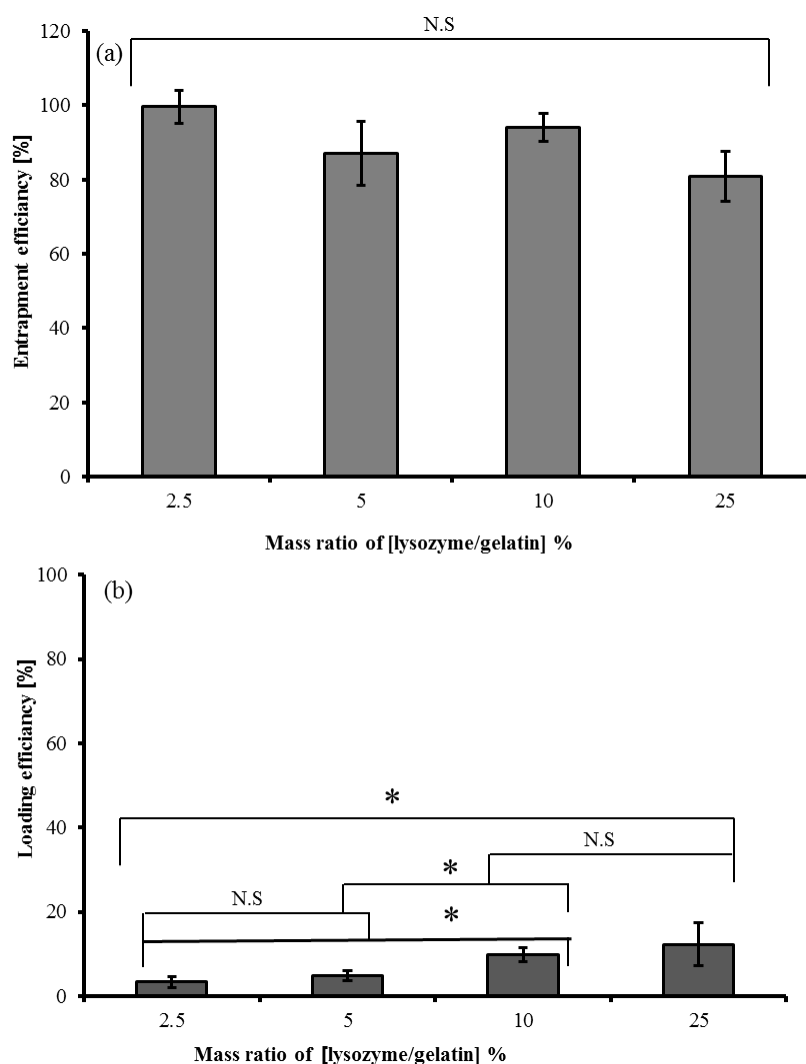


Figure 5-11. (a) Entrapment efficiency of DIC-crosslinked GNPs loaded with different amounts of lysozyme (% EE was calculated for lysozyme-loaded GNPs without microfiltration). (b) Loading efficiency of GNPs loaded with different amounts of lysozyme. Loaded GNPs without microfiltration were analysed. Statistics (N.S.: statistically non-significant on the basis of $p > 0.01$ as per one-way ANOVA and t-test; (*) $p < 0.05$)

5.4.5. Summary of the physicochemical properties of lysozyme-loaded GNPs

In summary, the mean size of lysozyme-loaded nanoparticles does not change significantly with using lysozyme/gelatin up to 5-10 % (see Table 5-5). However, there is slight increase in mean size of about (15-30 nm) with loading of lysozyme above 10 % up to 25 %. For all formulations, the PDI was found to be below 0.2 showing a narrow size distribution. With loading of lysozyme above 25 % led to visible precipitates formation which ultimately led to phase separation of the dispersion system. Thus, the maximum loadable lysozyme-to-gelatin

Characterization and loading of Surface-Crosslinked Gelatin Nanoparticles with Hydrophilic Macromolecules

ratio was found to be 25 %. The zeta potential values of lysozyme-GNPs loaded with different lysozyme amounts measured at pH 6 were compared with the unloaded GNPs (see Table 5-5). It was observed that the zeta potential of blank GNPs and lysozyme-loaded GNPs loaded with lysozyme up to 5 % is similar. On the other hand, the positive zeta potential increases with increasing the amount of loaded lysozyme above 5%. The highly positive zeta potential of lysozyme-loaded GNPs could be attributed to the surface adsorbed lysozyme molecules which exist as cationic molecules because of its high isoelectric point (IEP 11-12). The entrapment efficiency is above 80 % for all amounts of loaded lysozyme. The loading is constantly increasing and the maximum loading efficiency achievable is 12 %.

Table 5-5. Summary of the physicochemical properties of lysozyme-loaded GNPs crosslinked with diisopropylcarbodiimide (DIC concentration used for crosslinking: 15 mg/mL)

[lysozyme/g elatin] %	^(b) Size \pm S.D. [nm]	PDI \pm S.D.	Zeta potential at pH 6 [mV]	Entrapment efficiency \pm S.D. [%]	Loading efficiency \pm S.D. [%]
Unloaded GNPs	184.19 \pm 5.20	0.09 \pm 0.05	9.94 \pm 2.30	-	-
2.5	178.84 \pm 10.26	0.07 \pm 0.01	10.56 \pm 2.35	99.60 \pm 3.35	3.35 \pm 1.33
5	184.76 \pm 7.20	0.08 \pm 0.02	10.67 \pm 0.76	87.01 \pm 4.79	4.79 \pm 1.16
10	205.00 \pm 10.00	0.09 \pm 0.02	28.14 \pm 0.97	93.97 \pm 9.87	9.87 \pm 1.71
25	221.25 \pm 7.00	0.07 \pm 0.02	-	80.92 \pm 12.20	12.20 \pm 5.11
30	ND ^a	ND ^a	ND ^a	ND ^a	ND ^a
40	-	-	-	-	-
50	-	-	-	-	-

ND^a: Not determined due to visible precipitate formation. ^(b) All samples were measured in acetone as dispersion medium for the DLS measurements and were 10 times diluted with acetone before measurements. The data is an average of three independent experiments.

5.4.6. Investigation of *in vitro* release

5.4.6.1. FITC-dextran

The *in vitro* release profile of DIC-crosslinked GNPs loaded with different molecular weight FITC-dextran has been shown in Figure 5-12. The rate and extent of FITC-dextran release is different for different molecular weights. It can be observed that FITC-dextran of low

Characterization and loading of Surface-Crosslinked Gelatin Nanoparticles with Hydrophilic Macromolecules

molecular weight shows faster release as compared to high molecular weight FITC-dextran (see Figure 5-12). For example, the FITC-dextran 20 kDa and 70 kDa showed almost 20 % release in the first 30 minutes. After 8 h, the FITC-dextran 20 kDa was released completely, while the FITC-dextran 70 kDa achieved a plateau concentration of around 40 % after 24 h. In the case of FITC-dextran 150 kDa, almost 40 % FITC-dextran was released after 72 h followed by a continuous release for 120 h. In the case of FITC dextran 2000 kDa, almost 17 % release was observed after 24 h which was maintained at 17 % for 120 h (see Figure 5-12). It has been previously reported that the slow release of high molecular weight FITC-dextran is not associated with the crosslinking of payload with the gelatin polymer as dextran is a polysaccharide lacking primary amino groups [98]. According to literature, it is believed that on contact with aqueous buffer, some pores or channels of defined porosity are produced in the gelatin matrix which are bigger than the low molecular weight FITC-dextran but smaller than the high molecular weight FITC-dextran. In the case of high molecular weight FITC dextran, after the releases of surface adsorbed FITC-dextran, the rest of payload is retained in the matrix of gelatin nanoparticles. In terms release kinetics pattern, almost similar release behaviour, *i.e.*, dependency of release kinetics on molecular weight of FITC-dextran has also been reported for glutaraldehyde crosslinked GNPs [98].

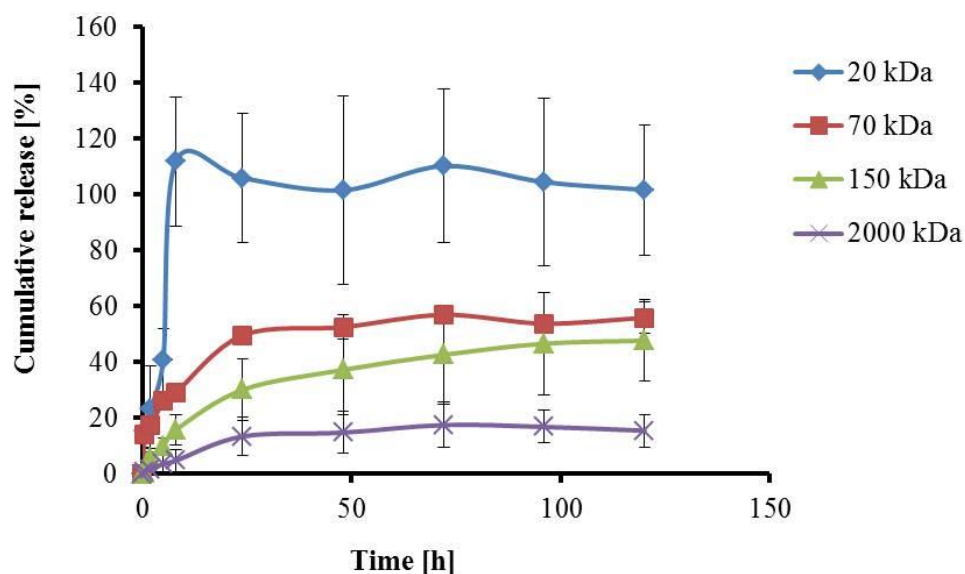


Figure 5-12. *In vitro* release profile of DIC-crosslinked gelatin nanoparticles loaded with FITC-dextran of different molecular weight in phosphate buffer saline (PBS) pH 7.4 as release medium at 37 °C.

5.4.6.2. Lysozyme

The *in vitro* release profile of lysozyme from DIC-crosslinked GNPs demonstrated that about 40% of lysozyme was released in the initial 0.5 h (Figure 5-13). This fast burst release has also been reported by other investigators [125]. The burst release of approximately 40-50 % was followed by a sustained release up to an extent of 90-100 % for 24 h. Lysozyme is a cationic polypeptide composed of 129 amino acids containing many basic as well as acidic amino acid residues [187] thus providing a favourable environment for crosslinking reaction by crosslinker (*e.g.*, DIC). Nevertheless, the maximum release of approximately 90-100 % release of lysozyme from DIC-crosslinked GNPs matrix reveals that the hydrophobic crosslinker, diisopropylcarbodiimide, is slightly involved in the crosslinking of lysozyme with gelatin thus allowing high fraction of lysozyme released in the medium. In contrast, the release from the GNPs stabilized by glutaraldehyde crosslinking demonstrated that some fraction of lysozyme (approximately 30-40 %) is released while a significant fraction (approximately 60-70 %) is still not released. Since, glutaraldehyde is a hydrophilic homo-

Characterization and loading of Surface-Crosslinked Gelatin Nanoparticles with Hydrophilic Macromolecules

bifunctional crosslinker which homogenously diffuses into the core of nanoparticulate matrix, it is believed that this low extent of release of lysozyme from glutaraldehyde crosslinked gelatin matrix is due to inter-molecular (lysozyme-gelatin) crosslinking following the formation of covalent linkages, *i.e.*, Schiff's bases. Therefore, it can be concluded that the crosslinker, diisopropylcarbodiimide, due to its hydrophobicity has a limited diffusion to the hydrophilic core of gelatin nanoparticles. Presumably, the surface restricted crosslinking behaviour of DIC due to its hydrophobic nature, led to the formation of surface crosslinked gelatin nanoparticles entrapping a hydrophilic peptidal cargo without being crosslinked inter-molecularly with GNPs matrix.

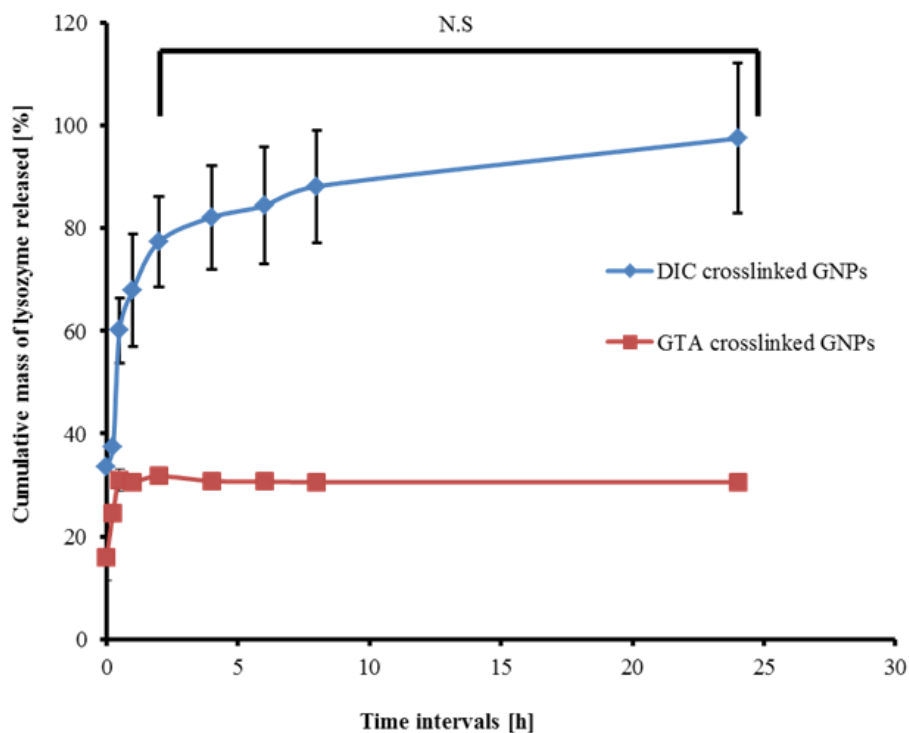


Figure 5-13. *In vitro* release profile of DIC-crosslinked and glutaraldehyde crosslinked GNPs loaded with different amounts of lysozyme in phosphate buffer saline (PBS) pH 7.4 as a release medium at 37°C. *Statistics* (N.S.: statistically non-significant on the basis of $p > 0.05$ as per one-way ANOVA).

5.4.7. Determination of biological activity

There is a linear relationship between lysozyme concentration and its corresponding enzymatic activity which was expressed in terms of turbidity clearance potential of its substrate suspension, *i.e.*, *Micrococcus lysodeikticus* ATCC No. 4698 cells. The turbidity lowering potential can be characterized as absorption change per unit time (*i.e.*, $\Delta A/\text{min}$). It was observed that the correlation between enzyme concentration and its activity was linear up to a concentration of approximately 80 $\mu\text{g/mL}$ as shown in Figure 5-14. Further increase in enzyme concentration has almost no influence on enzymatic activity. This phenomenon was expected as this is a general behaviour of all enzymes [188]. The enzymatic activity increases with increase in enzyme concentration at a given substrate concentration until an equilibrium is achieved. Further increase in enzyme concentration has no impact on enzymatic activity because of the substrate saturation with enzyme.

Moreover, when the rate of enzymatic reaction of lysozyme was studied after every minute for five minutes interval, it was observed that the rate of enzymatic reaction of lysozyme was found to be non-uniform. The activity is high initially (*i.e.*, during first minute) which slowly declines after each minute. This can be observed in the enzyme kinetics curves in Figure 5-15. Therefore, the enzymatic reaction rate during first minute which is the highest activity response was considered for making calibration curve as shown in Figure 5-14 (b).

Characterization and loading of Surface-Crosslinked Gelatin Nanoparticles with Hydrophilic Macromolecules

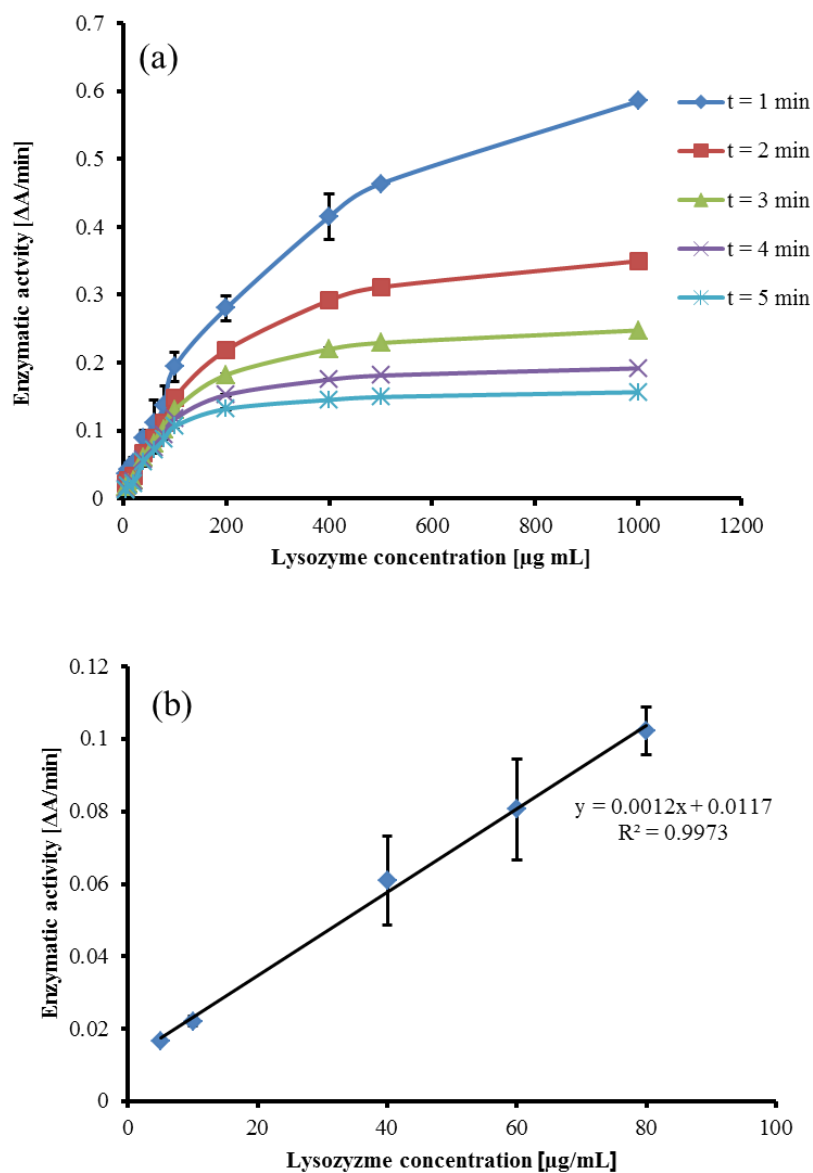


Figure 5-14.(a): Relationship between enzyme concentration ($\mu\text{g/mL}$) and corresponding enzymatic activity ($\Delta\text{A}/\text{min}$). (b): Calibration curve of lysozyme based on turbidimetric assay (Linearity between enzyme concentration and corresponding enzymatic activity in the concentration range of 5-80 $\mu\text{g/mL}$)

Characterization and loading of Surface-Crosslinked Gelatin Nanoparticles with Hydrophilic Macromolecules

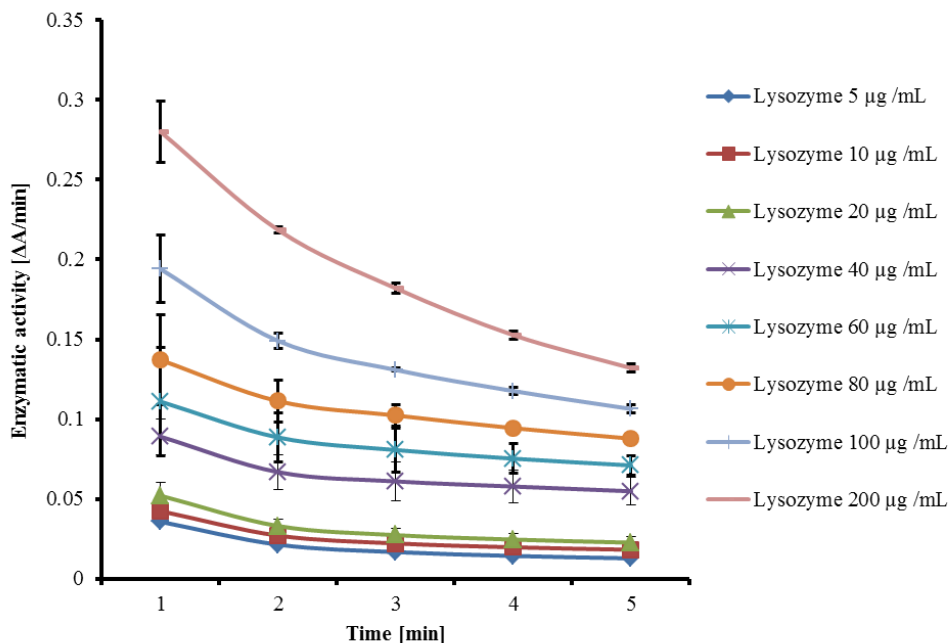


Figure 5-15. Standard kinetic curves using turbidimetric assay. The enzymatic activity is high initially which slowly declines with the passage of time. The calibration curve was constructed after 1st minute.

For the turbidimetry-based bioassay, the release samples from DIC and glutaraldehyde crosslinked GNPs were analysed after incubation of 8 mg of dried powder of lysozyme-loaded GNPs in 4 mL of PBS (pH 7.4) for 24 h at 37°C accompanied by continuous mechanical shaking at 400 rpm. The same samples were also analysed using the validated method of reverse-phase HPLC. Consequently, the calibration curve shown in Figure 5-16 was used for the determination of the total mass of released lysozyme from crosslinked (both DIC and GTA crosslinked gelatin nanoparticles).

The comparison between released lysozymes from GTA-crosslinked GNPs and DIC-crosslinked GNPs is summarized in Table 5-6.

Characterization and loading of Surface-Crosslinked Gelatin Nanoparticles with Hydrophilic Macromolecules

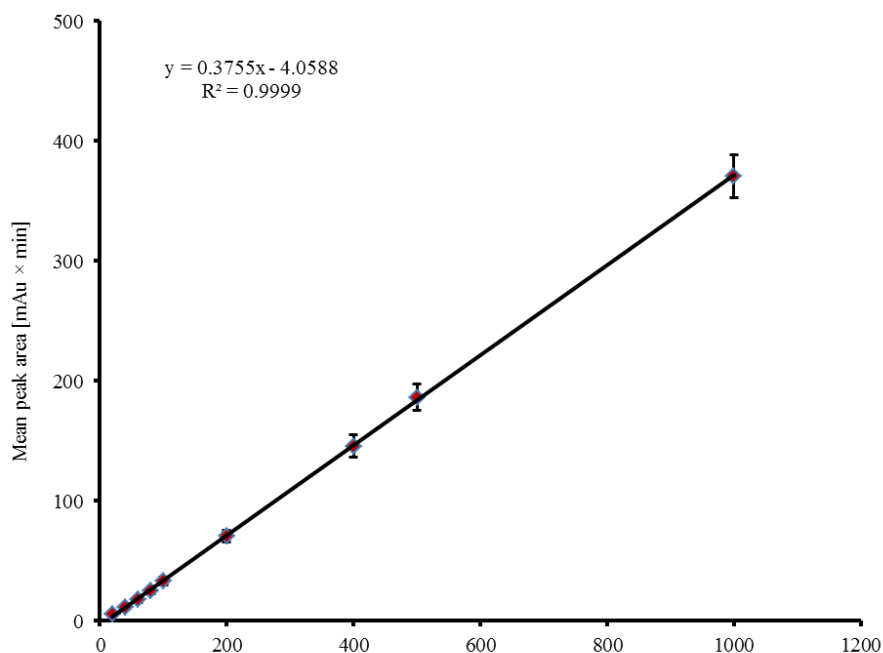


Figure 5-16. Calibration curve of lysozyme based on RP-HPLC

Table 5-6. Comparison between lysozyme amounts analysed via bioassay and HPLC assay

Sampling time [h]	Lysozyme released [%]			
	GTA-GNPs ^(a)		DIC-GNPs ^(b)	
	Bioassay	HPLC	Bioassay	HPLC
24	36.67 ± 4.26	48.11 ± 2.83	84.42 ± 8.18	95.15 ± 7.50

The data is an average of three independent experiments (n=3). ^(a)Crosslinking time: 24 h. Due to short crosslinking time, the release of lysozyme is comparatively higher than the release of previous experiment (5.4.6.2) in which the crosslinking time was 48 h. ^(b)Crosslinking time: 48 h

It is evident from the HPLC- and turbidimetry-based quantification of the released amount of lysozyme that the release extent from the DIC-crosslinked system is more as compared to the GTA-crosslinked system. The same phenomenon was also observed in section 5.4.6.2, Figure 5-13. From the biological assay it is evident that during the formulation of lysozyme-loaded GNPs and subsequently crosslinking with diisopropylcarbodiimide, the biological activity of encapsulated lysozyme is conserved. For both GTA and DIC-crosslinked GNPs, only a small fraction of approximately 11 % is released which seems to be biologically inactive (difference between the total amount released and the biologically active amount). In

Characterization and loading of Surface-Crosslinked Gelatin Nanoparticles with Hydrophilic Macromolecules

contrast, the enzymatic activity of lysozyme released from glutaraldehyde-crosslinked GNPs is significantly lower than the activity of the amount released from the DIC induced surface-crosslinked GNPs. The lower biological activity and the lower released amount of lysozyme in case of glutaraldehyde-crosslinked GNPs can be associated to glutaraldehyde mediated gelatin-lysozyme crosslinking which ultimately leads to hindrance in the release of lysozyme. On the other hand, the higher release extent and the corresponding higher activity of lysozyme from DIC-crosslinked gelatin nanoparticles demonstrates that the apolar crosslinker (DIC) is involved to a very lower degree in the inter-molecular crosslink formation between gelatin nanoparticulate matrix and the loaded lysozyme. Therefore, it can be extracted that the therapeutic activity of loaded protein-based hydrophilic macromolecule is not influenced after crosslinking with apolar zero length crosslinker, *i.e.*, diisoproylcarbodiimide.

5.5. Conclusions

This research work demonstrates a unique and novel approach of stabilization of protein-loaded GNPs with the aid of selective surface crosslinking of colloidal interface of GNPs. This was possible due to using hydrophobic zero length crosslinker, *i.e.*, diisopropylcarbodiimide. Crosslinking of lysozyme-loaded GNPs produced as a result of co-nanoprecipitation resulted in the formation of GNPs of 200-300 nm with narrow size distribution (PDI < 0.2). There is a negligible crosslinking between gelatin nanoparticulate matrix and lysozyme as evident from 90-100% release of lysozyme in the release medium. The nano-encapsulated polypeptidal compound of lysozyme in DIC-crosslinked GNPs also retains its intended therapeutic activity (anti-bacterial activity) after encapsulation and is not significantly influenced by the crosslinker during the crosslinking step of particles. In contrast, the glutaraldehyde crosslinked GNPs loaded with lysozyme show only 30-40 % release of free lysozyme while the remainder 60-70 % is believed to be covalently attached with the gelatin nanoparticulate matrix due to glutaraldehyde induced crosslinking. Therefore, it can be concluded that the DIC-induced surface-crosslinked gelatin nanoparticles (scGNPs) presents an excellent opportunity for the delivery of hydrophilic macromolecules especially peptide-based therapeutic compounds.

Summary and Outlook

The efficacy and therapeutic potential of hydrophilic macromolecules especially peptide-based drugs is limited by different obstacles after administration into the body. Some of these obstacles include short biological half, phagocytic clearance, poor membrane permeability and instability. In order to overcome these obstacles, one of the promising approaches is the nanoparticle-based delivery system. This involves the encapsulation of these hydrophilic compounds into hydrophilic polymer-based nanoparticles. Gelatin is one of the macromolecular hydrophilic biopolymers which has been predominantly used as a matrix material for hydrophilic macromolecular drugs. The main disadvantage of gelatin nanoparticles is that they are physicochemically un-stable in aqueous environment. Therefore, in order to maintain the structural integrity of these delivery systems in aqueous media, different stabilization approaches have been reported. Amongst these approaches, the chemical crosslinking has been frequently reported.

The main disadvantage of chemical crosslinking is that the crosslinker has a potential to penetrate inside the nanoparticle matrix thus making the delivery of protein-based drugs less flexible because crosslinkers will also react with protein-based drugs. The aim of this research work was to design gelatin nanoparticles via nanoprecipitation and subsequently stabilizing them with the help of selective interfacial crosslinking to overcome the main drawback for flexible protein delivery. For the selective interfacial crosslinking of GNPs, we employed diisopropylcarbodiimide (DIC), a zero-length hydrophobic crosslinker. The basic idea is that diisopropylcarbodiimide due to its hydrophobicity should not diffuse into the core of nanoparticles rather it would establish crosslinks exclusively on the colloidal interface by conjugating primary amino groups with the carboxylic functional groups. The effects of various critical parameters associated with crosslinking conditions and its possible impact on physicochemical properties of nanoparticles were investigated. The concentration of

crosslinker, crosslinking time, and temperature of crosslinking mixture were found to be critical parameters for the colloidal stability of nanoparticles in aqueous environment. The mean hydrodynamic diameter of nanoparticles was also influenced by changing gelatin type, its bloom number and concentration in the solvent phase. The surface restricted crosslinking behaviour of DIC was assessed in terms of limited crosslinking degree and limited extent of participation of the crosslinker (DIC) in the crosslinking reaction.

During the purification step of these DIC-surface crosslinked GNPs, the problem of non-redispersibility was observed. The issue was that the pellet formed after centrifugation was not redispersed in water despite applying vigorous mechanical shaking as well as ultrasonication. This problem was solved with the application of tangential flow filtration. The tangential flow filtration was found promising in terms of removing all the unwanted impurities from the crude nanosuspensions of surface-crosslinker gelatin particles.

The possibility of these surface-crosslinked gelatin nanoparticles (scGNPs) for the delivery of hydrophilic macromolecules was demonstrated using both peptide-based payloads, *e.g.*, lysozyme as well as non-peptide based payloads, *e.g.*, FITC-dextran with different molecular weights. The release from DIC-induced crosslinked gelatin nanoparticles was found to be dependent on the molecular weight of FITC-dextran. The release of low molecular weight FITC-dextran is characterized by fast burst release followed by a slow release. While, slow burst release was observed for high molecular weight FITC-dextran. This release behaviour was found to be almost similar to glutaraldehyde-crosslinked GNPs reported in literature [98]. In contrast to glutaraldehyde crosslinked GNPs, the rate and extent of FITC-dextran release from DIC-crosslinked GNPs was observed to be high. This shows a variability of crosslinks formation between glutaraldehyde and DIC-crosslinked GNPs.

In order to evaluate the surface restricted crosslinking behaviour in a more realistic way, a protein-based payload was necessary. For this purpose, lysozyme was selected as a model protein containing many crosslinkable primary amino groups. It was demonstrated that after crosslinking of lysozyme-loaded gelatin nanoparticles with DIC, no significant impact of the crosslinker was observed on the *in vitro* release of lysozyme. Approximately, 90-100 % of the encapsulated lysozyme was released in PBS (pH 7.4) demonstrating that the crosslinker (DIC) does not crosslink the loaded therapeutic protein with the polymeric matrix of gelatin, even though both the payload (*i.e.*, lysozyme) and polymer (*i.e.*, gelatin) possess plenty of primary amino groups as well as carboxylic groups. Furthermore, the evaluation of biological activity of lysozyme released from these surface-crosslinked GNPs demonstrated that the intended enzymatic activity of lysozyme, *i.e.*, anti-bacterial activity against gram positive microorganisms, is conserved to a significant extent. Therefore, it can be concluded that the surface-crosslinking of gelatin nanoparticles using zero length hydrophobic crosslinker (DIC) presents an excellent opportunity for the encapsulation of hydrophilic protein-based APIs.

However, the phenomenon of fast burst release of lysozyme from DIC-crosslinked GNPs matrix was observed. This is not surprising as the fast release of low molecular weight substances and slow release of high molecular weight substances was already reported in literature and this is believed to be due to porous structure of gelatin [189, 190]. Keeping in view the release data of FITC-dextran, there exists a specific molecular weight cut-off range in the DIC-crosslinked matrix, possibly up to 20 kDa which is equivalent to 4 nm. It is clear that lysozyme having molecular weight of 14 kDa is below 20 kDa ~ 4 nm. To overcome the fast burst release of low molecular weight macromolecules, it needs further optimization and formulation development to control the fast burst release of low molecular weight hydrophilic macromolecular payloads.

In this context, in order to overcome the fast high burst release phenomenon from surface crosslinked GNPs, we are planning to investigate the possible hydrophobization of the surface of GNPs via coating the particles with hydrophobic biodegradable polymers such as poly-(lactic acid). The coating of both un-crosslinked and surface crosslinked GNPs will be accomplished with the application of two-step nanoprecipitation [101] and nanoprecipitation-emulsion solvent evaporation techniques [122]. The idea would be that the hydrophobic coating layer deposited at the interface of GNPs composed of hydrophobic polymers will retard the fast burst release of loaded hydrophilic peptides. In this way, the release of encapsulated hydrophilic drugs will be prolonged. In parallel, these hybrid NPs composed of PLA coated GNPs can be exploited for the delivery of both hydrophobic as well as hydrophilic drugs. The hydrophilic drugs will be entrapped in the gelatin core and the hydrophobic drugs in the hydrophobic coating composed of poly-(lactic acid). These hybrid nanoparticles-based formulations can be used in cancer therapy for the co-administration of both hydrophilic and hydrophobic drugs. The co-delivery of hydrophilic and hydrophobic drugs in one particle based delivery system has also been reported for cancer treatment using other nanomaterials [191]. This coating with biodegradable hydrophobic polymers (*i.e.*, poly-lactic acid) will not only lead retard the high burst release of low molecular weight macromolecules from GNPs but also providing a stabilization mechanism for GNPs in hydrophilic environment without chemical crosslinking.

In order to investigate further the phenomenon of DIC surface crosslinking, we are also planning to extend the application of surface-crosslinked gelatin nanoparticles for the delivery of other therapeutic proteins, *e.g.*, cytochrome c (apoptosis inducer, anticancer drug), antibodies (anticancer drug) and α -chymotrypsin (anti-inflammatory drug).

Bibliography

1. Azad, N. and Y. Rojanasakul, *Macromolecular Drug Delivery*, in *Biopharmaceutical Drug Design and Development*, S. Wu-Pong and Y. Rojanasakul, Editors. 2008, Humana Press: Totowa, NJ. p. 293-323.
2. Agrahari, V. and A.K. Mitra, *Nanocarrier fabrication and macromolecule drug delivery: challenges and opportunities*. *Ther Deliv*, 2016. **7**(4): p. 257-78.
3. Mitragotri, S., P.A. Burke, and R. Langer, *Overcoming the challenges in administering biopharmaceuticals: formulation and delivery strategies*. *Nature reviews. Drug discovery*, 2014. **13**(9): p. 655-672.
4. Skalko-Basnet, N., *Biologics: the role of delivery systems in improved therapy*. *Biologics : targets & therapy*, 2014. **8**: p. 107-114.
5. Ibraheem, D., A. Elaissari, and H. Fessi, *Administration strategies for proteins and peptides*. *International Journal of Pharmaceutics*, 2014. **477**(1): p. 578-589.
6. Chen, M.C., et al., *Recent Advances in Chitosan-based Nanoparticles for Oral Delivery of Macromolecules*. *Advanced Drug Delivery Reviews*, 2012. **65**(6): p. 865–879.
7. des Rieux, A., et al., *Nanoparticles as potential oral delivery systems of proteins and vaccines: a mechanistic approach*. *Journal of Controlled Release*, 2006. **116**(1): p. 1-27.
8. Desai, M.P., et al., *The mechanism of uptake of biodegradable microparticles in Caco-2 cells is size dependent*. *Pharmaceutical Research*, 1997. **14**(11): p. 1568-1573.
9. Treuel, L., X. Jiang, and G.U. Nienhaus, *New views on cellular uptake and trafficking of manufactured nanoparticles*. *Journal of The Royal Society Interface*, 2013. **10**(82).
10. Jiang, W., et al., *Advances and challenges of nanotechnology-based drug delivery systems*. *Expert Opin Drug Deliv*, 2007. **4**(6): p. 621-33.
11. Liversidge, G.G. and K.C. Cundy, *Particle size reduction for improvement of oral bioavailability of hydrophobic drugs: I. Absolute oral bioavailability of nanocrystalline danazol in beagle dogs*. *International journal of pharmaceutics*, 1995. **125**(1): p. 91-97.
12. Liversidge, G.G. and P. Conzentino, *Drug particle size reduction for decreasing gastric irritancy and enhancing absorption of naproxen in rats*. *International journal of pharmaceutics*, 1995. **125**(2): p. 309-313.
13. Merisko-Liversidge, E., G.G. Liversidge, and E.R. Cooper, *Nanosizing: a formulation approach for poorly-water-soluble compounds*. *European journal of pharmaceutical sciences*, 2003. **18**(2): p. 113-120.
14. Bawa, R., *Nanoparticle-based therapeutics in humans: a survey*. *Nanotech. L. & Bus.*, 2008. **5**: p. 135.
15. Matsumura, Y. and H. Maeda, *A new concept for macromolecular therapeutics in cancer chemotherapy: mechanism of tumoritropic accumulation of proteins and the antitumor agent smancs*. *Cancer research*, 1986. **46**(12 Part 1): p. 6387-6392.
16. Almeida, A.J. and E. Souto, *Solid lipid nanoparticles as a drug delivery system for peptides and proteins*. *Advanced drug delivery reviews*, 2007. **59**(6): p. 478-490.
17. Pinto Reis, C., et al., *Nanoencapsulation II. Biomedical applications and current status of peptide and protein nanoparticulate delivery systems*. *Nanomedicine: Nanotechnology, Biology and Medicine*, 2006. **2**(2): p. 53-65.
18. Bilati, U., E. Allémann, and E. Doelker, *Nanoprecipitation Versus Emulsion-based Techniques for the Encapsulation of Proteins Into Biodegradable Nanoparticles and Process-related Stability Issues*. *AAPS PharmSciTech*, 2005. **6** (4): p. E593-E604.

19. Mundargi, R.C., et al., *Nano/micro technologies for delivering macromolecular therapeutics using poly(D,L-lactide-co-glycolide) and its derivatives*. Journal of Controlled Release, 2008. **125**(3): p. 193-209.
20. Rietscher, R., et al., *Impact of PEG and PEG-b-PAGE modified PLGA on nanoparticle formation, protein loading and release*. International journal of pharmaceutics, 2016. **500**(1-2): p. 187-195.
21. Rietscher, R., et al., *Antigen delivery via hydrophilic PEG-b-PAGE-b-PLGA nanoparticles boosts vaccination induced T cell immunity*. European Journal of Pharmaceutics and Biopharmaceutics, 2016. **102**: p. 20-31.
22. Xu, Y. and Y. Du, *Effect of molecular structure of chitosan on protein delivery properties of chitosan nanoparticles*. International Journal of Pharmaceutics, 2003. **250**(1): p. 215-226.
23. Vila, A., et al., *Low molecular weight chitosan nanoparticles as new carriers for nasal vaccine delivery in mice*. European Journal of Pharmaceutics and Biopharmaceutics, 2004. **57**(1): p. 123-131.
24. Singh, R. and J.W. Lillard, Jr., *Nanoparticle-based targeted drug delivery*. Experimental and molecular pathology, 2009. **86**(3): p. 215-223.
25. Verma, D., et al., *Protein Based Nanostructures for Drug Delivery*. Journal of pharmaceutics, 2018. **2018**: p. 9285854-9285854.
26. Coester, C., P. Nayyar, and J. Samuel, *In vitro uptake of gelatin nanoparticles by murine dendritic cells and their intracellular localisation*. Eur J Pharm Biopharm, 2006. **62**(3): p. 306-14.
27. Wang, G. and H. Uludag, *Recent developments in nanoparticle-based drug delivery and targeting systems with emphasis on protein-based nanoparticles*. Expert Opin Drug Deliv, 2008. **5**(5): p. 499-515.
28. Langer, R., *Drug delivery and targeting*. Nature, 1998. **392**(6679 Suppl): p. 5-10.
29. Gulfam, M., et al., *Anticancer drug-loaded gliadin nanoparticles induce apoptosis in breast cancer cells*. Langmuir, 2012. **28**(21): p. 8216-8223.
30. Zargar, B., et al., *Zein bio-nanoparticles: a novel green nanopolymer as a dispersive solid-phase extraction adsorbent for separating and determining trace amounts of azorubine in different foodstuffs*. RSC Advances, 2016. **6**(77): p. 73096-73105.
31. Scheffel, U., et al., *Albumin microspheres for study of the reticuloendothelial system*. J Nucl Med, 1972. **13**(7): p. 498-503.
32. Kreuter, J., *Nanoparticles and nanocapsules--new dosage forms in the nanometer size range*. Pharm Acta Helv, 1978. **53**(2): p. 33-9.
33. Marty, J.J., R.C. Oppenheim, and P. Speiser, *Nanoparticles--a new colloidal drug delivery system*. Pharm Acta Helv, 1978. **53**(1): p. 17-23.
34. Rubino, O.P., R. Kowalsky, and J. Swarbrick, *Albumin Microspheres as a Drug Delivery System: Relation Among Turbidity Ratio, Degree of Cross-linking, and Drug Release*. Pharmaceutical Research, 1993. **10**(7): p. 1059-1065.
35. Lin, W., et al., *Preparation of Sterically Stabilized Human Serum Albumin Nanospheres Using a Novel Dextranox-MPEG Crosslinking Agent*. Pharmaceutical Research, 1994. **11**(11): p. 1588-1592.
36. Sailaja, A. and P. Amareshwar, *Preparation of BSA nanoparticles by desolvation technique using acetone as desolvating agent*.
37. Lomis, N., et al., *Human serum albumin nanoparticles for use in cancer drug delivery: process optimization and in vitro characterization*. Nanomaterials, 2016. **6**(6): p. 116.
38. Noorani, L., et al., *Albumin nanoparticles increase the anticancer efficacy of albendazole in ovarian cancer xenograft model*. Journal of nanobiotechnology, 2015. **13**(1): p. 25.

39. Jithan, A., et al., *Preparation and characterization of albumin nanoparticles encapsulating curcumin intended for the treatment of breast cancer*. International journal of pharmaceutical investigation, 2011. **1**(2): p. 119.
40. Mirshahi, T., et al., *Adaptive immune responses of legumin nanoparticles*. Journal of drug targeting, 2002. **10**(8): p. 625-631.
41. Wu, Y., et al., *Fabrication of elastin-like polypeptide nanoparticles for drug delivery by electrospraying*. Biomacromolecules, 2008. **10**(1): p. 19-24.
42. Dhanya, A., et al., *Development of Zein-Pectin nanoparticle as drug carrier*. International Journal of Drug Delivery, 2012. **4**(2): p. 147-152.
43. Chen, H., *Fabrication of Zein Nanoparticle-Biopolymer Complexes to Deliver Essential Oils in Aqueous Dispersions*. 2014.
44. Huang, J., et al., *Layer-by-layer assembled milk protein coated magnetic nanoparticle enabled oral drug delivery with high stability in stomach and enzyme-responsive release in small intestine*. Biomaterials, 2015. **39**: p. 105-113.
45. Teng, Z., Y. Luo, and Q. Wang, *Nanoparticles synthesized from soy protein: preparation, characterization, and application for nutraceutical encapsulation*. Journal of agricultural and food chemistry, 2012. **60**(10): p. 2712-2720.
46. Liu, F. and C.-H. Tang, *Soy protein nanoparticle aggregates as Pickering stabilizers for oil-in-water emulsions*. Journal of agricultural and food chemistry, 2013. **61**(37): p. 8888-8898.
47. Karim, A.A. and R. Bhat, *Fish gelatin: properties, challenges, and prospects as an alternative to mammalian gelatins*. Food Hydrocolloids, 2009. **23**(3): p. 563-576.
48. Gómez-Guillén, M.C., et al., *Functional and bioactive properties of collagen and gelatin from alternative sources: A review*. Food Hydrocolloids, 2011. **25**(8): p. 1813-1827.
49. Choi, S.S. and J. Regenstein, *Physicochemical and sensory characteristics of fish gelatin*. Journal of Food Science, 2000. **65**(2): p. 194-199.
50. Elzoghby, A.O., W.M. Samy, and N.A. Elgindy, *Protein-based nanocarriers as promising drug and gene delivery systems*. J Control Release, 2012. **161**(1): p. 38-49.
51. Kaul, G. and M. Amiji, *J. Pharm. Sci.*, 2005. **94**(null): p. 184.
52. Sundar, S., J. Kundu, and S.C. Kundu, *Biopolymeric nanoparticles*. Science and technology of advanced materials, 2010. **11**(1): p. 014104-014104.
53. Patel, Z.S., et al., *Biodegradable gelatin microparticles as delivery systems for the controlled release of bone morphogenetic protein-2*. Acta biomaterialia, 2008. **4**(5): p. 1126-1138.
54. Ninan, G., J. Jose, and Z. Abubacker, *Preparation and characterization of gelatin extracted from the skins of rohu (Labeo rohita) and common carp (Cyprinus carpio)*. Journal of Food Processing and Preservation, 2011. **35**(2): p. 143-162.
55. Santoro, M., A.M. Tataru, and A.G. Mikos, *Gelatin carriers for drug and cell delivery in tissue engineering*. Journal of controlled release, 2014. **190**: p. 210-218.
56. Cui, L., et al., *Preparation and characterization of IPN hydrogels composed of chitosan and gelatin cross-linked by genipin*. Carbohydrate polymers, 2014. **99**: p. 31-38.
57. Li, J.-H., et al., *Preparation and characterization of active gelatin-based films incorporated with natural antioxidants*. Food Hydrocolloids, 2014. **37**: p. 166-173.
58. Prata, A.S. and C.R.F. Grosso, *Production of microparticles with gelatin and chitosan*. Carbohydrate Polymers, 2015. **116**: p. 292-299.
59. Finlayf, H., G.G. Millera, and R. Löbenberga, *Optimization of a two-step desolvation method for preparing gelatin nanoparticles and cell uptake studies in 143B osteosarcoma cancer cells*. 2006.

60. Rajan, M. and V. Raj, *Formation and characterization of chitosan-poly(lactic acid)-poly(ethylene glycol)-gelatin nanoparticles: a novel biosystem for controlled drug delivery*. Carbohydrate polymers, 2013. **98**(1): p. 951-958.
61. Lu, Z., et al., *Paclitaxel-loaded gelatin nanoparticles for intravesical bladder cancer therapy*. Clinical Cancer Research, 2004. **10**(22): p. 7677-7684.
62. Vandervoort, J. and A. Ludwig, *Preparation and evaluation of drug-loaded gelatin nanoparticles for topical ophthalmic use*. European Journal of Pharmaceutics and Biopharmaceutics, 2004. **57**(2): p. 251-261.
63. Nahar, M., et al., *Development, characterization, and toxicity evaluation of amphotericin B-loaded gelatin nanoparticles*. Nanomedicine: Nanotechnology, Biology and Medicine, 2008. **4**(3): p. 252-261.
64. Ofokansi, K., et al., *Matrix-loaded biodegradable gelatin nanoparticles as new approach to improve drug loading and delivery*. Eur J Pharm Biopharm, 2010. **76**(1): p. 1-9.
65. Cascone, M.G., et al., *Gelatin nanoparticles produced by a simple W/O emulsion as delivery system for methotrexate*. Journal of Materials Science: Materials in Medicine, 2002. **13**(5): p. 523-526.
66. Bajpai, A. and J. Choubey, *In vitro release dynamics of an anticancer drug from swellable gelatin nanoparticles*. Journal of applied polymer science, 2006. **101**(4): p. 2320-2332.
67. Leo, E., et al., *Doxorubicin-loaded gelatin nanoparticles stabilized by glutaraldehyde: involvement of the drug in the cross-linking process*. International journal of Pharmaceutics, 1997. **155**(1): p. 75-82.
68. Leo, E., et al., *General and cardiac toxicity of doxorubicin-loaded gelatin nanoparticles*. Farmaco (Societa chimica italiana: 1989), 1997. **52**(6-7): p. 385-388.
69. Leo, E., R. Camerani, and F. Forni, *Dynamic dialysis for the drug release evaluation from doxorubicin-gelatin nanoparticle conjugates*. International journal of pharmaceutics, 1999. **180**(1): p. 23-30.
70. Kaur, A., S. Jain, and A. Tiwary, *Mannan-coated gelatin nanoparticles for sustained and targeted delivery of didanosine: in vitro and in vivo evaluation*. Acta pharmaceutica, 2008. **58**(1): p. 61-74.
71. Bajpai, A. and J. Choubey, *Release study of sulphamethoxazole controlled by swelling of gelatin nanoparticles and drug-biopolymer interaction*. Journal of Macromolecular Science, Part A: Pure and Applied Chemistry, 2005. **42**(3): p. 253-275.
72. El-Shabouri, M., *Positively charged nanoparticles for improving the oral bioavailability of cyclosporin-A*. International journal of pharmaceutics, 2002. **249**(1-2): p. 101-108.
73. Singh, V. and A. Chaudhary, *Development and characterization of rosiglitazone loaded gelatin nanoparticles using two step desolvation method*. Int. J. Pharm. Sci. Rev. Res, 2010. **5**: p. 100-103.
74. Saxena, A., et al., *Effect of molecular weight heterogeneity on drug encapsulation efficiency of gelatin nano-particles*. Colloids and Surfaces B: Biointerfaces, 2005. **45**(1): p. 42-48.
75. Li, J.K., N. Wang, and X.S. Wu, *Gelatin nanoencapsulation of protein/peptide drugs using an emulsifier-free emulsion method*. J Microencapsul, 1998. **15**(2): p. 163-72.
76. Li, J.K., N. Wang, and X.S. Wu, *A novel biodegradable system based on gelatin nanoparticles and poly(lactic-co-glycolic acid) microspheres for protein and peptide drug delivery*. J Pharm Sci, 1997. **86**(8): p. 891-5.
77. Won, Y.-W. and Y.-H. Kim, *Recombinant human gelatin nanoparticles as a protein drug carrier*. Journal of Controlled Release, 2008. **127**(2): p. 154-161.

78. Zhao, Y.-Z., et al., *Experiment on the feasibility of using modified gelatin nanoparticles as insulin pulmonary administration system for diabetes therapy*. Acta Diabetologica, 2012. **49**(4): p. 315-325.
79. Wang, H., et al., *Comparison of micro- vs. nanostructured colloidal gelatin gels for sustained delivery of osteogenic proteins: Bone morphogenetic protein-2 and alkaline phosphatase*. Biomaterials, 2012. **33**(33): p. 8695-703.
80. Uesugi, Y., et al., *An ultrasound-responsive nano delivery system of tissue-type plasminogen activator for thrombolytic therapy*. Journal of Controlled Release, 2010. **147**(2): p. 269-277.
81. Uesugi, Y., et al., *Ultrasound-responsive thrombus treatment with zinc-stabilized gelatin nano-complexes of tissue-type plasminogen activator*. J Drug Target, 2012. **20**(3): p. 224-34.
82. Sudheesh, M.S., S.P. Vyas, and D.V. Kohli, *Nanoparticle-based immunopotentialization via tetanus toxoid-loaded gelatin and aminated gelatin nanoparticles*. Drug Deliv, 2011. **18**(5): p. 320-30.
83. Balthasar, S., et al., *Preparation and characterisation of antibody modified gelatin nanoparticles as drug carrier system for uptake in lymphocytes*. Biomaterials, 2005. **26**(15): p. 2723-2732.
84. Azarmi, S., W.H. Roa, and R. Löbenberg, *Targeted delivery of nanoparticles for the treatment of lung diseases*. Advanced Drug Delivery Reviews, 2008. **60**(8): p. 863-875.
85. Gupta, B., et al., *Preparation and characterization of in-situ crosslinked pectin-gelatin hydrogels*. Carbohydrate Polymers, 2014. **106**(0): p. 312-318.
86. Mohanty, B., et al., *Synthesis of gelatin nanoparticles via simple coacervation*. Journal of Surface Science and Technology, 2005. **21**(3/4): p. 149.
87. Choubey, J. and A.K. Bajpai, *Investigation on magnetically controlled delivery of doxorubicin from superparamagnetic nanocarriers of gelatin crosslinked with genipin*. J Mater Sci Mater Med, 2010. **21**(5): p. 1573-86.
88. Gupta, A.K., et al., *Effect of cellular uptake of gelatin nanoparticles on adhesion, morphology and cytoskeleton organisation of human fibroblasts*. Journal of Controlled Release, 2004. **95**(2): p. 197-207.
89. Landfester, K., *The generation of nanoparticles in miniemulsions*. Advanced Materials, 2001. **13**(10): p. 765-768.
90. Zinatloo-Ajabshir, S. and N. TaheriQazvini, *Inverse miniemulsion method for synthesis of gelatin nanoparticles in presence of CDI/NHS as a non-toxic cross-linking system*. Journal of Nanostructures, 2014. **4**(3): p. 267-275.
91. Ethirajan, A., et al., *Synthesis and optimization of gelatin nanoparticles using the miniemulsion process*. Biomacromolecules, 2008. **9**(9): p. 2383-2389.
92. Farrugia, C.A. and M.J. Groves, *Gelatin behaviour in dilute aqueous solution: designing a nanoparticulate formulation*. J Pharm Pharmacol, 1999. **51**(6): p. 643-9.
93. Kommareddy, S., D.B. Shenoy, and M.M. Amiji, *Gelatin nanoparticles and their biofunctionalization*. Nanotechnologies for the Life Sciences: Online, 2007.
94. Coester, C., et al., *Preparation of avidin-labelled gelatin nanoparticles as carriers for biotinylated peptide nucleic acid (PNA)*. International journal of pharmaceutics, 2000. **196**(2): p. 147-149.
95. Lee, S.J., et al., *Biocompatible gelatin nanoparticles for tumor-targeted delivery of polymerized siRNA in tumor-bearing mice*. Journal of controlled release, 2013. **172**(1): p. 358-366.
96. Quintanar-Guerrero, D., et al., *Preparation techniques and mechanisms of formation of biodegradable nanoparticles from preformed polymers*. Drug Dev Ind Pharm, 1998. **24**(12): p. 1113-28.

97. Lee, E.J., et al., *Studies on the characteristics of drug-loaded gelatin nanoparticles prepared by nanoprecipitation*. Bioprocess Biosyst Eng, 2012. **35**(1-2): p. 297-307.
98. Khan, S.A., *Gelatin Nanoparticles as Potential Nanocarriers for Macromolecular Drugs*, 2014, Philipps-Universität Marburg.
99. Bilati, U., E. Allémann, and E. Doelker, *Development of a nanoprecipitation method intended for the entrapment of hydrophilic drugs into nanoparticles*. European Journal of Pharmaceutical Sciences, 2005. **24**(1): p. 67-75.
100. Pérez, C., et al., *Recent trends in stabilizing protein structure upon encapsulation and release from bioerodible polymers*. Journal of Pharmacy and Pharmacology, 2002. **54**(3): p. 301-313.
101. Morales-Cruz, M., et al., *Two-step nanoprecipitation for the production of protein-loaded PLGA nanospheres*. Results in pharma sciences, 2012. **2**: p. 79-85.
102. Elzoghby, A.O., *Gelatin-based nanoparticles as drug and gene delivery systems: reviewing three decades of research*. J Control Release, 2013. **172**(3): p. 1075-91.
103. Kommareddy, S. and M.M. Amiji, *Preparation and loading of gelatin nanoparticles*. CSH Protoc, 2008. **1**(10).
104. Farris, S., J. Song, and Q. Huang, *Alternative reaction mechanism for the cross-linking of gelatin with glutaraldehyde*. Journal of agricultural and food chemistry, 2009. **58**(2): p. 998-1003.
105. Vandelli, M.A., et al., *Gelatin microspheres crosslinked with D,L-glyceraldehyde as a potential drug delivery system: preparation, characterisation, in vitro and in vivo studies*. Int J Pharm, 2001. **215**(1-2): p. 175-84.
106. Van Luyn, M.J.A., et al., *Calcification of subcutaneously implanted collagens in relation to cytotoxicity, cellular interactions and crosslinking*. Journal of Materials Science: Materials in Medicine, 1995. **6**(5): p. 288-296.
107. Tsai, C.-C., et al., *In vitro evaluation of the genotoxicity of a naturally occurring crosslinking agent (genipin) for biologic tissue fixation*. Journal of Biomedical Materials Research, 2000. **52**(1): p. 58-65.
108. Song, F., et al., *Genipin-crosslinked casein hydrogels for controlled drug delivery*. Int J Pharm, 2009. **373**(1-2): p. 41-7.
109. Rose, J., et al., *Gelatin-based materials in ocular tissue engineering*. Materials, 2014. **7**(4): p. 3106-3135.
110. Qazvini, N.T. and S. Zinatloo, *Synthesis and characterization of gelatin nanoparticles using CDI/NHS as a non-toxic cross-linking system*. Journal of Materials Science: Materials in Medicine, 2011. **22**(1): p. 63-69.
111. Heck, T., et al., *Enzyme-catalyzed protein crosslinking*. Applied microbiology and biotechnology, 2013. **97**(2): p. 461-475.
112. Fuchs, S., et al., *Transglutaminase: new insights into gelatin nanoparticle cross-linking*. Journal of microencapsulation, 2010. **27**(8): p. 747-754.
113. Duesberg, G., et al., *Separation of carbon nanotubes by size exclusion chromatography*. Chemical Communications, 1998(3): p. 435-436.
114. Lee, J.-S., S.I. Stoeva, and C.A. Mirkin, *DNA-induced size-selective separation of mixtures of gold nanoparticles*. Journal of the American Chemical Society, 2006. **128**(27): p. 8899-8903.
115. Latham, A.H., et al., *Capillary magnetic field flow fractionation and analysis of magnetic nanoparticles*. Analytical chemistry, 2005. **77**(15): p. 5055-5062.
116. Sweeney, S.F., G.H. Woehrle, and J.E. Hutchison, *Rapid purification and size separation of gold nanoparticles via diafiltration*. Journal of the American Chemical Society, 2006. **128**(10): p. 3190-3197.
117. Hanauer, M., et al., *Separation of nanoparticles by gel electrophoresis according to size and shape*. Nano letters, 2007. **7**(9): p. 2881-2885.

118. Xiong, B., et al., *Separation of nanorods by density gradient centrifugation*. J Chromatogr A, 2011. **24**(25): p. 3823-9.
119. Sharma, V., K. Park, and M. Srinivasarao, *Shape separation of gold nanorods using centrifugation*. Proc Natl Acad Sci U S A, 2009. **106**(13): p. 4981-5.
120. Dalwadi, G., H.A. Benson, and Y. Chen, *Comparison of diafiltration and tangential flow filtration for purification of nanoparticle suspensions*. Pharm Res, 2005. **22**(12): p. 2152-62.
121. Elmer, J., et al., *Purification of hemoglobin by tangential flow filtration with diafiltration*. Biotechnology progress, 2009. **25**(5): p. 1402-1410.
122. Khan, S.A. and M. Schneider, *Stabilization of Gelatin Nanoparticles Without Crosslinking*. Macromolecular Bioscience, 2014. **14**(11): p. 1627-1638.
123. Khan, S.A. and M. Schneider, *Improvement of nanoprecipitation technique for preparation of gelatin nanoparticles and potential macromolecular drug loading*. Macromol Biosci, 2013. **13**(4): p. 455-63.
124. Loth, T., et al., *Reactive and stimuli-responsive maleic anhydride containing macromers—multi-functional cross-linkers and building blocks for hydrogel fabrication*. Reactive and Functional Polymers, 2013. **73**(11): p. 1480-1492.
125. Zhai, X., *Gelatin nanoparticles & nanocrystals for dermal delivery*, 2014.
126. Janes, K., P. Calvo, and M. Alonso, *Polysaccharide colloidal particles as delivery systems for macromolecules*. Advanced drug delivery reviews, 2001. **47**(1): p. 83-97.
127. Bubnis, W.A. and C.M. Ofner, 3rd, *The determination of epsilon-amino groups in soluble and poorly soluble proteinaceous materials by a spectrophotometric method using trinitrobenzenesulfonic acid*. Anal Biochem, 1992. **207**(1): p. 129-33.
128. Mosmann, T., *Rapid colorimetric assay for cellular growth and survival: application to proliferation and cytotoxicity assays*. J Immunol Methods, 1983. **65**(1-2): p. 55-63.
129. Lee, E.J., S.A. Khan, and K.H. Lim, *Gelatin nanoparticle preparation by nanoprecipitation*. J Biomater Sci Polym Ed, 2011. **22**(4-6): p. 753-71.
130. Galindo-Rodriguez, S.A., et al., *Comparative scale-up of three methods for producing ibuprofen-loaded nanoparticles*. Eur J Pharm Sci, 2005. **25**(4-5): p. 357-67.
131. Khorana, H.G., *The Chemistry of Carbodiimides*. Chemical Reviews, 1953. **53**(2): p. 145-166.
132. Kurzer, F. and K. Douraghi-Zadeh, *Advances in the Chemistry of Carbodiimides*. Chemical Reviews, 1967. **67**(2): p. 107-152.
133. Mikoz, xl, et al., *Recent developments in the carbodiimide chemistry*. Tetrahedron, 1981. **37**(2): p. 233-284.
134. Williams, A. and I.T. Ibrahim, *Carbodiimide chemistry: recent advances*. Chemical Reviews, 1981. **81**(6): p. 589-636.
135. Carpino, L.A. and A. El-Faham, *The diisopropylcarbodiimide/1-hydroxy-7-azabenzotriazole system: segment coupling and stepwise peptide assembly*. Tetrahedron, 1999. **55**(22): p. 6813-6830.
136. Corbett, A.D. and J.L. Gleason, *Preparation of active esters on solid support for aqueous-phase peptide couplings*. Tetrahedron letters, 2002. **43**(8): p. 1369-1372.
137. Han, S.-Y. and Y.-A. Kim, *Recent development of peptide coupling reagents in organic synthesis*. Tetrahedron, 2004. **60**(11): p. 2447-2467.
138. Ofner, I., Clyde M. and W.A. Bubnis, *Chemical and Swelling Evaluations of Amino Group Crosslinking in Gelatin and Modified Gelatin Matrices*. Pharmaceutical Research, 1996. **13**(12): p. 1821-1827.
139. GMIA, G.H., *Gelatin Manufacturers Institute of America*. New York, 2012.
140. Shaw, R., *Dynamic Light Scattering Training*. Malvern Instruments Ltd, 2014.
141. Instruments, M., *Zetasizer Nano User Manual MAN0317*. Malvern Instruments Ltd.: Malvern, United Kingdom, 2009(5.0): p. 1-12.

142. Bhattacharjee, S., *DLS and zeta potential—What they are and what they are not?* Journal of Controlled Release, 2016. **235**: p. 337-351.
143. Tseng, C.-L., et al., *Cationic gelatin nanoparticles for drug delivery to the ocular surface: in vitro and in vivo evaluation.* Journal of Nanomaterials, 2013. **2013**: p. 7.
144. Aramwit, P., et al., *A comparative study of type A and type B gelatin nanoparticles as the controlled release carriers for different model compounds.* Materials Express, 2015. **5**(3): p. 241-248.
145. Fröhlich, E., *The role of surface charge in cellular uptake and cytotoxicity of medical nanoparticles.* International journal of nanomedicine, 2012. **7**: p. 5577.
146. Hafidz, R., et al., *Chemical and functional properties of bovine and porcine skin gelatin.* International Food Research Journal, 2011. **18**: p. 813-817.
147. Blouza, I.L., et al., *Preparation and characterization of spirinolactone-loaded nanocapsules for paediatric use.* International journal of pharmaceutics, 2006. **325**(1-2): p. 124-131.
148. Hornig, S., et al., *Synthetic polymeric nanoparticles by nanoprecipitation.* Journal of Materials Chemistry, 2009. **19**(23): p. 3838-3840.
149. Lezanska, M., et al., *Type A and B gelatin as precursors of silica-templated porous carbon with a specified number of nitrogen-and oxygen-containing functionalities.* Materials Express, 2017. **7**(2): p. 123-133.
150. Maxey, C. and M. Palmer, *Photographic Gelatin II*, 1967, Academic Press, London.
151. Hermanto, S. and W. Fatimah, *Differentiation of bovine and porcine gelatin based on spectroscopic and electrophoretic analysis.* Journal of Food and Pharmaceutical Sciences, 2013. **1**(3).
152. Fitch, C.A., et al., *Arginine: Its pKa value revisited.* Protein Sci, 2015. **24**(5): p. 752-61.
153. Weiss, A.-V., et al., *Mechanical Properties of Gelatin Nanoparticles in Dependency of Crosslinking Time and Storage.* Colloids and Surfaces B: Biointerfaces, 2018.
154. Govender, T., et al., *PLGA nanoparticles prepared by nanoprecipitation: drug loading and release studies of a water soluble drug.* Journal of Controlled Release, 1999. **57**(2): p. 171-185.
155. Murakami, H., et al., *Further application of a modified spontaneous emulsification solvent diffusion method to various types of PLGA and PLA polymers for preparation of nanoparticles.* Powder technology, 2000. **107**(1-2): p. 137-143.
156. Calvo, P., et al., *Chitosan and chitosan/ethylene oxide-propylene oxide block copolymer nanoparticles as novel carriers for proteins and vaccines.* Pharmaceutical research, 1997. **14**(10): p. 1431-1436.
157. Nguyen, C.A., et al., *Synthesis of a novel fluorescent poly (D, L-lactide) end-capped with 1-pyrenebutanol used for the preparation of nanoparticles.* European journal of pharmaceutical sciences, 2003. **20**(2): p. 217-222.
158. Beck, P., D. Scherer, and J. Kreuter, *Separation of drug-loaded nanoparticles from free drug by gel filtration.* Journal of microencapsulation, 1990. **7**(4): p. 491-496.
159. Kwon, H.-Y., et al., *Preparation of PLGA nanoparticles containing estrogen by emulsification–diffusion method.* Colloids and Surfaces A: Physicochemical and Engineering Aspects, 2001. **182**(1-3): p. 123-130.
160. Tishchenko, G., et al., *Purification of polymer nanoparticles by diafiltration with polysulfone/hydrophilic polymer blend membranes.* Separation and purification technology, 2001. **22**: p. 403-415.
161. Tishchenko, G., et al., *Ultrafiltration and microfiltration membranes in latex purification by diafiltration with suction.* Separation and purification technology, 2003. **30**(1): p. 57-68.

162. Quintanar-Guerrero, D., et al., *Influence of the stabilizer coating layer on the purification and freeze-drying of poly (D, L-lactic acid) nanoparticles prepared by an emulsion-diffusion technique*. Journal of microencapsulation, 1998. **15**(1): p. 107-119.
163. Martin, T.M., et al., *Preparation of budesonide and budesonide-PLA microparticles using supercritical fluid precipitation technology*. AAPS PharmSciTech, 2002. **3**(3): p. 16-26.
164. Prabha, S., et al., *Size-dependency of nanoparticle-mediated gene transfection: studies with fractionated nanoparticles*. Int J Pharm, 2002. **244**(1-2): p. 105-15.
165. Chiellini, E., et al. *Polymeric nanoparticles based on polylactide and related copolymers*. in *Macromolecular Symposia*. 2003. Wiley Online Library.
166. Ghebeh, H., A. Handa-Corrigan, and M. Butler, *Development of an assay for the measurement of the surfactant pluronic F-68 in mammalian cell culture medium*. Analytical biochemistry, 1998. **262**(1): p. 39-44.
167. Chung, H.H., et al., *Direct determination of residual Pluronic F-68 in in-process samples from monoclonal antibody preparations by high performance liquid chromatography*. Journal of Chromatography A, 2011. **1218**(15): p. 2106-2113.
168. Mao, Y., et al., *Quantitation of poloxamers in pharmaceutical formulations using size exclusion chromatography and colorimetric methods*. Journal of pharmaceutical and biomedical analysis, 2004. **35**(5): p. 1127-1142.
169. Zwioerek, K., et al., *Gelatin nanoparticles as a new and simple gene delivery system*. J Pharm Pharm Sci, 2004. **7**(4): p. 22-28.
170. Tao Liang, M., et al., *Particulate systems as adjuvants and carriers for peptide and protein antigens*. Current drug delivery, 2006. **3**(4): p. 379-388.
171. Nezhadi, S.H., et al., *Gelatin-based delivery systems for cancer gene therapy*. Journal of Drug Targeting, 2009. **17**(10): p. 731-738.
172. Kuo, W.-T., et al., *Surface modification of gelatin nanoparticles with polyethylenimine as gene vector*. Journal of Nanomaterials, 2011. **2011**: p. 28.
173. Price, W.S., F. Tsuchiya, and Y. Arata, *Lysozyme Aggregation and Solution Properties Studied Using PGSE NMR Diffusion Measurements*. Journal of the American Chemical Society, 1999. **121**(49): p. 11503-11512.
174. Wetter, L. and H. Deutsch, *Immunological studies on egg white proteins*. J. biol. Chem, 1951. **192**: p. 237-242.
175. Palmer, K., M. Ballantyne, and J. Galvin, *The molecular weight of lysozyme determined by the X-ray diffraction method*. Journal of the American Chemical Society, 1948. **70**(3): p. 906-908.
176. Masuda, T., N. Ide, and N. Kitabatake, *Structure–sweetness relationship in egg white lysozyme: role of lysine and arginine residues on the elicitation of lysozyme sweetness*. Chemical senses, 2005. **30**(8): p. 667-681.
177. Phillips, D.C., *The three-dimensional structure of an enzyme molecule*. Scientific American, 1966. **215**(5): p. 78-93.
178. Liao, Y.H., M.B. Brown, and G.P. Martin, *Turbidimetric and HPLC assays for the determination of formulated lysozyme activity*. J Pharm Pharmacol, 2001. **53**(4): p. 549-54.
179. Mörsky, P., *Turbidimetric determination of lysozyme with Micrococcus lysodeikticus cells: reexamination of reaction conditions*. Analytical biochemistry, 1983. **128**(1): p. 77-85.
180. Chipman, D.M. and N. Sharon, *Mechanism of lysozyme action*. Science, 1969. **165**(3892): p. 454-465.
181. Held, J. and S. van Smaalen, *The active site of hen egg-white lysozyme: flexibility and chemical bonding*. Acta crystallographica. Section D, Biological crystallography, 2014. **70**(Pt 4): p. 1136-1146.

182. Lesnierowski, G. and J. Kijowski, *Lysozyme*, in *Bioactive Egg Compounds*, R. Huopalahti, et al., Editors. 2007, Springer Berlin Heidelberg: Berlin, Heidelberg. p. 33-42.
183. Young, S., et al., *Gelatin as a delivery vehicle for the controlled release of bioactive molecules*. Journal of controlled release, 2005. **109**(1-3): p. 256-274.
184. Tabata, Y. and Y. Ikada, *Protein release from gelatin matrices*. Advanced drug delivery reviews, 1998. **31**(3): p. 287-301.
185. Hines, D.J. and D.L. Kaplan, *Mechanisms of controlled release from silk fibroin films*. Biomacromolecules, 2011. **12**(3): p. 804-812.
186. Bajpai, A. and J. Choubey, *Design of gelatin nanoparticles as swelling controlled delivery system for chloroquine phosphate*. Journal of Materials Science: Materials in Medicine, 2006. **17**(4): p. 345-358.
187. Phillips, D.C., *The Hen Egg-White Lysozyme Molecule*. Proceedings of the National Academy of Sciences of the United States of America, 1967. **57**(3): p. 483-495.
188. Robinson, P.K., *Enzymes: principles and biotechnological applications*. Essays in biochemistry, 2015. **59**: p. 1-41.
189. Akhter, K., J. Zhu, and J. Zhang, *Nanoencapsulation of protein drug for controlled release*. J Physic Chem Biophysic, 2012: p. 2161-0398.
190. Khan, S.A., *Gelatin Nanoparticles as Potential Nanocarriers for Macromolecular Drugs*. 2014.
191. Garbuzenko, O.B., et al., *Biodegradable Janus nanoparticles for local pulmonary delivery of hydrophilic and hydrophobic molecules to the lungs*. Langmuir, 2014. **30**(43): p. 12941-12949.

Scientific Output

Publications

1. **Abdul Baseer**, Aljoscha Koenneke, Josef Zapp, Saeed A. Khan & Marc Schneider, **Design and Characterization of Surface-Crosslinked Gelatin Nanoparticles for the Delivery of Hydrophilic Macromolecular Drugs**. *Macromolecular Chemistry and Physics*. 2019. 220(18): p. 1900260.

Poster Presentation

1. **Abdul Baseer**, Marc Schneider, Synthesis and Characterization of Gelatin Nanoparticles for the Delivery of Hydrophilic Macromolecules, DPhG Annual Conference, 26-29 September 2017, Saarland University, Saarbrücken.
2. **Abdul Baseer**, Marc Schneider, Synthesis and Characterization of Gelatin Nanoparticles for the Delivery of Hydrophilic Macromolecules, 22nd Annual Meeting of CRS Germany Local Chapter, March 2018, Martin-Luther University, Halle-Wittenberg, Germany.
3. **Abdul Baseer**, Marc Schneider, Gelatin Nanoparticles Stabilized via interfacial crosslinking: A Novel delivery system for Hydrophilic macromolecules, 12th International Conference and Workshop on Biological Barriers, 27-29 August 2018, Saarland University, Saarbrücken, Germany.

Curriculum Vitae

Personal Information

Name Abdul Baseer
Date of Birth 14th March 1981
Place of Birth Malakand (Pakistan)

Academic Record

2014-2019 Doing PhD (Pharmaceutical Technology), Phillips University Marburg, Germany, and Saarland University, Saarbrücken, Germany.
Thesis title: Surface-Crosslinked Gelatin Nanoparticles as New Tool for the Delivery of Hydrophilic Macromolecular Drugs.

2004-2007 M.Pharm (Pharmaceutics), Faculty of Pharmacy, Karachi University, Karachi, Pakistan
Thesis title: Formulation Development of famotidine tablets using Dry Granulation.

1999-2003 Bachelor of Pharmacy, University of Peshawar, Pakistan.

Practical Experience

2004-2005 Production officer at **Atco Laboratories** ltd, Karachi, Pakistan.

2005-2006 Production officer at **Abbott Laboratories** ltd, Karachi, Pakistan.

2006-2008 Consultant at **Parke-Davis (now merged with Pfizer laboratories)** and co. ltd, Karachi, Pakistan

2008-2009 Senior Production Officer at **Ali Gohar Pharmaceuticals** ltd, Karachi, Pakistan.

2009-2012 Lecturer at the Department of Pharmacy, **Sarhad University of Science and Information Technology (SUIT)**, Peshawar, Pakistan.

2012-2014 Lecturer at the Department of Pharmacy, **Kohat University of Science and Technology (KUST)**, Kohat, Pakistan.

Acknowledgment

In the name of Al-mighty ALLAH, the most gracious and the most merciful! Who always bestowed on me infinite bounties and blessings. I am highly grateful to Allah who granted me several opportunities in my life.

During my doctorate research, I got supported from many people in my institute as well as from other departments of Saarland University, so I can only name some of them in my acknowledgments.

Firstly, I would like to express my grateful acknowledgement to my supervisor Prof. Dr. Marc Schneider. Thank you Marc for providing me the excellent opportunity to work in a highly intellectual, professional and scientific environment. You have always been there for kind advices. I have greatly enjoyed working in such a comfortable atmosphere. I will always appreciate your highly accommodative nature, stress-free supervision and encouragement for new ideas. I am very thankful to you for having such a magnificent scientific atmosphere and a friendly environment.

I would like to thank all my ex- and present colleagues for their full support. In this connection, I would like to acknowledge especially Dr. Agnes Weiß, Dr. Saeed Ahmed Khan, Marcel, Alexandra, Nesma Ibrahim, Nashrawan, Dr. Carolin Thum, Aljoscha, Thorben and Dr. Michael Möhwald. I am also very grateful to Dr. Daniel Primaveßy for scientific discussion and sharing knowledge. I must also acknowledge the contribution of Dr. Afra Torge and Dr. Sara Barthold in regards of SEM measurements and scientific discussions. In addition to the PhD students, I would like to thank all diploma students joining our lab, like Madona, Inga, Sami, Camila. Thanks for the scientific discussions and input, the enjoyable working atmosphere and thanks for all the friendships developing over the time.

I thank Dr. Phil Sevatus, research fellow of Prof. Dr. Uli Kazmaier for the analysis of my samples using Gas chromatography-Mass spectrometry and Gas Chromatography coupled

with flame ionization detector (GC-MS & GC-FID). I would also like to acknowledge gratefully the contribution of Dr. Josef Zapp, Department of Pharmaceutical Biology, Saarland University, for his kind support and guidance in context of ^1H NMR spectroscopic analysis of my samples. I also thank Professor Dr. Gerhard Wenz, Department of Macromolecular Chemistry, and his entire research group members, especially, Mr. Devid Hero who helped me a lot in the FT-IR measurements of my samples.

I am also grateful to Prof. Claus-Michael Lehr and the entire HIPS drug delivery group for sharing knowledge, help, support and beneficial scientific discussions. Many thanks to Dr. Chiara De Rossi (HIPS) for the SEM analysis.

I gratefully acknowledge the kind assistance of Peter Meiers (Uni. Saarland) for his kind guidance and training me on HPLC and routine laboratory works. Off course, Marijas, who was not only a technician but also a great friend of mine. Thank you, Marijas, for helping me in cell culture experiments.

Finally, I would like to thank my family. I thank my lovely parents, for their love and encouragement throughout my life. I thank all my brothers for their prayers. Special thanks to my loving elder brother Abdul Sadiq who always fully supported me throughout my academic carrier. I also thank my lovely and supportive wife who always fortify my confidence by standing by me in all situations. I am also thankful to my parents-in-law, my brothers-in-law, Muhammad Sajjad and Muhammad Jawad Nasim for their moral support and encouragement. Without their support my aim wouldn't have been accomplished.

I gratefully acknowledge HEC, Pakistan and DAAD whose funding made my PhD possible.

Abdul Baseer